

Understanding the structure and dynamics of bacteria-phage infection networks

Rosanna Christina Taylor Wright

PhD

University of York

Biology

September 2018

Abstract

As rising levels of antibiotic resistance limit treatment options against bacterial infections, phage therapy offers a promising alternative. However, as bacteria and phage have co-evolved for millennia within natural microbial communities, where lytic phages naturally regulate bacterial density, a diverse set of phage resistance mechanisms exist. Here, I explore how the structure of bacteria-phage communities influences the evolution of phage resistance, and how the evolutionary principles which shape these communities may be exploited to improve the rational design of phage therapeutics. Using network analysis to assess how environmental conditions influence the structure of bacteria-phage communities, I showed that imbalances in selection pressure can destabilise bacteria-phage communities and drive phage to extinction. The community structure of microbial communities is underpinned by extensive gene-gene interactions between multiple pairs of co-evolving species. By determining the breadth of cross-resistance individual resistance mutations can promote, I characterised how cross-resistance can structure a collection of phage strains, and how these interactions determine the evolution of multiple resistances. Further, I characterised how this could be exploited to limit the evolution of resistance against phage cocktails, revealing that the evolution of multi-phage resistances are influenced by the order of phage exposure, such that sequential exposure promotes accumulation of multiple strong phage-specific resistances whereas simultaneous exposure to phage pairs promotes weaker resistances. Finally, by comparing the efficacy of phage combinations of increasing diversity, I assessed the relative contributions of phage diversity, functional diversity and cross-resistance structure on the efficacy of phage cocktails. This revealed that functionally diverse phage combinations (i.e. those targeting multiple adsorption receptors) make more effective phage cocktails. These results provide insight into the fundamental evolutionary processes which determine the efficacy of phage cocktails, revealing simple concepts which may be implemented to simplify the rational design of therapeutic phage treatments, such as the maximisation of functional diversity.

List of Contents

Abstract	2
List of Contents	3
List of Figures	5
Acknowledgements	7
Author's declaration	8
Chapter One Introduction	9
1.1 Perpetual evolution can be driven by biotic interactions	10
1.2 Phage classification and biodiversity	12
1.3 Phage resistance mechanisms and counter-defence strategies	14
1.4 Network analysis as a tool to study evolutionary interactions	17
1.5 A model system to study the effect of phage therapy	19
1.6 Is phage therapy a realistic alternative to antibiotics?	24
1.7 Thesis outline	28
Chapter Two Ecological conditions determine extinction risk in co-evolving bacteria-phage populations	29
2.1 Introduction	29
2.2 Materials and Methods	31
2.3 Results	33
2.4 Discussion	37
Chapter Three Cross-resistance is modular in bacteria-phage interactions	41
3.1 Introduction	41
3.2 Materials and Methods	43
3.3 Results	49
3.4 Discussion	57
Chapter Four Effect of sequential versus simultaneous exposure to phages on host resistance evolution	63
4.1 Introduction	63
4.2 Materials and Methods	65
4.3 Results	69
4.4 Discussion	79

Chapter Five Functional diversity determines the efficacy of phage cocktails	84
5.1 Introduction	84
5.2 Materials and Methods	86
5.3 Results	88
5.4 Discussion	93
Chapter Six Discussion	97
6.1 Insights into community structure from network analysis	98
6.2 Genetic basis of resistance determines network modularity	99
6.3 Rational design of phage therapeutics	102
6.4 Conclusions	107
Appendices	108
Appendix A (Chapter Three)	108
Appendix B (Chapter Four)	123
Abbreviations	124
Bibliography	125

List of Figures

Chapter One

- Figure 1.1** The life cycle and morphological classification of phages 13
- Figure 1.2** Characterising the network structure of bacteria-phage infection networks 18
- Figure 1.3** Structure of the Type IV pilus 22
- Figure 1.4** Diversity of lipopolysaccharide structures which may be displayed on one bacterial cell 23

Chapter Two

- Figure 2.1** Survivorship of phage replicate populations through time is determined by treatment conditions 28
- Figure 2.2** Contrasting density profiles over time for bacteria and phage populations 35
- Figure 2.3** Changes in bacterial susceptibility across low resource treatments approaching phage extinction time points 36

Chapter Three

- Figure 3.1** Cross-resistance network describing quantitative cross-resistance between all possible phage combinations 50
- Figure 3.2** Effect of relative fitness and focal resistance on cross-resistance range 52
- Figure 3.3** Genetic basis of phage resistance 54
- Figure 3.4** Effect of cross-resistance type and mutational target on relative fitness of spontaneous resistant mutants 55
- Figure 3.5** Relative mutational frequency for resistance against phage pairs exerting symmetrical, asymmetrical and no cross-resistance 56

Chapter Four

- Figure 4.1** Trade-offs in the strength of resistance to each selection Phage 71
- Figure 4.2** Relative fitness of resistant mutants is determined by selection regime 74
- Figure 4.3** Treatment regimens determine the frequency and type of resistance mutations selected 76
- Figure 4.4** Contrasting fitness costs resulting from specific combinations of single and double mutations 78

Chapter Five

- Figure 5.1** Illustration of pathway analysis methodology 88

Figure 5.2 Saturating relationship between the efficacy and diversity of phage combinations	89
Figure 5.3 Receptor classification determines the linearity of the diversity-reduction relationship	91
Figure 5.4 Stepwise changes in cross-resistance structure reveal key transitions in the efficacy of phage combinations	92

Acknowledgements

Firstly, I would like to thank my supervisors, Mike Brockhurst, Ville Friman and Maggie Smith. I have been incredibly lucky to have benefitted from their support, advice and expertise, and sincerely appreciate all the effort they have made over the last four years.

Thanks to my TAP panel, Jon Pitchford and Peter Young, for invaluable advice and discussions.

Thank you to the NERC ACCE DTP Scheme for funding my PhD.

To the Brockhurst lab group - Thank you all for being so supportive and encouraging, but most importantly, for making work so fun! Huge thanks to Ellie Harrison and Jamie Hall for endless advice and problem-solving. And lastly a massive thank you to Cagla, Megan and Rachael, you guys are absolutely the best!

Finally, to my family, you are my foundation, and I simply couldn't have done this without you all – thank you.

Author's Declaration

I declare that this thesis is a presentation of original work and I am the sole author. This work has not previously been presented for an award at this, or any other, University. All sources are acknowledged as References.

The following publications have arisen from this thesis:

- Wright, R.C.T., Brockhurst, M.A., and Harrison, E. (2016). Ecological conditions determine extinction risk in co-evolving bacteria-phage populations. *BMC Evolutionary Biology*. 16, 227.
- Wright, R.C.T., Friman, V-P., Smith, M.C.M., and Brockhurst, M.A. (2018). Cross-resistance is modular in bacteria-phage interactions. *PLOS Biology*. 16 (10), e2006057

Chapter Two presents the published version of Wright et al (2016). I performed the experiments and analysed the data under the supervision of M.A.B. and E.H. All authors contributed towards the design of the experiment, interpretation of results and writing of the manuscript.

Chapter Three presents the accepted version of Wright et al (2018). I performed the experiments and analysed the data under the supervision of M.A.B., V-P.F. and M.C.M.S. All authors contributed towards the design of the experiment, interpretation of results and writing of the manuscript.

Chapter One

Introduction

Bacterial communities are ubiquitous across a wide range of natural ecosystems, from deep sea hydrothermal vents to soils, and play a fundamental role in ecological and evolutionary processes in all of these locations (DeLong et al., 2001; Fuhrman, 1999; Wilhelm and Suttle, 1999). Wherever bacteria exist it is likely that abundant and diverse communities of viral parasites of bacteria, bacteriophages, often abbreviated to phages, will co-occur. Phages are viruses that parasitise bacterial cells, hijacking their cellular machinery and reproduce (Weinbauer, 2004). This process results in lysis of the bacterial host. Therefore, phage are believed to play an important role in the regulation of bacterial populations, and consequently the composition of bacterial communities, whilst cell lysis also results in the release of nutrients (Weinbauer, 2004; Weinbauer and Rassoulzadegan, 2004). Hence, phage are considered key global regulators of carbon and nutrient cycling across both aquatic and terrestrial environments (Weinbauer and Rassoulzadegan, 2004; Wilhelm and Suttle, 1999).

Since phage were first discovered in the early 20th century (Duckworth, 1976; d'Herelle, 1917), it has been proposed that their bactericidal actions could be harnessed to treat bacterial infections, a treatment termed phage therapy (Carlton, 1999). Indeed, in many parts of Eastern Europe phage therapy has been used successfully for many years, however, the discovery of Penicillin less than 15 years after the discovery of phages meant that researchers in the western hemisphere largely ignored this research and phage therapy was not adopted (Levin and Bull, 2004). With rising rates of antibiotic resistance worldwide and greater understand of the propensity for bacteria to develop resistance by *de novo* mutation or horizontal gene transfer, new antimicrobial treatments are urgently required that can be used to combat drug resistant infections (World Health Organisation, 2014). Like antibiotics, bacteria can easily evolve resistance to phage attack, and, therefore, to maximise the potential benefits and durability of phage therapy a better understanding of the fundamental ecological and evolutionary processes that determine the efficacy of phage therapies is required.

Here, I examine the evolutionary principles governing phage resistance evolution in bacteria that structure natural communities and determine co-existence between bacteria and phage, towards developing an evolutionary framework to aid the rational design of phage therapy cocktails.

1.1 Perpetual evolution can be driven by biotic interactions

1.1.1 Antagonistic coevolution within bacteria-phage interactions

Infection of bacterial cells is an essential stage in the life cycle of phage, and hence links the evolutionary fate of phage to their bacterial host species through a process of antagonistic coevolution: Phage infection selects for bacterial adaptations which promote phage resistance, so phage must counter-adapt to maintain infectivity and continue to replicate, leading to continual cycles of adaptation and counter-adaptation. This follows the Red Queen hypothesis of coevolution (Van Valen, 1973) where biotic conflicts drive perpetual evolution of interacting species.

There are two main theories which describe the dynamics of antagonistic coevolution, these are not mutually exclusive and the prominent mode may be determined by the associated fitness costs within the local ecological context (Brockhurst et al., 2014). Arms race dynamics (ARD; Gandon et al., 2008), also known as Escalatory Red Queen (ERQ; Brockhurst et al., 2014), is driven by directional selection for increasingly resistant hosts and increasingly infectious parasites over time, in which novel mechanisms of phage infectivity or host resistance emerge and accumulate, being driven to fixation by recurrent selective sweeps (Lenski and Levin, 1985). In contrast, fluctuating selection dynamics (FSD; Gandon et al., 2008), also known as Fluctuating Red Queen (FRQ; Brockhurst et al., 2014), is driven by negative frequency-dependent selection whereby common host genotypes are targeted by phage infection and selected against, leading to an increased frequency of rarer host genotypes which eventually become the most common, and so the cycle repeats (Levin et al., 1988).

1.1.2 What are the costs of perpetual antagonistic coevolution?

Both dynamic models have been identified in experimental pairwise bacteria-phage systems using *Pseudomonas fluorescens* SBW25 with the associated phage Φ 2. Perpetual ARD results in directional selection and is therefore limited by the potential number of novel mutations which can arise and the impact of accumulating fitness costs (Buckling and Rainey, 2002; Hall et al., 2011a). As a

result, after several hundreds of generations of coevolution a switch to FSD is observed (Hall et al., 2011b). FSD removes the directional pressure for additional novel mutations and associated costs, making FSD more sustainable over time and in stressful environments where the fitness costs of ARD are magnified. Therefore, whilst novel interactions often result in strong directional selection on both species promoting an ARD period, persistent antagonistic coevolution appears to be maintained by switching to FSD. Thereafter bouts of ARD could occur in response to changes in environmental conditions or due to additional biotic interactions (Brockhurst et al., 2014).

Long term FSD promotes diversity within populations because genetic diversity is not purged by selective sweeps (Harrison et al., 2013; Lopez Pascua et al., 2014). Increased host diversity supports broader genetic polymorphism of resistance phenotypes which could in turn protect the population upon encountering new phage genotypes (Lively, 2010). Diversity can also be sustained in ARD coevolution, provided the cost of resistance is high enough that susceptible bacteria retain a fitness advantage (Sasaki, 2000). This diversity can result in compartmentalised specificity (Bascombe, 2010), allowing long-term bacteria-phage coexistence even if highly resistant bacterial genotypes emerge.

1.1.3 *The local environmental context determines co-evolutionary dynamics*

The Red Queen principle states that biotic factors are sufficient to drive perpetual evolution, however, this does not preclude evolutionary responses to abiotic factors. Nutrient availability can constrain evolutionary dynamics by limiting population sizes, and hence, limiting the genetic variation available to selection (Kassen et al., 2000). Therefore, whilst ARD seem prevalent in high quality environments, such as in nutrient rich media (Lopez Pascua et al., 2014) a switch to FSD has been observed in lower quality environments, such as experimental soil microcosms (Gómez and Buckling, 2011). Variation in nutrient availability may also limit ARD, by impeding the selective sweeps characteristic of coevolution driven by directional selection (Harrison et al., 2013). Environments which impose higher stress on one partner in the co-evolutionary relationship are likely to imbalance co-evolutionary dynamics and can result in extinction of one partner. For example, increasing temperatures impose stronger environmental stress on the phage than on the bacterial host, and therefore although the phage can survive if the bacteria is held in evolutionary stasis, when they are forced to co-evolve, the phage is driven to extinction (Zhang and Buckling, 2011). At the individual level, phage resistance is often associated with fitness costs, such as

reduced ability to utilise nutrients (Middelboe et al., 2009), and hence there are trade-offs between phage resistance (biotic factors) and adaptation to the local environment (abiotic factors) (Bohannan et al., 2002). Pleiotropic effects associated with resistance mutations can reduce the potential for the host to adapt to environmental changes (Scanlan et al., 2015a), especially in environments where the expression of many diverse traits is necessary.

Spatial heterogeneity of abiotic factors, such as resource levels, or of biotic factors, such as community composition can influence the mode and rate of coevolution across a landscape. Antagonistic coevolution accelerates molecular evolution (Paterson et al., 2010) and hence, minor changes which result in variation in the rate of coevolution can result in localised differences within communities (Lopez-Pascua and Buckling, 2008; Vogwill et al., 2009). Bacteria-phage coevolution may be reduced in static conditions due to decreased dispersal and lower encounter rates (Brockhurst et al., 2006), promoting FSD (Brockhurst et al., 2004). Further, population structure can develop in static conditions to create spatial refuges, such as wall dwelling sub-populations (Schrag and Mittler, 1996), which may promote co-existence as phage-free refuges maintain host diversity and allow maintenance of a susceptible host sub-populations. On the other hand, population mixing increases the rate of dispersal within an environment can enhance the encounter rate between hosts and parasites (Haraguchi and Sasaki, 2000), imposing stronger selection for resistance and thus accelerating the rate of coevolution and promoting ARD (Brockhurst et al., 2003, 2004). Interestingly, a shift from FSD to ARD was observed with increased population mixing in soil microcosms (Gómez et al., 2015a), indicating that even in low resource environments, the effect of mixing can substantially alter coevolutionary dynamics by altering the balance of the cost:benefit ratio of resistance.

1.2 Phage classification and biodiversity

1.2.1 Morphological diversity of phages

Phages can be classified by morphology, describing their component nucleic acid and the structural proteins surrounding this which form a protective capsid. Phages may contain DNA or RNA (either single or double stranded), with genomes ranging from only a few kb to examples of giant phages with large genomes of up to 300kb (Hertveldt et al., 2005). The phage genome is protected from the environment by protein structures built of repeating subunits; these often

form an icosahedral capsid, but can also form rod-like structures known as filamentous phages (Figure 1.1B).

Tailed phages, known collectively as *Caudovirales*, represent approximately 96% of known phages (Figure 1.1B; Ackermann, 2007). The phage tail is a complex multi-unit structure which is involved in attachment and entry into the host cell, and in the case of *Myoviridae*, the tail is covered in a contractile sheath which acts in a syringe-like mechanism to inject phage DNA into the host cell (Fokine and Rossmann, 2014).

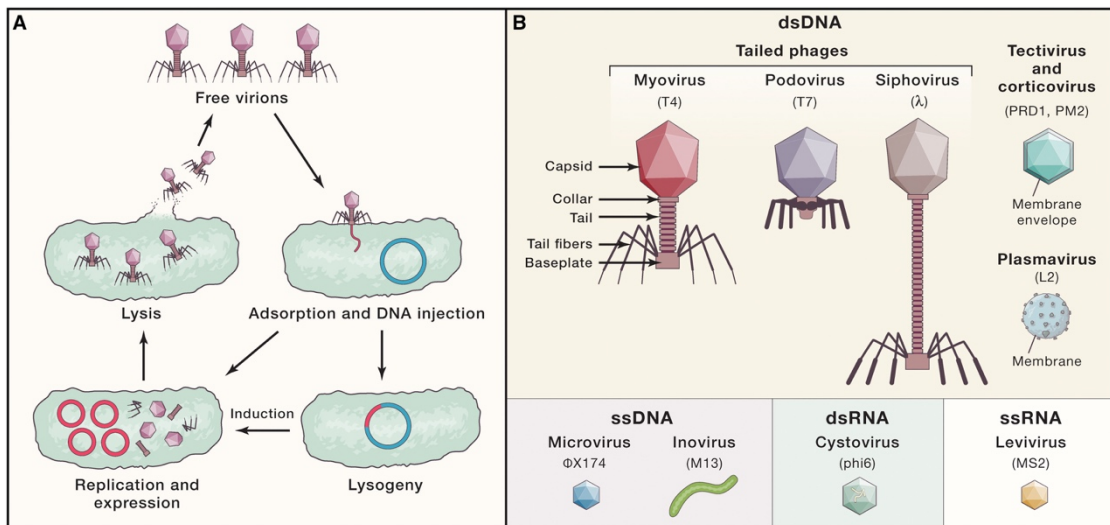


Figure 1.1 The life cycle and morphological classification of phages

Lytic versus lysogenic life cycles (A) and morphological diversity of phages (B)
Source: Ofir and Sorek, 2018

1.2.2 Phage life cycles

The life cycle of a phage determines how it interacts with a bacterial host, and can determine the influence of evolutionary interactions. Whilst some phages are strictly lytic (i.e. replicate and lyse the bacterial cell to release progeny; Figure 1.1A), other phages are able to adopt an alternative life cycle, termed lysogeny, where the phage DNA is incorporated within the host genome (Clokie et al., 2011). This lifestyle decision enables phage to minimise the risk of extinction if the chance of replication is reduced, for example, if there are multiple phage co-infecting one cell (Ofir and Sorek, 2018). Further, lysogeny can act as a bacterial regulatory switch, by disrupting bacterial gene expression at the insertion site, and relieving repression upon induction of phage replication (Ofir and Sorek, 2018). In contrast, filamentous phages (Inovirus, Figure 1B) are able to replicate without cell lysis as viral progeny is extruded from the bacterial cell (Ceysens

and Lavigne, 2010). Phage therapies therefore advocate the use of strictly lytic phages.

1.2.3 *Host ranges and other characteristics*

The nature of host attachment by recognition of cell surface receptors means that phages are often highly specialised to infect specific bacterial species, or even subsets of strains within a single bacterial species. However, there are examples of broad host range phages which can infect multiple bacterial species (Jensen et al., 1998), and of plasticity promoting expansion of host range (Ross et al., 2016). The global distribution of highly specialised phages may therefore be limited by the host distribution, and hence by host permissible environmental conditions. A global survey of phages infecting *Pseudomonas aeruginosa*, a ubiquitous bacterial species found in a diverse environments ranging from soil and aquatic ecosystems to human bacterial infections, found 15 novel and genetically distinct phages, with diverse morphological characteristics and genome sizes, yet highly overlapping host ranges (Ceysens et al., 2009). However, high levels of phage diversity can also occur within local geographical scales; a set of 83 phages isolated from the same urban sewage sample displayed variation in their tolerance to various stressors including pH, extremely high or low temperatures, organic solvents and detergents (Jurczak-Kurek et al., 2016).

1.3 **Phage resistance mechanisms and counter-defence strategies**

1.3.1 *The genetic basis of constitutive phage resistance*

The most basic form of resistance to phage infection is to prevent attachment to the bacterial cell by modifying cell-surface receptors to which phage adsorb (Bertozzi Silva et al., 2016; Rakhuba et al., 2010). Single nucleotide polymorphisms can sufficiently modify cell-surface receptors to prevent phage infection, and even provide cross-resistance to other phages targeting the same receptor (Betts et al., 2016a, 2018; Chan et al., 2016; Gurney et al., 2017). However, environmental context may modulate the degree of evolved surface modification, as complete receptor loss may impose much higher fitness costs with more complex environments, due to pleiotropic effects limiting nutrient acquisition, motility, and many other expressed traits (Bohannan et al., 2002; Cornforth et al., 2018; Scanlan et al., 2015a; Skurnik et al., 2013). Common phage adsorb targets include the Type IV pili, lipopolysaccharide (LPS) and TonB (Bertozzi Silva et al., 2016; Betts et al., 2016a, 2018), modification of which can

prevent twitching motility (Type IV pilus; Burrows, 2012), affect bacterial virulence (Type IV pilus and LPS; Cryz et al., 1984; Hahn, 1997; Lam et al., 2011), and prevent uptake of iron-siderophore complexes (TonB; Poole et al., 1996). Therefore alternative methods of modifying receptors, such as glycosylation, may be favoured to limit cost to the host (Harvey et al., 2018). Phage may counter-adapt to overcome surface modification by acquiring mutations in genes associated with host attachment, which also provides an evolutionary mechanism for host range expansion (Duffy et al., 2006). A more generalist mechanism of phage defence is the production of exopolysaccharides to mask cell-surface receptors (Labrie et al., 2010; Scanlan and Buckling, 2012). Whilst this mechanism can prove costly to the host (i.e. through investment in exopolysaccharide production), this type of defence mechanism can provide cross-resistance to other phages and antibiotics, and even protect bacteria from the host immune system (Hentzer et al., 2001; Leid et al., 2005). However, inevitably, phage counter-defence mechanisms do exist in the form of lytic enzymes which can degrade extracellular matrix (Davidson et al., 1977; Hanlon et al., 2001).

Restriction modification (RM) systems provide active phage defence and act by recognising and degrading foreign DNA, therefore they can provide a generalist mechanism of defence against phages and other mobile DNA. Host DNA is modified to prevent recognition by degradation complexes (Stern and Sorek, 2011), and as such is energetically costly. Even so, RM defence mechanisms are not infallible; if phage DNA is not degraded before the host enters a reproductive cycle, the phage DNA will be modified along with the host DNA, resulting in production of phage viruses which are able to avoid this resistance mechanism (Sneppen et al., 2015). Active phage counter-adaptation has also been identified ranging from DNA modification to avoid detection to more complex mechanisms such as co-injection of binding proteins along with phage DNA which sequester the restriction enzymes (Samson et al., 2013).

1.3.2 *Inducible resistance mechanisms and adaptive immunity*

Phage DNA can also be recognised and degraded by CRISPR-Cas systems (clustered regularly interspaced short palindromic repeats), which provide the bacterial host with adaptive immunity against phages and other mobile DNA (Horvath and Barrangou, 2010). CRISPR-based defence works by building up a library of fragments of foreign DNA within the CRISPR array, a process known as 'spacer acquisition', which are transcribed to produce short guide RNAs which

direct the CRISPR-cas complex to cleave matching DNA within the cell, thereby degrading invasive phage DNA (Barrangou et al., 2007; Marraffini, 2015). Thus, a bacterial host may acquire a diverse spacer library, providing adaptive immunity against a broad range of phages. Expression of this mechanism of phage defence is costly, but these costs are limited if expression is only induced upon phage infection (Westra et al., 2015). High nutrient levels can sustain constitutive expression of phage resistance mechanisms, whereas in low resource environments inducible mechanisms may limit unnecessary expenditure of energy if phage are not present (Westra et al., 2015). Phage can overcome CRISPR recognition by simple single point mutations to escape recognition by the spacer (Deveau et al., 2008). Active phage counter-defence mechanisms have also been identified, including the production of anti-CRISPR proteins which can inhibit DNA-binding and even modulate CRISPR activity to promote transcriptional repression (Bondy-Denomy et al., 2015).

Abortive infection (Abi) systems offer a last-ditch line of defence against phage infection for the bacterial population: programmed cell death can be triggered by phage components recognised within the bacterial cell resulting in cellular suicide of infected cells via a toxin-antitoxin mechanism (Dy et al., 2014). This limits phage reproduction and therefore protects the remaining susceptible bacterial population from phage infection. Phage mechanisms exist to defeat Abi mechanisms, and include production of phage anti-toxin molecules which bind the bacterial toxin component to prevent cell death (Samson et al., 2013).

1.3.3 *Novel anti-phage defence mechanisms*

Whilst the mechanistic basis of some phage resistance mechanisms are becoming well characterised (e.g., the RM and CRISPR-Cas systems), it is predicted that many mechanisms of phage resistance remain to be discovered (Koonin et al., 2017). For example, a potentially novel mechanism of resistance, termed BREX ('Bacteriophage Exclusion'), was recently discovered. Unlike the RM and CRISPR-Cas systems, BREX does not appear to work via cleavage or degradation of phage DNA, but rather blocks the replication of phage DNA (Goldfarb et al., 2015). Searching for new phage defence systems clustered nearby to known systems in bacterial genomes recently led to the identification of nine new mechanisms of anti-phage defence, and an additional anti-plasmid system (Doron et al., 2018). Clustering of phage defence systems on genomic islands may promote horizontal gene transfer, for example, the presence of RM systems correlates with high rates of genetic exchange (Koonin et al., 2017;

Oliveira et al., 2016), and many Abi systems are encoded on plasmids (Hoskisson and Smith, 2007; O'Driscoll et al., 2006). The wide taxonomic prevalence of CRISPR, with up to ~40% of bacterial genomes and ~ 90% of archaea containing CRISPR-like DNA repeats (Horvath and Barrangou, 2010), and on-going discovery of new phage defence mechanisms [e.g. BREX is present in ~10% of bacterial genomes (Goldfarb et al., 2015)], indicates an ancient origin of these mechanisms of phage resistance.

1.4 Network analysis as a tool to study evolutionary interactions

1.4.1 Bacteria-phage infection networks

The evolutionary trajectory of each member of a complex community is likely to be influenced by ecological interactions with other species (Barraclough, 2015). These interactions can be characterised using bipartite bacteria phage infection networks (BPINs), which are often visualised as a 2-dimensional matrix, where bacteria are represented on one axis, and phage on the other (Figure 1.2). These networks may contain quantitative information, such as the frequency or strength of observed interactions. Key network properties include connectance (i.e. the proportion of interactions which are realised), nestedness and modularity, which describe the population level structure of interactions, and robustness, which calculates the stability of the network in response to sequential loss of members (Dormann et al., 2008, 2009). The network structure provides information about the range of interactions and co-evolutionary dynamics which have shaped the bacteria-phage community, for example modularity describes the specialisation of the network. At one extreme end, each bacteria and phage have a specialised interaction (Figure 1.2: one-to-one), but more commonly this would resolve as modules of specialised interactions (Figure 1.2: modular) (Beckett, 2015; Weitz et al., 2013). Nested networks display a hierarchy of phage host range (i.e. specialist to generalist) on one axis and a hierarchy of bacterial resistance range on the other (Figure 1.2: nested) (Beckett, 2015; Weitz et al., 2013). Although nested-modular networks have been predicted in nature (Beckett and Williams, 2013), a comprehensive meta-analysis of 38 bacteria-phage studies, revealed that nested structures predominate (Flores et al., 2011).

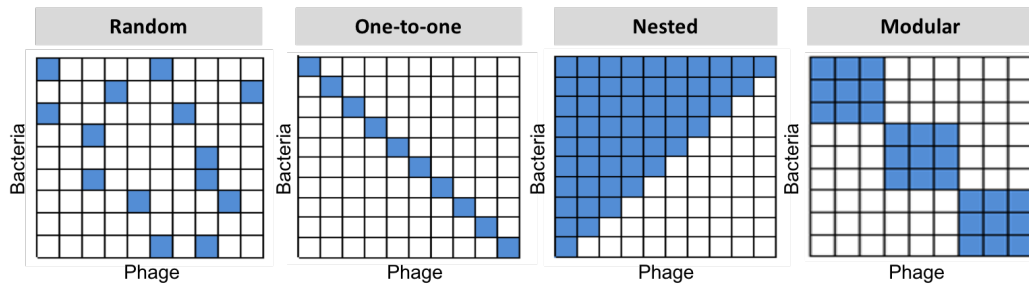


Figure 1.2 Characterising the network structure of bacteria-phage infection networks

Each matrix indicates a different potential structure of a bacteria-phage community. Each column designates one phage strain, and the coloured boxes indicate host range as the number of different bacteria (rows), which the phage can infect.

1.4.2 Using interaction structure within a community to distinguish background dynamics

Identifying all of the interacting species within a bacteria-phage community can reveal the signature of the coevolutionary dynamics which have shaped the population structure to date (Weitz et al., 2013). The directionality of ARD means that each novel mutation providing further resistance or infectivity is added to the previous background, and so resistance or infectivity ranges increase as ARD proceeds. This means that within a population there will exist a hierarchical structure where each genotype present is a subset of a more generalist genotype, which is one step further down the coevolutionary race. Using bipartite networks to visualise bacteria-phage interactions in a population undergoing ARD demonstrates this hierarchy as a nested pattern (e.g. Figure 1.2) where interaction range for each bacteria or phage is nested within a more generalist pattern.

The network signature of FSD is more complicated to characterise; as only the most abundant bacteria are targeted, numerous genotypes may co-exist and if each independently co-evolves against specialised phages, each interaction would have its own evolutionary trajectory potentially forming their own hierarchy of genotypes as they diversify. Therefore, separate modules may develop where bacteria and phage specialise to resist/infect one another, and genotypes within each module may form a nested structure of resistance/infectivity range. Therefore, a modular nested bacteria-phage infection network would be observed (Beckett and Williams, 2013). However, this same pattern could theoretically be

achieved by ARD on a multi-species level if bacteria-phage interactions are species specific.

1.4.3 *Community structure can determine robustness of microbial communities*

The degree of connectivity within a community can also help us assess the robustness of a community to changes in the environment, or invasion by novel competitors or parasites. For example, highly modular networks may be more stable, as collapse of a single module will not necessarily influence the surrounding community, whereas changes to a hierarchical nested structure could have a domino effect, such that loss of one member could destabilise the whole community (Thébault and Fontaine, 2010). As such, key community members may create network 'hubs' which, if lost, could have wide-reaching collateral effects on connected species (Agler et al., 2016). By understanding the genetic interactions which shape a community, it may therefore be possible to predict how communities would respond to change, and how diverse bacterial infections may respond to treatment.

1.5 A model system to study the effect of phage therapy

1.5.1 *Pseudomonas aeruginosa – a multi-drug resistant pathogen*

Numerous mechanisms of antimicrobial resistance exist which can limit the success of antibiotic treatments, including efflux pumps, target modification and enzymes which bind and degrade the drug (Blair et al., 2015). These resistances are commonly encoded on mobile elements, such as plasmids, and multiple different resistances can be clustered together to form resistance 'cassettes', promoting the spread of multi-drug resistance by horizontal gene transfer (Alekhun and Levy, 2007; Bennett, 2008; Reece and Phillips, 1995). Encoding antibiotic resistance determinants can increase the fitness of bacterial pathogens even at low, environmental, concentrations of antibiotics (Bottery et al., 2016) which further promotes the spread of resistance.

Pseudomonas aeruginosa is an opportunistic pathogen, which commonly colonises burn wounds and the lungs of cystic fibrosis (CF) and bronchiectasis patients (Driscoll et al., 2007). It is associated with very high occurrence and range of antibiotic resistance, with some strains displaying pandrug resistance to all antibiotics in current use, due to a combination of both chromosomal and plasmid-encoded resistance mechanisms (Breidenstein et al., 2011; Lister et al., 2009; Livermore, 2002).

1.5.2 *The complexity of interactions within a clinical infection may influence therapy success*

The interaction between biotic and abiotic factors could be an important consideration for phage therapy, as many pathogens, such as *P. aeruginosa*, are commonly contracted from environmental reservoirs rather than from patient-patient contact (Rogues et al., 2007; Trautmann et al., 2005). As such, evolution in the environmental niche, which is influenced by both abiotic conditions and biotic interactions in the presence of both lytic and lysogenic phage strains as well as protist predation and inter-specific competition, has major consequences for the evolutionary strategies adopted during human infection (Friman et al., 2009). Treatment may therefore be hindered by bacterial evolutionary adaptation. In chronic infections, such as that of the CF airways, *P. aeruginosa* undergoes evolutionary diversification leading to a genetically diverse population adapted to the local environment which is difficult to eradicate, often persisting over numerous years (Burns et al., 2001; Conrad et al., 2013; Winstanley et al., 2016). Once within the CF lung, whilst the environment provides a rich nutrient source there are numerous new challenges, including defending against host immune response and antibiotic treatments (Smith et al., 2006). Most CF patients undergo intensive antibiotic therapy from a very young age, and whilst this appears to clear intermittent infections, this commonly only delays the development of chronic infections (Burns et al., 2001; Frederiksen et al., 1997). The respiratory system provides a range of compartmentalised environments, each with distinct abiotic characteristics; the paranasal sinuses have been suggested to provide a niche in which bacteria are protected from both antibiotics and immune responses enabling the pathogen to re-colonise the remainder of the respiratory system following antibiotic treatment, eventually forming a chronic infection (Folkesson et al., 2012). Therefore, the potential for use of phage therapy could be greatly influenced by the heterogeneity within an infection, in terms of the localised differences in pathogen virulence and susceptibility in response to varying selection pressures, which develop as bacteria adapt and diversify (Harrison, 2007; Winstanley et al., 2016).

1.5.3 *Using phage to combat P. aeruginosa infections*

Due to high rates of antibiotic resistance in *P. aeruginosa* the possibility of using phage therapy to combat these infections has recently been revisited. Phage cocktails have proven to be highly effective in suppressing the growth of *P. aeruginosa in vitro*, performing better than individual phage strains (Betts et al.,

2016a, 2018), and although rates of evolved resistance were similar, the strength of resistance increased with parasite diversity as the rate of host adaptation accelerated (Betts et al., 2018). However, pre-adapting phages to evolved host resistance has been shown to improve their efficacy against this pathogen, and constrain the evolution of resistance (Betts et al., 2013; Friman et al., 2016). Further, phage cocktails have been shown to cure otherwise lethal *P. aeruginosa* infections in waxmoth models (Hall et al., 2012), and eliminate this bacterium in tissue cultures of biofilm-forming CF airway cells (Alemayehu et al., 2012). The potential use of phages to prevent biofilm formation in medical devices has been explored using an *in vitro* model using hydrogel-coated catheters, and showed promising results, which were maximised by using phage cocktails over single phage strains (Fu et al., 2010). In addition to these promising *in vitro* results, a number of studies have shown that phages can effectively treat *P. aeruginosa* infections within various models of disease within mice, including lung infections (Morello et al., 2011; Waters et al., 2017), burn wounds (McVay et al., 2007), and gut-derived septicaemia (Watanabe et al., 2007). These studies also demonstrate simple and successful methods of phage therapy administration, for example, nasal inhalation of phage products was sufficient in the murine lung model (Waters et al., 2017) and oral administration was used in the murine gut-disease model (Watanabe et al., 2007).

1.5.4 Phage adsorption targets of *P. aeruginosa*

Determining the cell-surface receptors which are recognised by phage to allow adsorption is important in understanding the potential for bacteria to evolve resistance by surface modification. Two common targets on the membrane of *P. aeruginosa*, which are commonly mutated in the presence of phages, include the Type IV pilus and Lipopolysaccharide (LPS) (Betts et al., 2016a; Gurney et al., 2017).

Type IV pili are protein structures which adhere to surfaces, extend and retract to allow twitching motility, and are important in biofilm formation, hence Type IV pili have a fundamental role in colonisation of new hosts, and therefore modification of these structures may attenuate bacterial virulence (Figure 1.3; Burrows, 2012). Due to the complex protein structure of the Type IV pilus, consisting numerous protein subunits which act together mechanically, and the further genes involved in biosynthesis and regulation of pilus expression (Mattick et al., 1996), there are a vast number of genetic targets which can influence the structure of the Type IV

pilus resulting in a wide variety of phenotypes ranging from complete loss to hyperpiliation (Chiang and Burrows, 2003). Further, phage attachment to Type IV pilus can also be deterred by glycosylation of the pilus structure (Harvey et al., 2018).

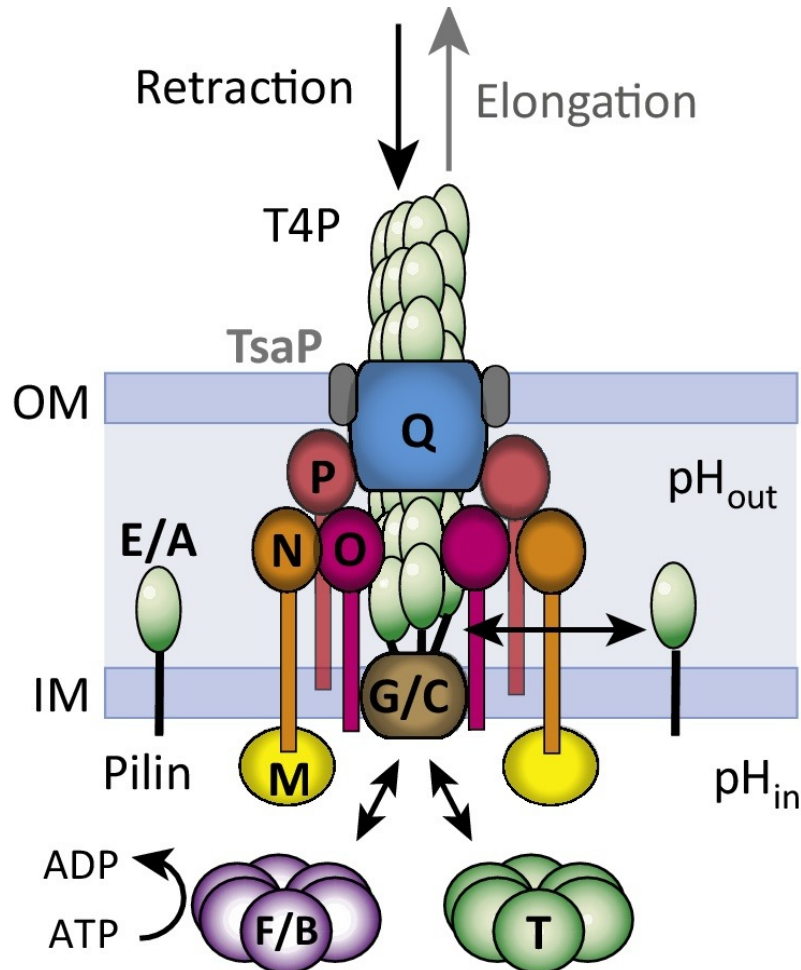


Figure 1.3 Structure of the Type IV pilus

Multiple subunits of the protein PilA form the major pilin which is inserted into the bacterial membrane through a pore formed by PilQ. Extension and retraction of the major pilin is co-ordinated by the motor proteins PilB and PilT. Figure adapted from Maier and Wong, 2015.

Lipopolysaccharide (LPS) is also an important virulence factor of *P. aeruginosa* as a target for the human immune system, and therefore has evolved a variable structure such that one bacterial cell may present multiple different variations of LPS (Figure 1.4; Lam et al., 2011). LPS is composed of three main sections: lipid A anchors the structure to the bacterial membrane and is attached to the core oligosaccharide to form the uncapped LPS (Figure 1.4, far left), which can then

be capped by a variable O-antigen structure composed of A- and B-bands (King et al., 2009). The mutation of specific LPS biosynthesis genes may prevent biosynthesis of individual variations whilst maintaining other forms within the cell, with the most drastic mutations leading to loss of all but the uncapped LPS (Figure 1.4, $\Delta wbpL$; Lam et al., 2011).

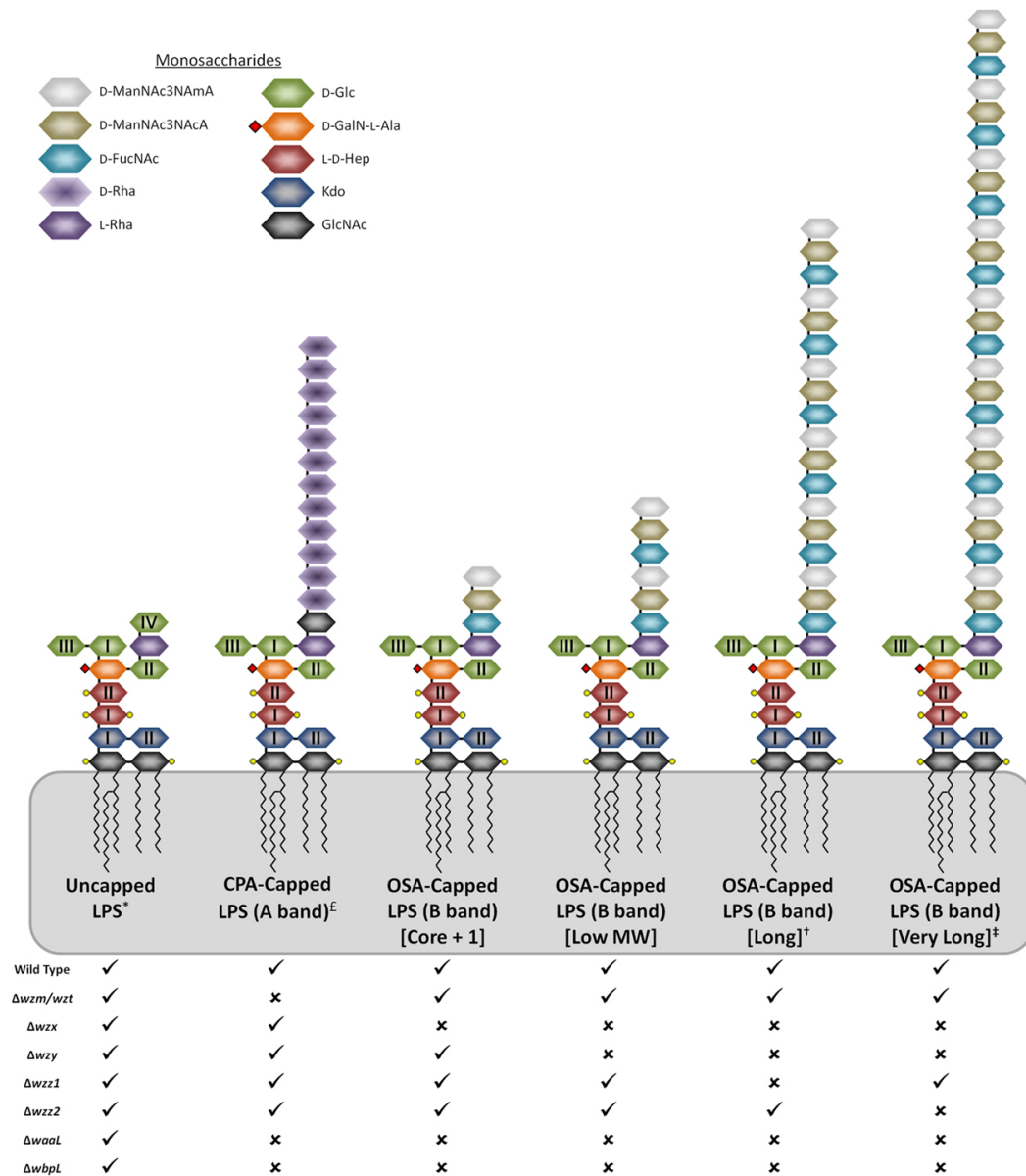


Figure 1.4 Diversity of lipopolysaccharide structures which may be displayed on one bacterial cell

Structural diversity of LPS within one bacterial cell is achieved by variation in the O-antigen structure which caps the core LPS. Mutation of biosynthesis genes can limit the diversity of LPS structures displayed; (✓) indicates presence and (X) indicates the absence of each structure across a range of genotypes. Figure adapted from Lam et al., 2011.

1.6 Is phage therapy a realistic alternative to antibiotics?

1.6.1 *Historical and current use of phage therapy*

The therapeutic use of phages to treat antibiotic infections dates back to the 1920s, where Felix d'Herelle experimented with phage treatments against bacterial dysentery in Paris, and later developed the first commercially available phage cocktails (Pirnay et al., 2012). Whilst the western world turned its back on phage therapy as a lack of scientific understanding of phage biology led to expansive and unfulfilled claims about the effectiveness of phage treatments and antibiotics were discovered, phage therapy has been continually used in eastern Europe for over 60 years (Monk et al., 2010). The Eliava Institute in Georgia have developed an expansive collection of phages, frequently replenishing these stocks from environmental samples, which is screened against specific pathogenic strains to develop cocktails of multiple phages, some of which are available over-the-counter (Kutter et al., 2010; Pirnay et al., 2012). These combinations may be highly diverse, targeting as many as 23 different bacterial strains (Kutter et al., 2010). This methodology allows rapid adaptation of therapeutics in response to the evolution of resistance, which is further enhanced by 'training' phages against problematic bacterial strains (Pirnay et al., 2012). In fact, two of the phage products first designed by d'Herelle (*pyophage* and *intestiphage*) are still in use in Georgia today; this is achieved by regular testing (every 6 months) against bacterial strains in current circulation which allows the phage formula to be continually updated to maintain efficacy (Kutter et al., 2010). In contrast to the use of commercially available diverse phage cocktails in Georgia, the Hirszfeld Institute in Poland promote the use of personalised phage therapeutics, selected from a phage bank against patient-specific bacterial strains and implemented either as individual phages, or combinations (Kutter et al., 2010). These practices allow rapid isolation and implementation of new therapeutic products in response to the evolution of resistance, however, these methodologies are generally incompatible with pharmaceutical regulations in western Europe and the USA, where Good Manufacturing Practice (GMP) requires extensive testing, clinical trials for each component and interaction within a medicinal product (Pirnay et al., 2012).

1.6.2 *Evolutionary hurdles for phage therapy*

Before it can be employed routinely, there are a number of considerations in the use of phage therapy that must first be addressed. Firstly, phage have co-evolved

with bacteria for millions of years and as such, many bacterial resistance mechanisms are present to resist phage infection (see section 1.2), therefore even weak resistance may prevent phage from completely clearing a bacterial infection. A better strategy may be to use phage to re-structure microbial communities or reduce pathogen virulence (León and Bastías, 2015), so that either multiple phage in combination or the combined use of phage with antibiotics could together eradicate a bacterial infection (Chan et al., 2016; Schmerer et al., 2014). Secondly, much more research is needed to fully understand the pharmacology of phage infection, i.e. how phage are influenced by the patient's immune system (pharmacokinetics) and how the body reacts to phage (pharmacodynamics) (Abedon, 2014; Abedon and Thomas-Abedon, 2010). For example, can auto-dosing (i.e. relying on phage to self-propagate; Abedon and Thomas-Abedon, 2010; Loc-Carrillo and Abedon, 2011) provide sufficiently high phage titres to clear an infection? On the other hand, the patient's immune system may be required to clear even phage-sensitive cells from the infection site (Roach et al., 2017). Finally, it is important to realise that bacterial infections are not clonal populations in which every individual will respond identically to the treatment, but diverse, often multi-species, communities, and treat them as such (Levin and Bull, 1996). The evolution of resistance to phage therapies is unavoidable, however, if we can understand how and why different resistance mechanisms are selected, perhaps we can rationally design phage-based therapies to limit the evolution of broad resistances.

1.6.3 *Rational design of phage therapeutics*

Maximising host range is important to enable treatment of diverse bacterial genotypes and even multiple species, therefore the isolation of broad-spectrum phages using multiple hosts (Ross et al., 2016), and continued characterisation of novel phages (Amgarten et al., 2017; Ceysens et al., 2009; Sepúlveda-Robles et al., 2012), is an important factor in optimising phage treatments. However, current strategies in the development of phage cocktails are often based solely on maximising the host range targeted (e.g. Ross et al., 2016), commonly taking only the most virulent and generalist phage available against each target species, and do not take into account many of the fundamental aspects of bacteria-phage coevolution within a community context. This is in part due to the lack of simple experimental mechanisms of characterising interactions between multiple phage species, a gap in knowledge which is being filled by the use of bacteria-phage infection network (BPIN) analysis (e.g. Gurney et al., 2017). This tool will

hopefully enable rational design of phage cocktails to test the importance of multiple factors such as between-phage interactions and complementation of specialist and generalist phage infection strategies.

Limiting the evolution of resistance is, fundamentally, one of the most promising ways to prolong durability of phage treatments. One way of tackling this issue is to pre-adapt phages to the possible mechanisms of host-resistance which may arise during treatment (Betts et al., 2013; Friman et al., 2016; Kelly et al., 2011). Alternatively, maximising differences in selection pressures imposed by combined treatments, either as multiple phages targeting different receptors (McCallin et al., 2013; Tanji et al., 2004; Yen et al., 2017), or by combining phages with antibiotics (Torres-Barceló and Hochberg, 2016), could limit the resistance options available to the host. This works in two ways; firstly, by limiting mutation frequency as the chance two resistance mutations targeting distinct receptors occurring in the same cell is lower than if only one mutation is required, and secondly, by maximising fitness costs to the host. Cumulative fitness costs and in particular negative epistasis between individual resistance mutations can limit the potential for accumulation of multiple resistances, or result in a trade-off in resistance strength to multiple phages if phage-specific mutations interact negatively (Bohannon et al., 2002; Koskella et al., 2011; Scanlan et al., 2015a).

With the emergence of pandrug resistance [PDR; i.e. non-susceptibility to all classes of antibiotics (Sweeney et al., 2018)], there is growing interest in combination therapies, whereby multiple antibiotics, or phage-antibiotic combinations, are employed with the idea that resistance is harder to evolve against multiple targets at once (Baym et al., 2016; Torres-Barceló and Hochberg, 2016). The evolution of resistance to antibiotics commonly results in cross resistance, but can also cause collateral sensitivity, as strengthening one resistance trades-off against a second (Pál et al., 2015). By mapping these collateral effects using network analysis, it is possible to design treatment combinations, or sequential cycles, which can limit the evolution of cross-resistance, and optimise collateral sensitivity (Baym et al., 2016; Imamovic and Sommer, 2013). Sequential application of antibiotics has shown promising results, with the development of treatment cycles which limit the evolution of collateral resistance and promote sensitivity to further treatment (Imamovic and Sommer, 2013). However, comparison of simultaneous and sequential phage treatments showed that whilst sequential phage treatments may be as effective as simultaneous ones, exposure to phage cocktails promoted the highest

decreases in bacterial density (Hall et al., 2012). Further work is required to determine how these principles should be best employed to optimise the rational design of phage treatments.

1.6.4 *Clinical trials of phage therapy*

The use of phage therapy in the treatment of *P. aeruginosa* infections has been widely studied and has even progressed to clinical trials in human patients. Topical use of phage suspensions has been shown to clear *P. aeruginosa* infections within skin grafts of burns victims (Sivera Marza et al., 2006). A six-phage cocktail (Biophage-PA), reduced clinical indicators of disease in chronic infections of the ear (otitis) involving antibiotic-resistant *P. aeruginosa* (Wright et al., 2009). Phage cocktails can also be developed to treat multi-species infections, such as combinations of *P. aeruginosa* and *Staphylococcus aureus* within burn wounds; the safety of one such cocktail, BFC-1 (Merabishvili et al., 2009), has been demonstrated in a small clinical trial in Belgium, but the efficacy of the cocktail was undetermined (Rose et al., 2014). Clinical trials can be limited by a range of factors, and often by a failure to recruit patients due to regulatory constraints on recruitment and variable incidences of disease (Sybesma et al., 2018). One such trial which has encountered these issues involves the phage cocktail Phagoburn, which is designed to target *P. aeruginosa* and *Escherichia coli*; the trial was completed in 2017, and full results are expected to be published soon (Servick, 2016; <http://www.phagoburn.eu/>). Phage therapy has also been implemented in numerous individual cases, many with successful outcomes, under the Declaration of Helsinki (Verbeken et al., 2007), which allows the use of phage therapy when no other therapeutic options exist. For details of additional clinical trials currently in progress, and reports of individual case studies implementing phage therapy, see Sybesma et al, (2018).

1.6.5 *Regulatory challenges facing phage therapy approval*

There are a number of regulatory hurdles which must also be considered to allow implementation of phage therapy across the EU. Firstly, despite widespread use of phage therapy for nearly 100 years across Eastern Europe, there are only a limited number of clinical trials which have run to completion, leading to concerns about the safety of phage therapy (Pirnay et al., 2015; Sybesma et al., 2018), although as mentioned above, no adverse responses have been recorded to date from clinical trials in progress (section 1.5.4). Secondly, the current European framework for production of medicinal products imposes heavy restrictions on the

production of phage therapeutics, requiring the same good manufacturing practices as other medicinal drug production (Sybesma et al., 2018). However, this limits the potential for personalised cocktails to be prepared and imposes time delays on processing of novel phages and pre-adapting stock phages to resistant genotypes in current circulation. An alternative regulatory framework is under development in Belgium, through which phage therapies can be considered as a 'Magistral preparation', which would allow phage preparations to be tailor-made to meet the requirements of individual patients within a hospital pharmacy (Pirnay et al., 2018). This suggests that any principles of rational design which can simplify the production requirements for phage therapy would greatly simplify the regulatory process of phage production.

1.7 Thesis outline

This thesis explores how the structure of bacteria-phage interactions, and the underlying gene-gene interactions, influence the evolution of phage resistance. Firstly, I used bacteria-phage infection networks to characterise the changes in community structure through time to determine the abiotic factors which influence the evolution of phage resistance and constrain bacteria-phage co-existence (Chapter Two). Next, I defined how genetic interactions may underpin bacteria-phage community structure by determining how resistance evolution creates modular cross-resistance networks based upon adsorption receptor modification (Chapter Three). By contrasting the evolution of resistance against phage pairs applied either simultaneously or sequentially, I found that these different modes of selection influence the strength and cost of evolved resistances (Chapter Four). Finally, I assessed the effect of phage diversity, and the potential influence of cross-resistance structure, on the efficacy of phage combinations, (Chapter Five). These data provide valuable insight into the mechanisms of resistance evolution which influence the efficacy of phage therapies, which I expand upon in Chapter Six to discuss the potential implications for the rational design of phage therapies.

Chapter Two

Ecological conditions determine extinction risk in co-evolving bacteria-phage populations¹

2.1 Introduction

Microbial communities are subject to a broad range of biotic and abiotic selection pressures and are capable of rapid evolutionary change in response (Barraclough, 2015). Antagonistic interactions, such as between bacteria and bacteriophages (phages), in particular drive continuous evolutionary change through recurrent cycles of adaptation and counter-adaptation, known as Red Queen coevolution (Brockhurst et al., 2014; Koskella and Brockhurst, 2014; Van Valen, 1973). This process may be driven by directional selection favouring ever broader ranges of resistance and infectivity achieved by recurrent selective sweeps [Arms Race dynamics (ARD) (Lenski and Levin, 1985)], or proceed by sustained allele frequency oscillations driven by negative frequency-dependent selection [Fluctuating Selection dynamics (FSD) (Levin et al., 1988)]. The stability of coevolutionary interactions relies upon interaction symmetry, both in terms of the selection acting upon each partner and correspondingly their potential for adaptation (Brockhurst et al., 2014). Failure of either partner to adapt quickly enough could result in their extinction (Smith, 1976). Host-parasite communities are vulnerable to host extinction through failure to evolve resistance against increased parasite virulence (Rafaluk et al., 2015), whereas parasite extinction could result from either an inability to overcome evolved host resistance (Zhang and Buckling, 2016), or via extinction of the host. The risk of extinction may be dependent on the pattern of coevolutionary dynamics, which have been shown to vary depending on ecological conditions (Gómez and Buckling, 2011; Lopez Pascua et al., 2014). Strong directional selection under ARD coevolution may exacerbate asymmetries in evolutionary potential between the coevolving partners [e.g. phage infectivity evolution requires more mutational steps than reciprocal bacterial resistance evolution (Buckling and Brockhurst, 2012)] driving the more constrained partner to extinction. We are interested here in how

¹ Wright, R.C.T., Brockhurst, M.A., and Harrison, E. (2016). Ecological conditions determine extinction risk in co-evolving bacteria-phage populations. *BMC Evolutionary Biology*. 16, 227.

ecological context, and associated abiotic selection pressures, influences the risk of coevolution-induced extinction.

Although not extensively investigated, recent studies suggest that abiotic environmental conditions can affect coevolution-induced extinction risk (Gómez et al., 2015b; Zhang and Buckling, 2011, 2016). Phage adapting to deteriorating thermal conditions, for example, were able to adapt to thermal stress when their bacterial host was held in evolutionary stasis, but were driven to extinction in the presence of co-evolving hosts (Zhang and Buckling, 2011). Additional selection from gradually increasing temperatures, to which phage are far more sensitive, constrained the phage's ability to adapt to increased bacterial resistance, leading to extinction of the phage population (Zhang and Buckling, 2011). Imbalanced antagonistic coevolution can therefore increase the extinction risk for phage populations, however it is unclear how this varies with the intensity of coevolution. Numerous ecological factors are known to alter the strength of reciprocal selection driving bacteria-phage coevolution. Increasing resource supply, by supporting larger population sizes, increases bacteria-phage encounter rates (Lopez-Pascua and Buckling, 2008), and has been shown to drive phage extinction in both liquid media (Zhang and Buckling, 2016) and in soil (Gómez et al., 2015b). However, the effects of nutrient enrichment go beyond demography; increased resource availability reduces the fitness costs associated with host resistance (Zhang and Buckling, 2016). There is a documented trade-off between bacterial resistance and growth rate (Scanlan et al., 2015a), which is fundamental to the maintenance of diversity in microbial communities, by preventing highly competitive and resistant host strains from dominating the population (Jessup and Forde, 2008). The allocation of this trade-off varies across environmental conditions; when resource availability is high more energy can be allocated to resistance mechanisms (Boots, 2011), effectively reducing the fitness costs associated with bacterial resistance. Therefore, it is challenging to distinguish the impact of intensity of coevolution from the effect of reduced fitness costs in driving phage extinction in nutrient enriched conditions.

Population mixing (Brockhurst et al., 2003) accelerates coevolution in a similar way to increased resource availability (Lopez-Pascua and Buckling, 2008); increased bacteria-phage encounter rates strengthen reciprocal selection for the evolution of increased resistance and infectivity in bacteria and phage populations respectively. However, whereas increased resource availability mitigates the

fitness costs associated with bacterial resistance (Lopez-Pascua and Buckling, 2008; Zhang and Buckling, 2016), population mixing does not. In contrast, unmixed populations experience reduced encounter rates due to the development of spatial and temporal host refuges against phage infection (Schrag and Mittler, 1996).

In this study, we explore how two ecological variables altering the intensity of bacteria phage coevolution, population mixing and resource level, affect the extinction risk of coevolving bacteria-phage populations in the *Pseudomonas fluorescens* SBW25 – lytic phage SBW25 ϕ 2 model system (Brockhurst et al., 2007). We predicted that environments supporting more intense coevolution, i.e. well-mixed, high resource supply environments, would be those most likely to drive coevolution-induced extinction. To test this hypothesis, we experimentally coevolved replicate bacteria-phage populations by serial transfer under high or low resource supply, with or without population mixing in a full factorial experimental design and monitored population densities of each species over time.

2.2 Materials and Methods

2.2.1 Culture techniques

All cultures were grown in microcosms (30 ml glass universal bottles with loose fitting plastic lids) containing 6ml of either high or low nutrient level media. Low nutrient level was obtained by 100-fold dilution of standard (high resource level) King's Media B (KB) into M9 salt solution. Cultures were grown at 28°C in either a static incubator or orbital shaker set to 200rpm for 1min in every 30min (mixed treatment). Cultures were propagated by serial transfer, sub-culturing 1 percent into fresh media every 48h, for twenty transfers.

2.2.2 Experimental design

Four treatments were established consisting of high and low resource levels with mixed and static environments of each. Independent clones of *P. fluorescens* SBW25 and bacteriophage SBW25 ϕ 2 were isolated and used to found 24 replicate populations (4 treatments x 6 replicates). Each replicate microcosm was inoculated with 10^8 *P. fluorescens* SBW25 cells and 10^6 SBW25 ϕ 2 particles. Bacteria and phage densities were calculated every second transfer; bacterial

density as colony forming units (CFU/ml) by plating diluted cultures on KB agar plates, and phage density as plaque forming units (PFU/ml) by plating a serial dilution of filtered culture on a soft agar lawn of ancestral bacteria.

2.2.3 Sampling techniques

At every second transfer whole population samples, phage populations and 20 individual bacterial clones were isolated and stored at -80°C in glycerol solution (20%). Phage populations were obtained by filtration (0.22µm filters) to remove bacteria.

2.2.4 Resistance and infectivity profiles approaching phage extinction

To investigate the mechanism of phage extinction in low resource level treatments, we characterised bacterial resistance and phage infectivity levels within each population approaching the phage extinction time point. The transfer at which early phage extinction events were most common was designated as the 'extinction time point' (T=4 for low static; T=6 for low mixed), and the previous sampling point as the 'pre-extinction time point' (T=2 for low static; T=4 for low mixed). Twenty phage clones per replicate were isolated from phage population glycerol stocks of the pre-extinction time point by plating phage filtrate on 0.8% agar containing exponentially growing ancestral bacteria. The twenty bacterial clones from each low resource level replicate at the pre-extinction time point (henceforth 'contemporary bacteria') and at the extinction time point (henceforth 'future bacteria') were each assayed for resistance against their respective pre-extinction phage set.

Assays were performed in 96 well microtitre plates containing standard concentration of KB media in M9 salts for all treatments. Phage were added at a density approximately 10 times higher than bacterial density (multiplicity of infection, MOI = 10). The absorbance at 600nm was measured at t=0 and t=20h to give a relative bacterial growth rate (RBG) (Poullain et al., 2008) compared to a control in the absence of phage, given by equation 1.

For phage *i*, bacteria *j*:

$$RBG_{ij} = \frac{[Abs_{600}(t=20) - Abs_{600}(t=0)]_{ij}}{[Abs_{600}(t=20) - Abs_{600}(t=0)]_{controlj}} \quad (1)$$

The threshold for binary infection outcome was calculated by modelling a normal distribution over the resistance peak of the RBG distribution and taking the 95% confidence interval (RBG=0.781). The proportion of possible pairwise interactions within each replicate population (20 bacteria clones x 20 phage clones = 400 possible interactions) that resulted in infection (RBG<0.781), describes qualitative population-level susceptibility. This is referred to (e.g. Figure 2.3) as the 'Proportion of realised interactions'. Link strength (1-RBG) of realised interactions measures quantitative susceptibility at the individual level, such that 0 describes completely resistant bacteria and 1 completely susceptible bacteria.

2.2.5 Statistical analysis

Phage extinction was analysed using a survival model (fitted to a parametric Weibull distribution) on the time of extinction taken as the time point phage became undetectable in each replicate, with censoring to account for phage populations which survived the entire experiment. Analysis of the bacterial densities over time was performed using a generalised least squares (GLS) linear model with auto-correlation over time within replicates on \log_{10} transformed CFU values. In this model, time, presence or absence of phage, nutrient level and mixing status were given as fixed effects. Individual linear mixed effect models were made for both population-level (proportion of realised interactions) and individual-level (link strength) susceptibility as the response variable, fitting mixing, phage extinction status and bacterial time point (contemporary or future) as interacting fixed effects, and replicate population as a random effect. Tukey post hoc testing was used to isolate the drivers of significant main effects.

2.3 Results

Out of six replicate populations per treatment, phage extinction was observed in all low resource replicates under population mixing and half of those in static conditions. Phage extinction was less common in high resource conditions, with only one extinction event in static conditions, and three out of six replicates in mixed populations (Figure 2.1). The likelihood of phage extinction was increased by low resource levels and population mixing (survival model: resource level $Z=-2.59$, $p=0.00954$; population mixing $Z=-2.28$, $p=0.0226$). There was no significant interaction between these two treatments (survival model: interaction between resource and mixing $Z=0.106$, $p=0.915$); the individual effects were additive to

give the highest likelihood of phage extinction in the low resource, mixed environment. In contrast, no bacterial population extinctions were observed. Bacterial population densities were approximately 4-fold higher in high compared to low resource environments whilst population mixing had a small effect, increasing bacterial density by approximately 45% (GLS: high resource $t=9.83$, $p<0.0001$; mixing $t=2.36$, $p=0.0185$; Figure 2.2).

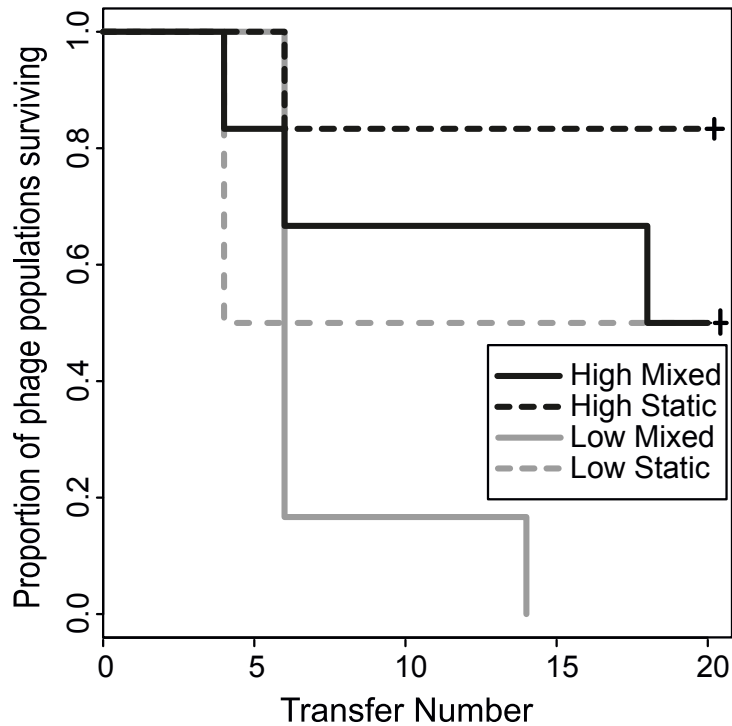


Figure 2.1 Survivorship of phage replicate populations through time is determined by treatment conditions

Survivorship is given as the proportion of replicate populations within each treatment in which phage are present at each transfer. Phage populations were judged to be extinct if phage were undetectable by plating undiluted filtrate of the respective replicate population.

Extinction events occurring in low resource populations were further investigated by estimating the susceptibility of bacterial populations to infection by phage clones from their sympatric populations approaching the extinction time points. Bacterial susceptibility was characterised by two distinct measurements. Firstly, population-level susceptibility is described by the proportion of realised interactions on a scale from 0, where all bacteria sampled are resistant to infection from all phage sampled, to 1, indicating all bacteria were susceptible to all phage

(i.e. ancestral level susceptibility). The second metric, link strength, gives an estimate of the mean quantitative susceptibility of bacteria, measured as the reduction in bacterial growth caused by phage infection, for each replicate population. We observed high levels of resistance to phage from the pre-extinction time point in contemporary (pre-extinction) bacteria irrespective of whether phage subsequently survived or became extinct (Figure 2.3A-B). There was no difference in the proportion of realised interactions between bacterial sampling points for extinction populations (Figure 2.3A; PRI Tukey $p=0.9036$).

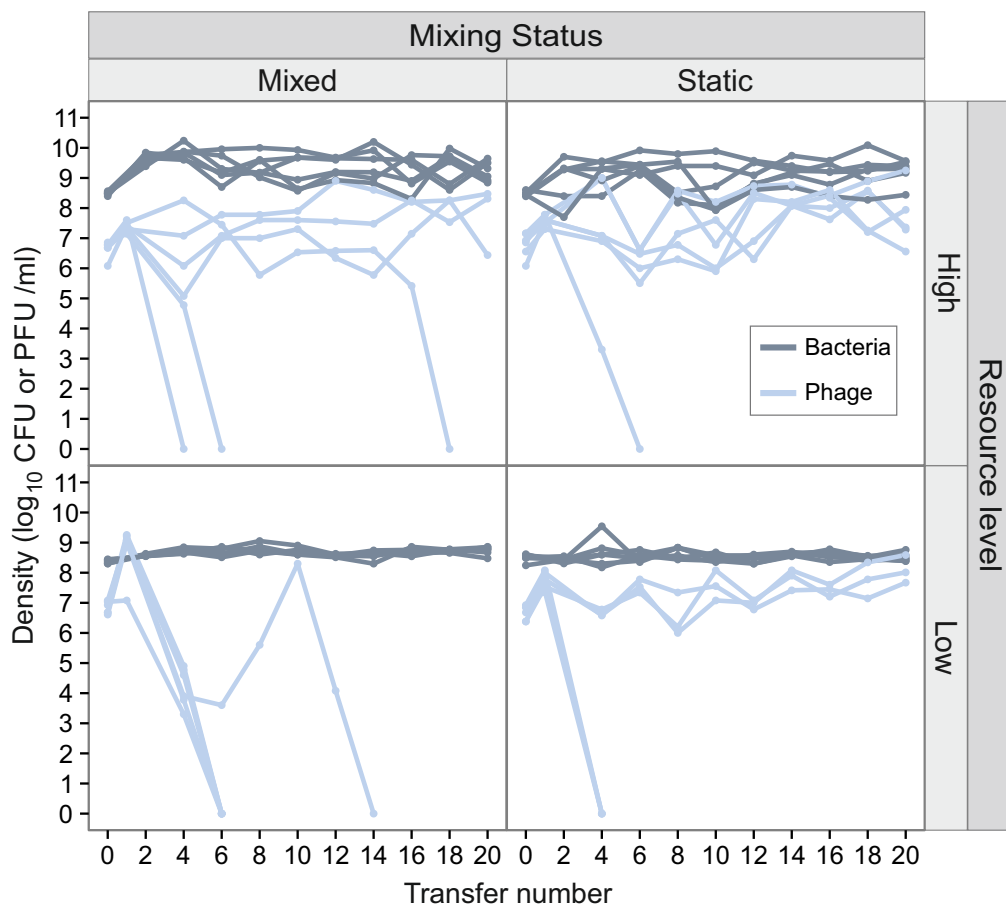


Figure 2.2 Contrasting density profiles over time for bacteria and phage populations

Phage densities (blue) denote plaque forming units (PFU/ml) and bacterial densities (red) are colony forming units (CFU/ml). Different lines represent the 6 replicate populations within each treatment.

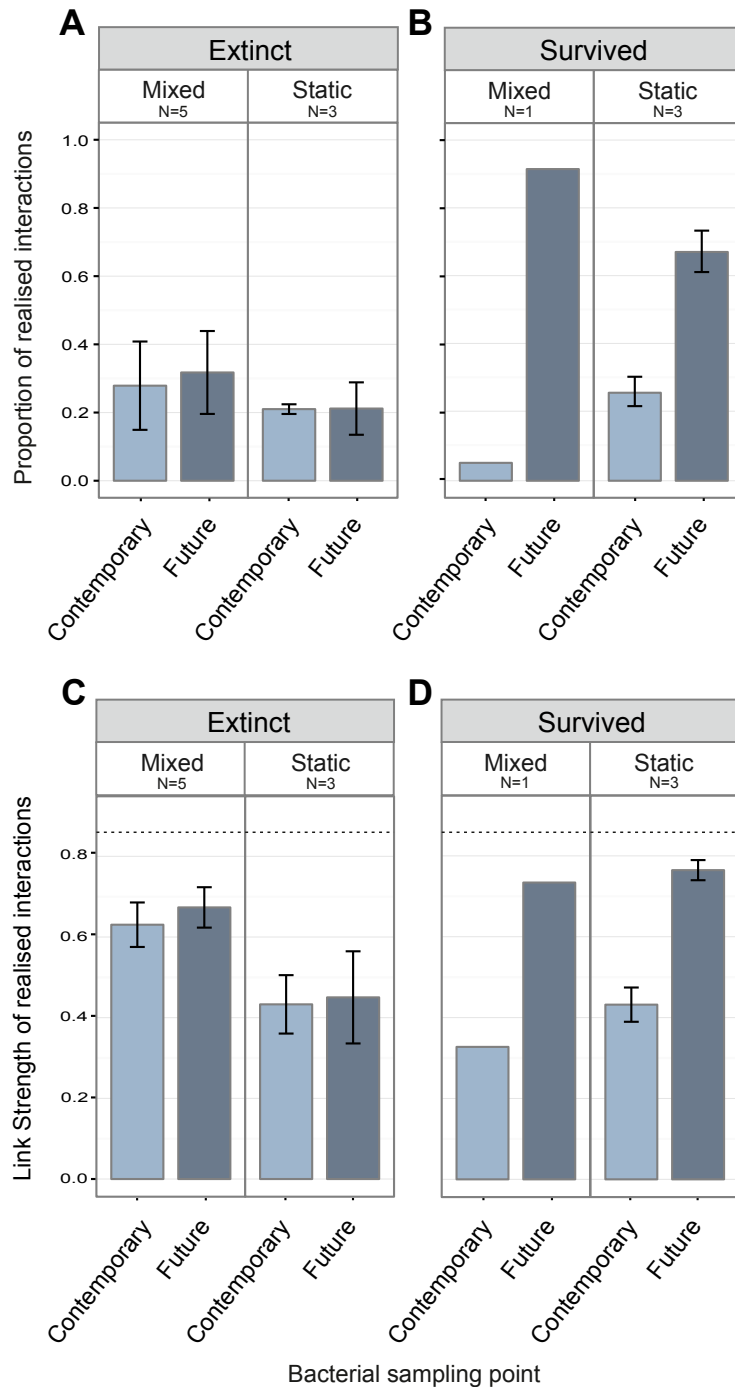


Figure 2.3 Changes in bacterial susceptibility across low resource treatments approaching phage extinction time points.

A, B mean (\pm SE) proportion of realised interactions (using binary threshold of susceptibility) and **C, D** mean (\pm SE) link strength of realised interactions within replicate populations of mixed and static low resource treatments. Bacteria sampled at pre-extinction time points (Contemporary) or extinction time points (Future) assayed against phage sampled from the same replicate population at the pre-extinction time point. Designated 'Extinct' (**A, C**) or 'Survived' (**B, D**) based on phage presence at transfer 10. 'N' describes the number of replicate populations represented under each heading. The dashed line in **C** and **D** shows the link strength of ancestral phage against ancestral bacterial.

However, in replicates where phage survived beyond the time-point where extinctions were observed in other replicates, bacteria sampled from the extinction time point (future) were significantly more susceptible to infection by pre-extinction time point phage (Figure 2.3B; PRI Tukey $p < 0.0001$). In addition, increased link strength in future compared to contemporary bacteria in survival populations indicated greater quantitative susceptibility at the individual level (Figure 2.3D; LS Tukey $p = 0.0337$) suggesting that phage survival relied upon the reinvasion of highly phage-susceptible bacterial genotypes. This pattern was consistent for both mixed and unmixed environments. Population mixing had no significant effect on proportion of realised interactions in extinction populations (Figure 2.3A, PRI Tukey $p = 0.9551$). However, link strength was greater in mixed than static conditions (Figure 2.3C, LS Tukey $p = 0.0410$), indicating population mixing promoted higher individual-level susceptibility in extinction populations.

2.4 Discussion

We have found that low resource conditions and population mixing both act to increase the likelihood of phage extinction. These findings, in part, contradict our predictions that more intense coevolution, known to be accelerated by both high resource availability and high rates of population mixing, should promote coevolution-induced phage extinction.

Our predictions were based on previous studies that found elevated phage extinction in nutrient-enriched environments using the same bacteria-phage model system (Gómez et al., 2015b), which Buckling and Zhang formalised as a 'coevolutionary paradox of enrichment' (Zhang and Buckling, 2016). They hypothesised that increasing nutrient levels can destabilise the coevolutionary interaction between bacteria and phage by increasing the intensity of antagonistic coevolution, selecting for increased bacterial resistance to phage infection, whilst ameliorating the costs associated with resistance mutations. As a result, the stronger selection for increased phage infectivity destabilises the coevolutionary interaction between bacteria and phage, and may therefore result in phage extinction in enriched environments (Zhang and Buckling, 2016). However, we found the opposite; the likelihood of phage extinction was increased at low resource levels.

Whilst these studies are not directly comparable (our experiment was conducted using different culture media and at different population sizes) these broadly contrasting outcomes are likely to be due to differences in the magnitude of the resource manipulations in each study. In our study we implemented a much more minimal low-resource condition [100-fold dilution of KB growth media compared with a maximum 10-fold dilution of LB media used by Zhang and Buckling (2016)]. Under comparable (i.e. static growth) conditions we observed far higher rates of extinction in low resource conditions (3 out of 6 replicates) than the more intermediate resource levels used in the previous study (0.1 and 0.3LB), where no extinctions were observed. Extinction rates under high resources were more similar between experiments (1 out of 6 replicates in our static 1KB treatment compared to 2 out of 8 replicates in their 2.7LB treatment). High rates of phage extinction may therefore be a result of the ecological effects of very low resource environments, suggesting that the stability of coevolutionary interactions may be maximised under intermediate resource levels.

Interestingly, however, the mechanisms driving extinction at high and low resources are likely to derive from the same fundamental process; limiting the potential of phage to evolve infectivity in response to bacterial resistance. Under high resource environments accelerated rates of antagonistic coevolution increases demand for novel resistance and infectivity mutations. In contrast, low resource levels sustained smaller population sizes which can limit the supply of resistance and infectivity mutations (Gandon and Michalakis, 2002). Because phage infectivity is known to require several mutational steps to overcome a single bacterial resistance mutation (Buckling and Brockhurst, 2012; Samson et al., 2013) both increasing demand or limiting supply of mutations is likely to disproportionately constrain the ability of phage to adapt compared with bacteria and thus lead to an imbalance in bacteria-phage coevolution and ultimately phage extinction.

Under very low resources these effects are likely to be further exacerbated by the impact of reduced host diversity due to more stringent bottlenecks, which can result in coevolution-induced phage extinction through stochastic loss of susceptible bacteria (Hesse and Buckling, 2015). An important caveat of our experimental design is that the magnitude of bottlenecking imposed by experimental transfers varies dependent on the population density supported by each treatment, such that the reduced population sizes in low resource conditions

also translate to a more stringent bottleneck. Furthermore, low resource conditions have been shown to inhibit the establishment of bacteria-phage interactions, reducing connectivity of the population (i.e. lower density of realised interactions) and thus further increasing vulnerability to extinction (Poisot et al., 2011). This mechanism is supported by our resistance assays which show that phage extinction in low resource treatments was associated with high levels of bacterial population-level resistance (Figure 2.3A). Moreover, populations in which phage were maintained experienced reinvasion of highly susceptible bacteria, displacing resistant host genotypes (Figure 2.3B,D).

Differences in resistance and infectivity profiles between treatments may also be influenced by variation in the type of resistance evolved by hosts, and in phage infection dynamics (e.g. adsorption, burst size, latent period), in response to different ecological pressures. However, as the literature strongly supports the intensification of co-evolution with increasing resources levels, our interpretation is based on the assumption that the changes in resistance and infectivity we have observed are primarily influenced by the differences in co-evolutionary rate and dynamics across resource levels and with population mixing (Brockhurst et al., 2003; Lopez-Pascua and Buckling, 2008; Zhao et al., 2017). Lopez-Pascua et al (2008) observed correlated changes in bacterial resistance and infectivity indicating reciprocal selection, the hallmark of co-evolution, which increased at higher resources levels (up to 1KB) indicating more intense co-evolution, and stalled at low resources equivalent to those we employed (0.01KB). Further, a recent study which characterised the rate of bacteria-phage co-evolution and the frequency of phage extinction across a similar range of nutrient levels (0.01-1KB) observed similar results, with the greatest stability in bacteria-phage coexistence at intermediate resource levels (0.1KB). Therefore, whilst resistance and infectivity are complex traits which may be influenced by complex and interacting selection effects across different ecological conditions (i.e. fitness effects of resistance evolution, changes in infection dynamics etc.), differences in the rate of co-evolution across ecological gradients are a primary factor in determining changes in these traits, and thus in the stability of bacteria-phage co-existence.

As predicted, population mixing was shown to increase the risk of phage extinction. Higher encounter rates in mixed environments, which stimulate more intense coevolution (Brockhurst et al., 2003), increased the risk of phage extinction consistently across high and low resource supply levels. Population

mixing may act to intensify the coevolutionary imbalances promoted in each resource condition, which limit phage adaptation, thereby increasing the likelihood of phage extinction. Conversely, static conditions provide spatial refuges for susceptible bacteria by reducing dispersal and lowering encounter rates (Brockhurst et al., 2006), thereby limiting selection for bacterial resistance. In turn, this alleviates selection for increased phage infectivity and as a result may stabilise the coevolutionary interaction, promoting co-existence. Bacterial spatial refuges may be 'self-organised' in nature: Modelling of bacteria-phage populations demonstrates that density-dependent mechanisms, such as biofilm formation, may promote formation of phage-exclusion zones (Heilmann et al., 2012). High phage densities could develop on the boundaries, but do not penetrate such zones, enabling susceptible bacterial genotypes to persist thereby promoting stable bacteria-phage coexistence.

Our results suggest that coevolution-induced phage extinction is promoted by abiotic conditions which destabilise the symmetry of antagonistic coevolution. This highlights the importance of feedbacks between ecological processes and the co-evolutionary interactions embedded within communities. We currently understand little about the effects of environmental changes across space and time on the stability of microbial populations, or the impact of short term responses to such changes on the long-term evolutionary trajectory of these communities. Whilst a predator-prey style paradox of enrichment may apply to bacteria-phage interactions in some situations, it is clear that the multivariate ecological and evolutionary effects of resource enrichment or depletion depend on the broader ecological and evolutionary context.

Chapter Three

Cross-resistance is modular in bacteria-phage interactions²

3.1 Introduction

Natural microbial communities are comprised of complex networks of species interactions, wherein each species may be engaged in ecological interactions with many other species (Friman and Buckling, 2013; Hambly and Suttle, 2005; Waterbury and Valois, 1993). In this community context, the evolutionary response of a focal species to a given pairwise species interaction can promote an “evolutionary cascade” through the adjacent interacting species (Betts et al., 2016b; Toju et al., 2017). In the context of bacteria-phage interaction networks, we expect that the impact of a given phage resistance mutation will depend on the connectivity of that bacterial host within the community network (Dallas and Cornelius, 2015), and the degree of cross-resistance provided by the mutation against other phage species in the network (Koskella et al., 2011). While the statistical structure of interactions in bacteria-phage networks has been well-studied (Weitz et al., 2013), the structure and underlying genetic basis of cross-resistance networks remain poorly understood. This considerably limits our ability to predict how cross-resistance evolution affects bacteria-phage communities across different environmental, agricultural and clinical contexts.

The extent of cross-resistance provided by a given resistance mutation is likely to depend on the genetic correlations between bacterial resistance traits selected by the different phage species. Cross-resistance is likely for cases of positive genetic correlation; for example, binding to shared receptors can cause synergistic pleiotropy between specific resistances, e.g. a mutation in the lipopolysaccharide (LPS) biosynthesis pathway is likely to promote cross-resistance to other phages that also adsorb to LPS (Lenski, 1984, 1988). In contrast, cross-resistance is less likely if there is antagonistic pleiotropy, where resistance to one phage increases susceptibility to an alternative phage [e.g. through replacement of a CRISPR spacer (Horvath and Barrangou, 2010)], or no

² Wright, R.C.T., Friman, V-P., Smith, M.C.M., and Brockhurst, M.A. (2018). Cross-resistance is modular in bacteria-phage interactions. *PLOS Biology* 16 (10), e2006057

genetic correlation, for instance if the phages bind to different receptors and accumulation of multiple resistance mutations is therefore required (Bohannon et al., 1999). Because individual resistance mechanisms frequently incur fitness costs by impairing the normal functioning of the molecule acting as the phage receptor, accumulation of multiple resistance mechanisms may be limited by their combined fitness costs, particularly if there is negative epistasis among the fitness costs of resistance mutations (Bohannon et al., 2002; Koskella et al., 2011). Even though pleiotropic costs should limit the evolution of generalist resistance, cross-resistance is commonly observed (Betts et al., 2016a; Hall et al., 2012). Most of this evidence is however based on relatively simple phage communities and it is less clear how the range of cross-resistance provided by different resistance mutations is related to the magnitude of fitness costs in more complex bacteria-phage networks.

Understanding the structure of bacterial cross-resistance to phage infection also has important applied implications with relation to phage therapy, i.e., the use of phages as antimicrobials to treat bacterial infections (Kutter et al., 2010). Phage cocktails (i.e. combinations of different phages) have been shown to delay the evolution of resistance in bacteria, both *in vitro* (Barbosa et al., 2013) and *in vivo* (Fischer et al., 2013), compared to challenge with a single phage. Effective phage cocktails often contain phages that target different bacterial receptors, e.g. (McCallin et al., 2013; Yen et al., 2017), and as a result multiple resistance mutations in different receptor genes are required to provide resistance to all the phages present in the cocktail (Tanji et al., 2004). The requirement for bacteria to accumulate multiple resistance mutations is thought to enhance the evolutionary robustness of phage cocktails because there is a lower probability of resistance emerging. Furthermore, resistance to multiple phages is likely to be associated with greater fitness costs assuming additivity of fitness costs associated with each resistance mutation (Koskella et al., 2011). These assumptions may not apply, however, if very generalist cross-resistance is available via a single mutation affecting the expression of multiple phage receptors. This suggests therefore that minimising the potential for cross-resistance could be a key feature of effective phage cocktail design. However, this has not been tested experimentally.

Here we determined the network structure and genetic basis of cross-resistance against a collection of 27 phages infecting the opportunistic human pathogen, *Pseudomonas aeruginosa*. The cross-resistance network contained both

symmetric (reciprocal) and asymmetric (non-reciprocal) interactions forming two cross-resistance modules defined by high within- but low between-module cross-resistance. Within cross-resistance modules, resistance mutations targeted distinct phage receptors, whereas between module cross-resistance was caused by mutations targeting a global regulator likely to control the expression of multiple phage receptors. The range of cross-resistance provided by a mutation was not correlated to its fitness cost, except that global regulator mutations causing between module cross-resistance were costlier than mutations causing within module cross-resistance. Furthermore, the degree and symmetry of cross-resistance predicted the ability of phage combinations to suppress bacterial growth and the frequency of resistance mutations. Together, our data suggest that an understanding of cross-resistance interactions could help to predict the impact of resistance evolution on host-parasite community structure and aid the rational design of therapeutic phage cocktails.

3.2 Materials and Methods

3.2.1 Study organisms

A total of 27 different phage strains (Table S3.1) that were able to infect *P. aeruginosa* PA01 strain were used. Four of the phage strains have been previously characterised and are known to be phylogenetically, structurally and serologically different (Friman et al., 2016; Merabishvili et al., 2007) and promote bacterial resistance evolution to differing degrees (Hall et al., 2012). The remaining 23 phage strains were isolated at the same time and location [Sewage water treatment facility, Jyväskylä, Finland; for isolation protocols and infectivity ranges see (Mattila et al., 2015)]. Sequence data is available for only two of these strains.

3.2.2 Characterisation of phage genetic relatedness

The genetic similarity of all phage strains was characterised using RAPD PCR (random amplification of polymorphic DNA) that uses a set of primers (Table S3.2) to amplify random sections of DNA, giving a unique PCR banding pattern for each distinct phage genotype. Phage DNA was extracted using the QIAamp DNA Mini Kit (Qiagen, Hilden, Germany), then a PCR was performed on each phage DNA sample (27 phages), with each primer (0.8µM final primer concentration; Table S3.3) under the following conditions: 4 initial cycles of 94°C for 45s, 30°C for 120s, 72°C for 60s, followed by 25 cycles of 94°C for 5s, 30°C

for 30s, 72°C for 30s, ending with 72°C for 10 mins. PCR products were run on 1% Agarose gels, for 30 mins at 200V. A difference matrix based on these banding patterns (i.e. the proportion of bands which two phage do not have in common), was used to make a neighbour joining tree [R package 'ape', (Paradis et al., 2004)].

3.2.3 *Culture conditions*

All bacterial cultures were grown in 6ml King's media B (KB) in 30ml glass microcosms with loose fitting plastic lids and incubated at 37°C with orbital shaking (200rpm). Phage cultures were prepared by inoculating frozen stocks into 30ml microcosms containing 6ml KB with 60µl of PA01 overnight culture (approximately 10^9 cells ml⁻¹). Following overnight incubation at 37°C, shaken, phage stocks were isolated by filtration (0.22µm) and stored at 4°C.

3.2.4 *Selecting spontaneous phage-resistant mutants*

To select spontaneous phage-resistant mutants, a modified fluctuation test was used (Harrison et al., 2015). To establish 135 independent sub-populations of PA01, we selected a single colony and incubated for 8h before diluting by 1 in 10 into individual wells of 96-well microplates containing 200µl of KB medium. Following overnight incubation, each of the bacterial populations was exposed to one of the 27 phages. Specifically, the overnight bacterial cultures were diluted by 10^{-2} directly into 200µl of a phage stock solution, giving a multiplicity of infection of approximately 100 phage particles per bacterial cell, and 5 independent bacterial populations per phage strain. From each bacteria-phage mixture 100µl was plated on KB solid agar and incubated overnight. Two colonies per plate were then re-streaked onto KB agar plates and grown overnight to remove phage particles. We then picked a single colony from each streak plate to give 10 resistant mutants per phage strain (270 in total), which were then grown overnight in KB before preparing glycerol stocks (40% glycerol) and storing at -80°C. These overnight cultures were also filter sterilised (0.22µm) and plated on KB soft agar (0.8%) containing ancestral PA01 to check for any remaining phage particles. If phages were detected, phage-free stocks were created by re-streaking the resistant mutant from glycerol stocks and repeating the last step. For seven replicates, we were unable to isolate phage-free stocks, therefore these replicates were excluded from the analysis, leaving 263 resistant mutants in total.

3.2.5 Cross-resistance assays

To assess the extent of cross-resistance conferred by resistance against individual phage strains, all 263 resistance mutants were assayed against each of the 27 phage strains individually. Cross-resistance assays were performed in 96 well microplates (final volume of 150µl) in KB media, at an approximate multiplicity of infection of 10 phage particles per bacterial cell. The relative bacterial growth (RBG; Poullain et al., 2008), was calculated by comparing absorbance readings (600nm at $t = 0$ and $t = 8h$) in the presence and absence of phage (Eq. 1). RBG is a quantitative measure of bacterial resistance where 1 indicates equal growth in the presence and absence of phage (i.e. complete resistance), and 0 indicates zero growth (i.e. complete susceptibility).

For phage i , bacteria j :

$$RBG_{ij} = \frac{[Abs_{600}(t=8h) - Abs_{600}(t=0h)]_{ij}}{[Abs_{600}(t=8h) - Abs_{600}(t=0h)]_{controlj}} \quad (1)$$

Cross-resistance range describes the proportion of phages to which each resistant bacterial replicate mutant is resistant to, using a resistance threshold (RBG = 0.798) calculated as the 95% confidence interval of a normal distribution modelled over the peak of resistance within the complete RBG distribution (Figure S3.1).

3.2.6 Measuring the fitness costs associated with cross-resistance

To determine the fitness costs associated with different cross-resistance profiles, the growth of all resistant mutants was measured in the absence of phage and compared to growth of the ancestral PA01 strain. Bacterial cultures were inoculated directly from glycerol stocks into 150µl of KB media in 96 well microplates. Absorbance at 600nm measured every 30min for 24h (37°C, shaken) to create a growth curve for each resistant mutant. Due to variation in the type of fitness costs observed (i.e. increased lag, reduced maximum OD and reduced growth rate; Figure S3.2), we used the integral of each growth curve as a combined measure of the effect of resistance mutations on bacterial growth. The integral of the growth curve correlates well with each of the other growth parameters (Figure S3.3, Figure S3.4). The integral of each growth curve gives the total growth for each bacterial strain; dividing this value by the average integral for the ancestral PA01 strain gives an estimate of relative fitness.

3.2.7 *Determining the cross-resistance network*

Cross-resistance interactions between two phage strains can be quantified as the proportion of resistance mutants screened against one phage that display cross-resistance (RBG above 0.798) against the second phage, giving a directional metric of cross-resistance strength (CRF). To enable comparison of pairwise phage interactions a non-directional cross-resistance index (CRI) was used as the mean of the two directional CRF values.

CRF can be used to construct an interaction network showing all directional cross-resistance interactions within a phage community. Firstly, an adjacency matrix is produced, containing directional CRF values for all possible phage pairs. The R package 'igraph' (Csardi and Nepusz, 2006) was used to convert the adjacency matrix into a network graph (a list of all the realised links in the network, and their associated weights; `graph.adjacency` function), which can then be plotted (`plot.igraph` function) as a directional weighted network. In the network, each node represents a single phage strain and the directional connections are weighted by CRF, showing the frequency of cross-resistance against each phage. A community-detection algorithm [`cluster_edge_betweenness` function in the 'igraph' R package (Csardi and Nepusz, 2006)] was used to identify the phage strains within the cross-resistance network that formed modules. This edge-betweenness algorithm (Girvan and Newman, 2002; Newman and Girvan, 2004) finds the optimum community structure of a given network by assigning a 'betweenness' value to every link in the network based on the frequency with which the link is used to create pathways between all possible pairs in the network. High 'betweenness' values indicate links between poorly connected modules. By removing these links in a stepwise manner (recalculating 'betweenness' values each time), the algorithm can define modules within the community. The subnetwork of the ten phages used in further analysis was extracted from this full network.

3.2.8 *Quantifying the frequency of phage resistance mutations*

Modified fluctuation tests (Harrison et al., 2015) were used to estimate bacterial mutation frequencies against either individual phage strains or combinations of two phage strains. Three microcosms were inoculated from single colonies of the ancestral PA01 strain. After overnight incubation, each microcosm was sub-cultured into 55 wells of a 96 well microplate, diluting by 10^{-1} to a final volume of 200 μ l then allowed to grow overnight at 37°C in a static incubator. Concurrently,

stock solutions of 10 phage strains (a subset representing each node within the CRF network; Figure S3.5) were prepared (as above). Phage combinations were assembled, consisting of each phage alone (100µl) and 1:1 mixtures of each possible phage pair (final volume 100µl), to give 55 different phage combinations. One independent 200µl PA01 culture from each of the three replicate microplates was then diluted 100-fold into each of the phage solutions, giving a multiplicity of infection of approximately 100 phage particles per bacterial cell, and incubated for 30 mins at 37°C in a static incubator.

Initial bacterial cell density was estimated by plating serial dilutions of six random 200µl PA01 cultures per replicate microplate. The number of phage-resistant spontaneous mutants was then calculated by plating 60µl of each bacteria-phage mixture onto solid KB agar to give colony forming units per ml (CFU/ml). The ratio of phage-resistant mutants to initial bacterial cell density provides an estimate of the mutational frequency (MF, Eq. 2) against each phage combination, then comparison to the individual phage strains gives relative mutational frequency (RMF, Eq. 3).

For phage suspension i , bacteria j :

$$MF_i = \frac{[CFU/ml]_{ij}}{[CFU/ml]_{controlj}} \quad (2)$$

For phage pair i_1 and i_2 ,

$$RMF = \frac{MF_{i_1 i_2}}{\sqrt{MF_{i_1} \cdot MF_{i_2}}} \quad (3)$$

3.2.9 *Suppression of bacterial growth by phage combinations*

To determine the ability of phage combinations to suppress growth of the ancestral PA01 strain, bacterial growth was measured over 24h in the presence of individual phage strains and all possible pairwise phage combinations of 10 phage strains. This phage subset contains all four phages from module 1, and six module 2 phage (Figure S3.5), and is comprised of asymmetric (N=11) and symmetric (N=13) cross-resistance interactions, as well as pairwise interactions which promote no cross-resistance (N=21). Individual colonies of ancestral PA01

were inoculated into KB media, and following overnight incubation, were transferred to fresh KB media in 96 well microplates, diluting ten-fold. Phage suspensions were added at an approximate multiplicity of infection of 100, for both individual phage and pairwise phage combination treatments (prepared from phage stock solutions with a 1:1 ratio). Absorbance at 600nm was measured every 30min for 24h during incubation at 37°C with regular orbital shaking to produce growth curves for PAO1 in the presence of each individual phage strain and all possible pairwise phage combinations within the phage subset (Figure S3.5), each replicated three times.

3.2.10 *Sequence analysis*

To assess the genetic basis of cross-resistance, we randomly chose one resistant mutant screened against each phage within the cross-resistance subnetwork (Figure S3.5), along with additional mutants representing symmetrical and asymmetrical cross-resistance profiles within resistance module 1, to be sequenced (22 independent spontaneous mutants in total). Bacteria were sequenced using the Illumina MiSeq platform, followed by bioinformatic analysis as follows: reads were aligned using Burrows-Wheeler Aligner (Li and Durbin, 2009), SNPs and small indel variants were called by GATK HaplotypeCaller (McKenna et al., 2010), then gene information was added using SNPeff (Cingolani et al., 2012). Variants were filtered for quality by the following parameters: coverage of >20 reads per base pair, and frequency of alternative allele in >80% of reads. The quality of each variant was further assessed visually using an alignment viewer [igv; (Robinson et al., 2011)]. Additionally, called variants occurring in all 22 sequenced mutants were discarded as these represent mutations present in the ancestral PAO1 compared to the available reference strain used (accession ID AE004091). All sequence data has been uploaded to the European Nucleotide Archive (accession ID PRJEB27828).

3.2.11 *Confirmation of phage surface receptor targets*

To confirm that distinct cell surface receptors are required for infection by module 1 phages compared to module 2, we tested the ability of all 27 phage strains to infect a *pilB* transposon mutant (PW8623 *pilB*-G07::ISlacZ/hah; *Pseudomonas aeruginosa* Two Allele Library) versus wildtype PAO1. Bacteria lawns were prepared as follows: three colonies were selected for each bacterial strain, inoculated into KB media (6ml) and grown overnight at 37°C, shaken; 200ul of

each culture was added to 12ml of soft KB agar (0.6% agar) and poured over set standard KB agar (1.2% agar) in a 120mm square petri dish to form a bacterial lawn. Filtered phage stocks were serially diluted, and each dilution was spot plated (5 μ l) onto a lawn of each bacteria. Plates were incubated at 37°C for 24h, then phage plaques were counted and density calculated as plaque forming units per ml.

3.2.12 Statistical analysis

All analysis was conducted in R (R Core Team, 2016). Resistant mutants originating from the same subpopulation were treated as paired replicates to prevent pseudo-replication. This means for 263 resistant mutants, we have 133 independent replicates. Variation in cross-resistance range between different focal phages was analysed using the non-parametric Kruskal-wallis test, after averaging within subpopulations. To test for associations between cross resistance range and focal resistance or relative fitness, linear mixed effects models [R package 'lmerTest' (Kuznetsova et al., 2017)] were used with subpopulation included as a random effect. Variation in relative fitness between mutants with different network-level cross-resistance (i.e. within/between modules) was analysed using a one-way anova followed by post-hoc testing (Tukey test). Comparison of phage densities between transposon mutant (*pilB*) and wild type hosts was performed using a linear mixed effects model, with bacteria and phage treated as interacting fixed effects. Statistical analysis of the effect of cross-resistance interaction type (i.e. symmetric/asymmetric) on RMF data was performed using the Kruskal-Wallis test, followed by post-hoc testing (pairwise Mann-Whitney U) to compare interaction types.

3.3 Results

3.3.1 Variation in cross-resistance provided by individual resistance mutations

To determine the extent of cross-resistance we tested 263 spontaneous resistant mutants of *P. aeruginosa* PAO1 selected against each of 27 phages (i.e. 10 resistant mutants were selected against each focal phage; 7 mutants were discarded due to persistent phage contamination) for their ability to resist infection by all other phages (cross-resistance). Resistance was determined by measuring relative bacterial growth (RBG) of each spontaneous mutant in the presence versus absence of each phage where mutants were classified as resistant if their RBG exceeded a binary resistance threshold [RBG = 0.798; calculated as the

95% confidence interval of a normal distribution modelled over the peak of resistance within the complete RBG distribution (Figure S3.1)]. We observed variation in the pattern and range of cross-resistance among spontaneous resistance mutations (Figure 3.1; Figure S3.6). First, the degree of cross-resistance selected by the different focal phages varied extensively, ranging from conferring resistance against less than 10% to up to 80% of all phages (Figure S3.6; Kruskal-Wallis $\chi^2_{26}=66.6$, $p<0.0001$). Second, both focal resistance and cross-resistance phenotypes varied considerably between independently evolved resistant mutants selected against the same focal phage (Figure S3.6). Together these results suggest that the magnitude of cross-resistance depends on the focal resistance selected, and that multiple resistance mechanisms may exist against the same focal phage, resulting in different levels of cross-resistance between independent replicate mutants.

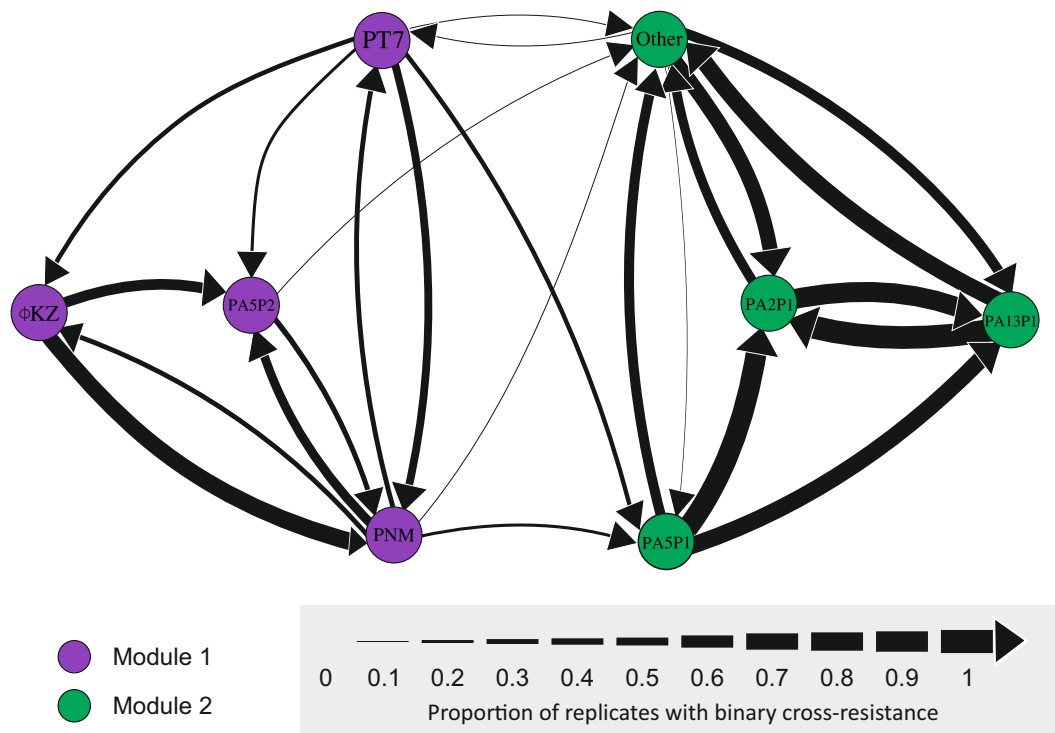


Figure 3.1 Cross-resistance network describing quantitative cross-resistance between all possible phage combinations

Each node represents a phage strain and arrows between nodes show directional cross-resistance frequency (CRF) between two phages. The line widths are scaled by the proportion of replicate mutants selected against the focal phage (origin node) which have resistance above the binary threshold (Figure S3.1) to the second phage (target node). Node colours define resistance modules identified using an ‘edge-betweenness’ algorithm. A subset of 20 phage strains that all showed strong symmetric cross-resistance were grouped together as the node labelled ‘Other’.

3.3.2 *Cross-resistance range was not limited by fitness costs or strength of focal resistance*

The evolution of broad, generalist cross-resistance could be constrained if it was associated with relatively higher costs compared to more specialised resistance, or if mutations providing cross-resistance concomitantly provided only weak resistance against the focal phage. In contrast, while all resistance mutations selected against focal phage were costly (Figure 3.2A; one-sided t-tests: all $p < 0.005$), we observed no overall relationship between the range of cross-resistance provided by resistance mutations and their associated costs (Figure 3.2A; linear mixed effects model: $t_{236} = -0.655$, $p = 0.513$). Moreover, we observed a positive relationship between the strength of focal resistance and the range of cross-resistance provided by resistance mutations (Figure 3.2B; linear mixed effects model: $t_{245} = 15.09$, $p < 0.0001$). These results suggest that the evolution of cross-resistance is unlikely to be constrained by trade-offs due to associated fitness costs or the strength of the focal resistance.

3.3.3 *The structure of the cross-resistance network*

Network analysis of the directional cross-resistance frequency (CRF) of all pairwise phage combinations produced a cross-resistance network with two distinct modules (Figure 3.1). Within each module, all possible pairwise phage combinations were connected by some degree of cross-resistance, whereas cross-resistance between the two modules was more limited (narrower arrows between nodes denote low frequency of cross-resistance interactions) and observed only between a small proportion of all the potential phage pairs (8/92, i.e. around 8.7%, Figure 3.1). Within modules, asymmetric (i.e. non-reciprocal) cross-resistance was more common within module 1, while module 2 was dominated by symmetric (i.e. reciprocal) cross-resistance (note that the 'other' node in module 2 of Figure 3.1 contains a subset of 194 mutants providing consistently strong symmetric cross-resistance against 20 phages). The high degree of symmetric cross-resistance observed in module 2 could not be explained simply by the genetic similarity of the focal phages as estimated from their RAPD PCR banding patterns (Figure S3.7). Between module cross-resistance was always asymmetric and typically from module 1 to module 2 (Figure 3.1). This network structure was robust to the binary threshold value used to classify resistance, although using lower thresholds led to increased numbers of asymmetric connections between modules (Figure S3.8). Symmetric cross-

resistance is likely to occur where both phages select for similar modifications to a shared receptor, whereas asymmetric cross-resistance could result if phages selected for different modifications to a shared receptor that varied in the extent of disruption or for entirely different resistance mechanisms that varied in the extent of generalism. To study this at the genetic level, we next obtained whole genome sequences for resistant mutants selected against a subset of 10 focal phages that represented all nodes of the cross-resistance network (Figure S3.5).

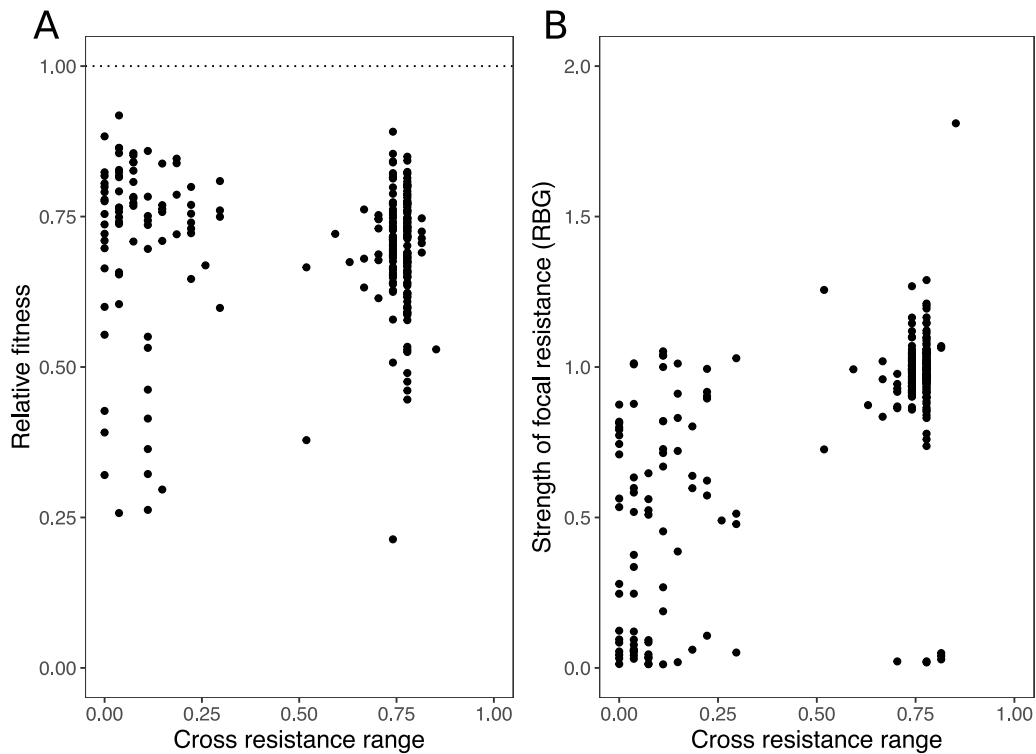


Figure 3.2 Effect of relative fitness and focal resistance on cross-resistance range

Relationship between cross-resistance range (the proportion of non-focal phages to which the bacterial mutant has resistance above the binary threshold) and relative fitness of spontaneous resistance mutants (**A**) measured as growth relative to the ancestral strain in phage-free standard media conditions, and (**B**), the strength of focal resistance, given as growth in the presence of the phage selected against, relative to growth in the absence of phage (RBG).

3.3.4 Molecular basis of within and between module cross-resistance

We obtained whole genome sequences for 22 independent spontaneous resistant mutants of PAO1 selected against 10 focal phages to identify mutational changes associated with specific phage resistance profiles (Figure 3.3; Figure S3.5). Cross-resistance within module 2 was associated with mutations in LPS

biosynthesis genes, *wzy* and *wbpL*, whereas cross-resistance within module 1 was associated with mutations in various genes encoding type IV pilus biosynthesis (Figure 3.3; Table S3.3). These included genes encoding mechanical components of the type IV pilus, such as the motor proteins PilB and PilT, and enzymes involved in type IV pilus biosynthesis and assembly such as PilD, a prepilin peptidase. These data confirm that cross-resistance modules were determined by distinct phage adsorption cell-surface receptors, specifically, the LPS for module 2 phages and the type-IV pilus for module 1 phages. We confirmed distinct receptor usage by testing the ability of all 27 phages to infect an unpiliated *pilB* transposon mutant: whereas module 1 phages were unable to form plaques on the unpiliated host, module 2 phages infected the unpiliated mutant at the same efficiency as they infected the pilated wild type PAO1 host (all $p > 0.1$; Figure S3.9). Between module cross-resistance was associated with mutations in genes encoding the transcriptional regulators, RpoN and PilS (Figure 3.3; Table S3.3). This suggests that more generalist phage resistance required changes in bacterial gene regulation, which are likely to have broader-scale effects on the bacterial phenotype than mutations affecting structural genes performing steps in biosynthetic pathways. In addition, weaker between module cross-resistance was associated with a mutation of the prepilin peptidase encoding gene *pilD* (Figure S3.10); here the likely mechanism of between module cross-resistance less clear.

3.3.5 *Fitness cost of between-module cross-resistance is gene-specific*

To test if the different classes of resistance mutations identified by sequencing were associated with different magnitudes of fitness cost we estimated the fitness of each of the genome sequenced strains relative to PAO1 in the absence of phage. Between module cross-resistance was associated with higher fitness costs than within module cross-resistance (Figure 3.4A; ANOVA with post-hoc Tukey test: module 1, $p = 0.009$; module 2, $p = 0.015$), but this was entirely due to far higher fitness costs caused by resistance mutations in the *rpoN* gene compared to resistance mutations in either type-IV pilus or LPS biosynthesis associated genes (Figure 3.4B). Thus, between module cross-resistance mutations in global regulators that are likely to disrupt many cellular functions are highly costly in the absence of phage, which may limit their long-term survival in bacterial populations.

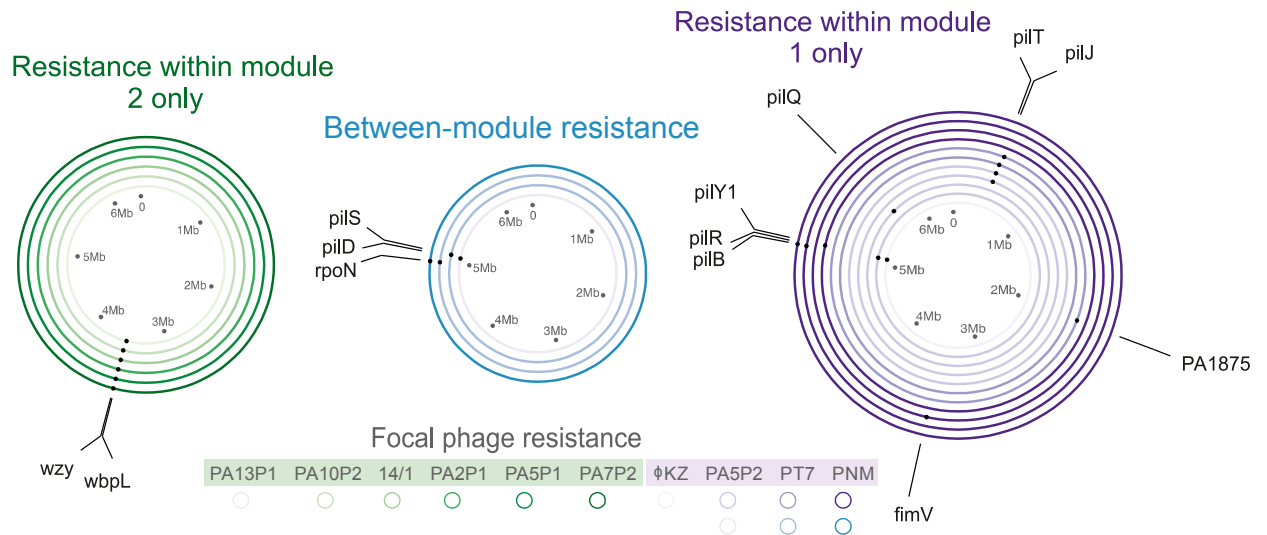


Figure 3.3 Genetic basis of phage resistance

Circles represent different phage resistant mutants selected against different focal phages (indicated by the colour shade; see key) and dots on each circle show the position of mutated genes. Colour represents the cross-resistance profile of each sequenced resistant mutant: resistance within module 1 (purple), within module 2 (green), and between-modules (generalist resistance, blue).

3.3.6 Cross-resistance determines the evolution of resistance to phage combinations

We hypothesised that the degree and symmetry of cross-resistance between a pair of phages would predict the frequency of resistance evolution against phage combinations. Specifically, we predicted the highest frequency of resistance mutation would occur against pairs selecting for symmetric cross-resistance, followed by asymmetric cross-resistance, and lowest for no cross-resistance. To test this, we first estimated the frequency of resistance mutations against phage pairs relative to individual phages for all possible combinations of the subset of 10 phages representing all nodes of the cross-resistance network (Figure S3.5). One phage (PA5P2) was excluded from further analysis because the absolute resistance mutation frequencies observed against this phage were unfeasibly high ($\sim 1.7 \times 10^{-3}$ for PA5P2 alone; Figure S3.11). This could possibly indicate that a physiological mechanism of resistance against PA5P2 infection exists, in addition to the Type IV pilus-associated mutational mechanism observed in the sequenced resistant clone (Figure 3.3; Table S3.3).

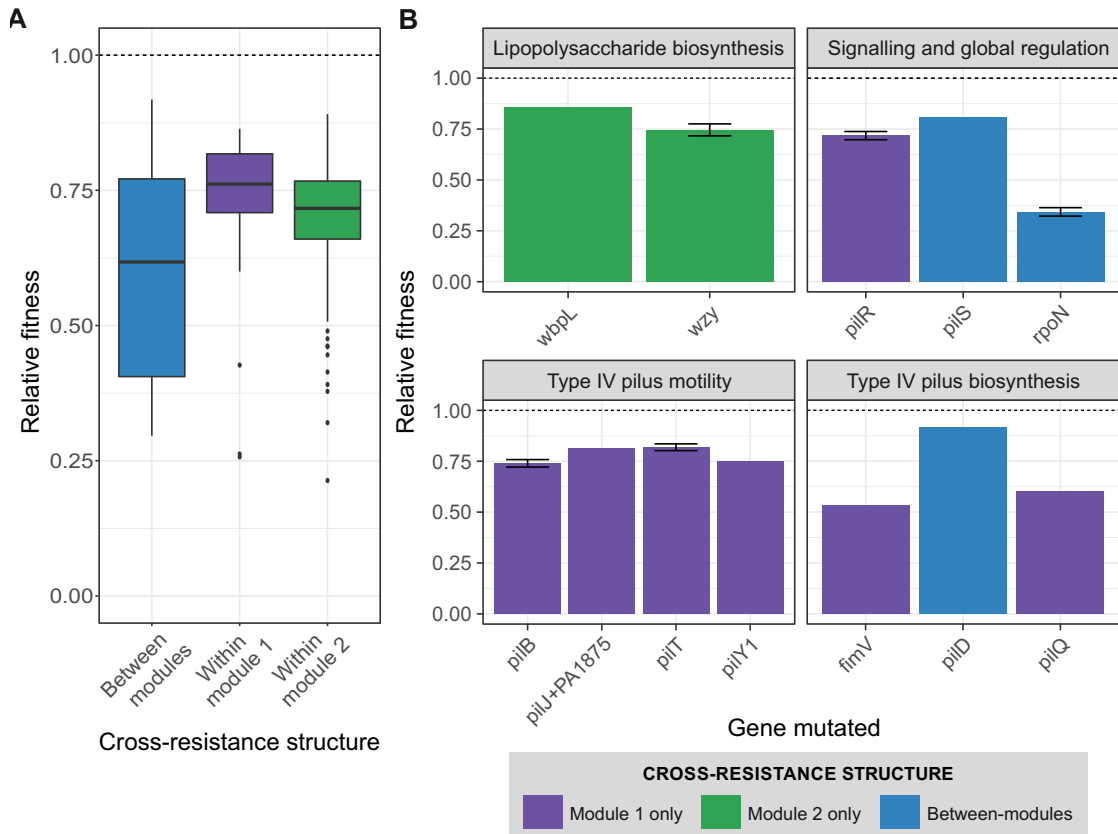


Figure 3.4 Effect of cross-resistance type and mutational target on relative fitness of spontaneous resistant mutants

Fitness relative to the phage-susceptible PAO1 ancestor of 263 spontaneous resistant mutants sorted by **A**) cross-resistance type or **B**) mutated locus. Colours denote cross-resistance type: within module 1 only (purple), within module 2 only (green), and between modules (blue). The dashed line (relative fitness = 1) represents equal fitness to the ancestor.

We found a positive relationship between the cross-resistance index (CRI; a non-directional measure of cross-resistance) and the relative mutation frequency (linear regression $R^2=0.280$, $F_{1,106}=42.7$, $p<0.0001$). Moreover, consistent with our hypothesis, the relative mutation frequency was highest for phage pairs that selected for symmetric cross-resistance (Figure 3.5; Symmetrical vs. Asymmetrical $p=0.001$; Symmetrical vs. None $p<0.0001$) and lowest for phage pairs that selected no cross-resistance (Figure 3.5; Asymmetrical vs. None $p<0.0001$). Thus, cross-resistance *per se* increased the frequency of resistance mutations, with the effect being strongest when cross-resistance was symmetric.

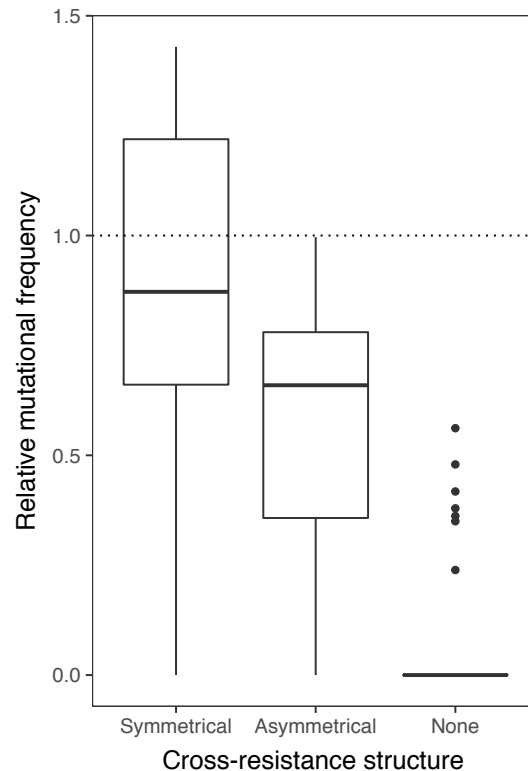


Figure 3.5 Relative mutational frequency for resistance against phage pairs exerting symmetrical, asymmetrical and no cross-resistance

Relative mutational frequency compares the frequency of resistance mutations against phage pairs to the geometric mean of mutational frequency against each individual phage. Dashed line represents equal frequency of resistance mutations against a phage pair versus the constituent phages individually.

Consistent with the observed resistance mutation frequencies, phage pairs that selected no cross-resistance suppressed the growth of PAO1 most effectively during 24h, whereas the effect of phage pairs that selected symmetric cross-resistance rarely differed from the best-performing individual phage (Figure S3.12). Interestingly, two phages did not conform to this pattern: Firstly, phage PA10P2 alone was sufficient to completely suppress bacterial growth, and all pairs including this phage were highly effective regardless of the symmetry of the cross-resistance. Secondly, phage pairs containing PA2P1 consistently performed poorly irrespective of the symmetry of cross-resistance. These results suggest that structure of cross-resistance predicts the performance of phage combinations, but that strong phage identity effects can override this by either increasing or decreasing the efficacy of a phage combination more than expected by cross-resistance alone.

3.4 Discussion

We analysed the network structure and underlying genetic basis of cross-resistance evolution in the bacterium *P. aeruginosa* PAO1 selected against 27 phages. Our data show that spontaneous resistance mutations against a focal phage commonly provide cross-resistance against other phages. The cross-resistance network was highly modular, containing two cross-resistance modules with high within- but weak between-module cross-resistance interactions. At the genetic level, cross-resistance modules were defined by shared mutational targets encoding biosynthesis of phage adsorption receptors (LPS or type IV pilus, respectively), while between module cross-resistance was associated with mutations targeting regulatory genes. The strength, direction and symmetry of cross-resistance between phage pairs predicted both the frequency of resistance mutation and the efficacy with which the phage pair suppressed bacterial growth: The highest performing phage combinations were those that selected no cross-resistance, whereas the lowest performing combinations selected symmetric cross-resistance. Taken together, these data suggest that cross-resistance will commonly shape the dynamic structure of bacteria-phage communities, and that it is likely to be an important predictor of the robustness of phage therapy to resistance evolution. Further experiments will be required, however, to test whether cross-resistance predicts the efficacy of phage cocktails in more complex *in vivo* environments.

Our finding that cross-resistance was common for our phage collection suggests that resistance evolution events may frequently disrupt the structure of bacteria-phage interaction networks. Cross-resistance evolution has the effect of reducing connectance at the whole community level more than would be expected if all interactions were strictly pairwise. The effect of connectance on community stability is dependent on underlying species interaction network architecture; reduced connectance can increase stability in trophic networks by enhancing modularity, but may reduce stability in networks with nested structures (Thébault and Fontaine, 2010). Bacteria-phage networks typically have a nested-modular network structure (Beckett and Williams, 2013; Flores et al., 2013), thus the impact of cross-resistance-mediated reduced connectance is likely to depend on precisely where in the network cross-resistance interactions occur. It seems reasonable to assume that modularity in bacteria-phage interaction networks may be caused by the same mechanism that causes cross-resistance modularity,

namely shared phage receptors. If this assumption is correct, then cross-resistance evolution may frequently lead to the collapse of isolated nested modules without destabilising the broader interaction network. Resistance in our experiments arose largely through mutations affecting the expression or biosynthesis of surface receptors. Notably, PAO1 lacks a CRISPR-Cas system and it is likely that CRISPR-mediated phage resistance would cause cross-resistance to only very closely related phages that are sequence identical for the genomic region targeted by the newly integrated spacer. In systems where both resistance mechanisms occur, by which mechanism resistance evolves is thought to depend on ecological conditions, with surface receptor modification favoured in high resource environments with high phage densities (Westra et al., 2015), suggesting that in such systems the structure of cross-resistance evolution may be highly ecologically contingent.

While resistance mutations were costly, we found no overall relationship between the range of cross-resistance provided by resistance mutations and their associated fitness costs, suggesting that the evolution of cross-resistance is unlikely to be constrained by fitness trade-offs except for rare cases of very generalist between-module cross-resistance (Figure 3.4B). This finding is somewhat surprising since previous studies of pairwise bacteria-phage interactions and interactions between bacteria and multiple phage species have reported that broader resistance ranges are associated with higher costs (Gómez and Buckling, 2011; Koskella et al., 2011). In contrast to these studies, however, we did not allow broad resistance ranges to evolve via accumulation of multiple sequential mutations but instead measured the effects of single spontaneous resistance mutations on cross-resistance. It seems likely therefore that higher costs of generalist phage resistance described previously arise from negative epistasis between multiple resistance mutations rather than from inherent costs of cross-resistance itself. At a community level, cross-resistance could limit the ability of phages to maintain bacterial diversity via density dependent killing (Thingstad, 2000). This could be mitigated by migration between local communities, promoting invasion of novel phages to which resistance is absent in the local community, or through phage counter-adaptation. For example, phage have been shown to switch hosts in multi-host environments (Betts et al., 2016b), and expand host range through spontaneous mutation (Duffy et al., 2006; Meyer et al., 2012). An important caveat is that fitness costs measured in simple lab environments are likely to underestimate the full extent of the pleiotropic effects

of resistance mutations in more complex *in vivo* environments relevant to phage therapy. For example, loss of the type-IV pilus is likely to be highly detrimental *in vivo* where type-IV pilus-mediated motility, attachment and biofilm formation play important roles in pathogenesis (Persat et al., 2015).

The modular structure of the cross-resistance network was determined by the shared phage receptors modified by resistance mutations. Within cross-resistance modules, mutations targeted biosynthesis of specific surface receptor targets for phage binding (Table S3.3), specifically the type IV pilus in module 1 or the LPS biosynthesis in module 2. Resistance to the same phage could be provided by mutations to different genes in the same pathway. For example, mutations selected against phage PA5P2 affected PilD [a peptidase which processes prepilins; (Nunn and Lory, 1991)], PilQ [which is involved in assembly and transport; (Martin et al., 1993)], and PilT [a motor protein which power pilus retraction; (Chiang et al., 2008)]. By contrast, mutations that provided very generalist between-module resistance targeted the regulatory genes, *rpoN* and *pilS*. RpoN is an alternative sigma factor which regulates transcription of approximately 700 genes, influencing a diverse range of functions including motility (via both type IV pilus and flagella associated genes), quorum sensing, mucoidy and biofilm formation (Lloyd et al., 2017). PilS is part of a two-component regulatory system which promotes pilus expression by activating RpoN (Hobbs et al., 1993). The diverse regulatory function of RpoN makes it difficult to identify the specific mechanism of generalist phage resistance. However, RpoN regulation of LPS-associated genes has been identified in *P. aeruginosa* [*rfaD*; (Lloyd et al., 2017)] and shown to directly influence LPS expression in *Salmonella enterica* [via *rfaH*; (Bittner et al., 2002, 2004)]. It is possible, therefore, that global regulatory mutations affecting the expression of multiple phage receptors could be typical for very generalist phage resistance. Crucially, only less than 10% of resistance mutants possessed generalist cross-resistance against both LPS and pilus binding phages, which suggest that these mutations are rarer. This is intuitive since there are many more mutational targets in each biosynthesis pathway compared to the single copy of the *rpoN* gene. Moreover, the evolutionary success of global regulator-mediated resistance may be limited by the extensive pleiotropic effects of such mutations on the bacterial phenotype. Consistent with this, *rpoN* mutants suffered the greatest impairment in growth rate of all the observed resistance mutations (Figure 3.4B). Interestingly, between module cross-resistance could be achieved at lower cost through mutations

affecting *pilS*, which were no more costly than other resistance mutations in type-IV pilus-associated genes, suggesting that loss of PilS-mediated activation of RpoN may have been less disruptive to the cell than loss of RpoN itself. Because RpoN controls expression of important virulence-related functions, such as quorum sensing and biofilm formation, phage combinations that select for these mutations may concomitantly drive reduced virulence.

Surprisingly, we observed that asymmetric cross-resistance was common within our cross-resistance network. Reducing the threshold used to define resistance further increased asymmetric connections between modules, suggesting that asymmetric cross-resistance may often be rather weak. While the mechanistic basis of symmetric cross-resistance appears conceptually straightforward - the two phages select for similar modifications to and/or loss of a shared receptor [e.g. via LPS modification (Betts et al., 2016a)] - the situation is likely to be more complex for asymmetric cross-resistance. We propose two potential routes to asymmetric cross-resistance: First, phages may select qualitatively different mechanisms of resistance offering different degrees of generality, for example one phage may select for mucoidy (Labrie et al., 2010; Scanlan and Buckling, 2012), masking a number of different phage receptors thus providing cross-resistance, whereas the other phage may select for modification of a specific receptor only and limited cross-resistance. Second, resistance mutations for each phage may target different points in a biosynthesis pathway, such that mutations affecting the start of the pathway will provide greater cross-resistance than those affecting targets downstream (Scanlan et al., 2015a). Consistent with the latter mechanism, within module 1, the observed mutations in *rpoN* which are likely to result in an unpiliated phenotype, provided complete cross-resistance within module 1, whereas mutations to genes lower down the pilus biosynthesis pathway [e.g. *pilB* and *pilT* encoding motor proteins which control extension and retraction of the pilus respectively; (Chiang et al., 2008)], provided cross resistance to only half of module 1 phage. Understanding the mechanistic basis of cross-resistance in general, and the symmetry of cross-resistance in particular, should be a target of future research.

Our findings show that cross-resistance and its symmetry predicts the efficacy of phage combinations both in terms of the frequency of resistance mutation and the efficiency of suppression of bacterial growth. Frequencies of resistance mutation were the highest for phage pairs with symmetric cross-resistance and

the lowest for phage pairs that showed no cross-resistance, suggesting either multi-step mutational changes or rarer generalist resistance mutations were required in the latter scenario. Consequently, phage pairs that exerted no cross-resistance often completely suppressed bacterial growth, whereas failure to suppress bacterial growth was more common for phage pairs that promoted some degree of cross-resistance evolution. Our analysis also identified individual phage strains that increased (or decreased) the performance of phage combinations more than predicted by cross-resistance alone. Although we observed an overall positive association between the strength of focal resistance and the strength of cross-resistance, in some cases focal resistance caused by a mutation was quantitatively weaker than the cross-resistance(s) or undetectable. Since spontaneous resistant mutants have not had the opportunity to specialise their resistance against the focal phage, it is perhaps unsurprising that stronger cross-resistance can arise by chance. More puzzling are the cases of undetectable focal resistance despite there being observable cross-resistance and a resistance mutation identified in the genome sequence. This phenomenon was limited to particular phages: ϕ KZ (*pilR* mutation), PA5P1 (*wzy* mutation) and PT7 (*pilS*, *pilT* and *pilJ* mutations). While we do not understand the mechanism underlying missing focal resistance, it is possible that this could be caused by extremely high rates of phage evolution to overcome the resistance mutation during the RBG assay, or particular phages being able to use an alternative surface receptor (Bertozzi Silva et al., 2016). This suggests that other properties of phage life-history are likely to affect their usefulness in phage combinations and that predictions based on cross-resistance networks could be sensitive to strong phage identity effects.

Pseudomonas aeruginosa is a common cause of opportunistic infections, frequently of burn wounds, and is also the major pathogen associated with chronic infections of the cystic fibrosis (CF) airway (Bjarnsholt et al., 2009; Driscoll et al., 2007; Pirnay et al., 2003; Willner et al., 2012). High-level antibiotic resistance frequently makes *P. aeruginosa* CF infections non-responsive to antibiotic treatments and consequently very difficult to eradicate (Deredjian et al., 2011). As a result, phage therapy has been suggested as a potential alternative or complementary treatment (Morello et al., 2011; Pires et al., 2015; Torres-Barceló et al., 2014). Phage therapy has shown promising results against *P. aeruginosa* in both artificial CF lung sputum-like environments and murine models (Waters et al., 2017). However, clinical trials of phage therapy on *P. aeruginosa*

colonised burn wounds have proved inconclusive thus far (Merabishvili et al., 2009; Rose et al., 2014). Our results suggest that unknown patterns of cross-resistance selected by the phages used in therapeutic cocktails could account for some degree of variation in the efficacy of phage therapies in these studies. Using combinations of phages that do not select for cross-resistance could potentially improve the efficacy and robustness of phage cocktails, increasing their ability to suppress bacterial growth by limiting resistance evolution. While caution is required when making inferences from simple lab experiments to far more complex *in vivo* environments, our data suggest that analysis of cross-resistance networks could aid the design process for improved therapeutic phage cocktails and warrants future *in vivo* experimental tests.

Chapter Four

Effect of sequential versus simultaneous exposure to phages on host resistance evolution

4.1 Introduction

As antimicrobial resistance continues to rise, with a potentially devastating impact on human health and the world economy (O'Neill, 2014), there has been renewed interest in the therapeutic use of phages to treat bacterial infections, which offers a viable alternative to antibiotics for some infections (Roach and Debarbieux, 2017). Yet as with antibiotics, the evolution of bacterial resistance to phages could limit treatment success (Rohde et al., 2018). Phage cocktails are considered better than single phage treatments as they can target a broader host range and are potentially more evolutionarily robust (Chan et al., 2013; Torres-Barceló, 2018). Conceptually, combining multiple phages into one treatment has the potential to suppress the evolution of resistance as multiple specific resistance mutations are less likely to arise in the same cell (Latino et al., 2016), and may impose additive fitness costs (Bohannan et al., 2002; Koskella et al., 2011). By delaying and/or moderating the evolution of resistance (Barbosa et al., 2013; Fischer et al., 2013), phage cocktails could therefore increase the likelihood of treatment success. However, co-evolution with multiple phage strains is also known to increase the rate of host evolution (Betts et al., 2016a, 2018), increasing the speed at which resistant genotypes could sweep through population making subsequent treatments more difficult. There is considerable interest therefore in understanding the evolutionary principles of phage cocktail design, for example, pre-adapting phage strains can improve their durability to the host evolving resistance (Betts et al., 2013; Friman et al., 2016; Kelly et al., 2011), and imposing concurrent selection for multiple resistances may limit the potential of host resistance evolution (Filippov et al., 2011; Tanji et al., 2004).

Host resistance is commonly acquired through mutations altering cell-surface receptors to prevent phage adsorption (Betts et al., 2016a, 2018; Gurney et al., 2017). As a collateral effect, this can provide cross-resistance to other phages targeting the same adsorption receptor (Chapter 3, Betts et al., 2016), and even to antibiotics (Chan et al., 2016). If single phage-specific resistance mechanisms

can protect the host from multiple phages targeting the same receptor, resistance may evolve as easily against multiple phages as against individual phage (Chapter 3). However, resistance to phage combinations targeting multiple adsorption receptors may be more difficult to acquire, requiring either generalist resistance (Betts et al., 2016a; Scanlan and Buckling, 2012), or multiple specific resistances (Tanji et al., 2004). We have previously found that phage combinations can be no more effective than a single phage if they promote cross-resistance, whereas phage combinations which do not promote cross-resistance to one another better suppress bacterial growth due to reduced frequencies of resistance mutations (Chapter 3). Similar to the concept of combining antibiotic and phage treatments (Torres-Barceló and Hochberg, 2016), by imposing selection on multiple different targets concurrently, we may impose additive, or even synergistic (i.e. higher than additive) stress on the bacterium.

Depending on the architecture of genetic correlations among multiple resistance mechanisms, concurrent selection may force a trade-off in resistance strength at a mechanistic level (e.g. mutation in receptor increasing antibiotic susceptibility; Chan et al., 2016; Kirby, 2012), or lead to untenably high fitness costs if the costs of each mutation accumulate additively or synergistically via negative epistasis (Bohannan et al., 2002; Koskella et al., 2011). Single mutations may be acquired which provide generalist resistance, however, this often either imposes substantial fitness costs (e.g. where mutations in transcriptional regulators such as RpoN disrupt many cell functions; Chapter 3), or only provides weak resistance (e.g. mucoidy; Betts et al., 2016; Scanlan and Buckling, 2012). Some sequential phage treatments have been proven equally as effective as simultaneous application (Hall et al., 2012), however it is unclear whether they promote different resistance profiles. Additionally, phage treatments prior to antibiotic treatment have been shown to improve bacterial killing more than either sequential treatments or the reverse order (i.e. antibiotic first; Chaudhry et al., 2017; Kumaran et al., 2018), suggesting there are important order effects when multiple selection pressures which are imposed. These differences may be compounded over longer evolutionary timescales; for example, over short timescales single mutations which can promote broad phage resistance may be selected for, whereas over longer timescales bacteria which accumulate multiple resistance mutations, along with potentially compensatory mutations, may be more dominant. We are interested in unravelling the mechanistic basis of resistance to multiple phage strains to determine if the degree of resistance evolution, and its

associated fitness costs, are dependent on the order of sequential exposure to phages, or if simultaneous exposure can produce equivalent resistance.

We compared the evolution of multi-phage resistance with *Pseudomonas aeruginosa* PAO1 strain against pairs of phage strains targeting either the same or different cell-surface receptors (LPS and Type IV pilus), selected in one-step (i.e. simultaneous exposure) or sequentially against one phage at a time for both sequential orders. For both treatments, resistant mutants were selected over limited time frames (less than 48h total growth per selection phase) to select only spontaneous mutants which would occur in a naturally diverse population. We found that sequential exposure allowed accumulation of multiple phage-specific resistances provided by mutations in cell surface receptor targets of phage adsorption without imposing any trade-offs in resistance strength. Further, the order of phage exposure determined the fitness costs of sequential resistance, such that certain sequential orders imposed much higher fitness costs than the same phage pair in the reverse order. In contrast, simultaneous selection for phage resistances resulted in weaker resistance to both phages compared to the strength of sequential resistance yet imposed similar fitness costs. This suggests that phage combination treatments can be rationally designed to limit the strength of evolved resistances and to maximise fitness costs associated with resistance.

4.2 Materials and Methods

4.2.1 Strains and culture conditions

Bacterial cultures of *P. aeruginosa* PAO1 were grown in King's media B (KB), as 6ml volumes in a 30ml glass microcosm with loose plastic fitting lids, and incubated at 37°C, shaken (180rpm). Four genetically distinct phage strains with characterised adsorption targets (see Chapter 3), were used to select phage resistance: PA5P2 and PT7 (Type IV pilus-binding phage), PA10P2 and 14/1 (LPS-binding phage). Phage cultures were prepared directly from frozen glycerol stocks, added to approximately 10^7 cells ml⁻¹ of ancestral PAO1 from overnight culture and incubated overnight at 37°C, shaken (180rpm). Phage stocks were purified by filtration to remove bacteria (0.22µm), and stored at 4°C.

4.2.2 Selection of spontaneous phage-resistant mutants

We used a modified fluctuation test (Harrison et al., 2015) to select spontaneous phage-resistant mutants against all pairwise phage combinations, under both

simultaneous and sequential selection. Three independent bacterial colonies were selected by streaking out the ancestral bacteria directly from glycerol stock onto KB agar (incubated overnight at 37°C); colonies were inoculated into 6ml KB and incubated at 37°C (shaken) for 8h, then used to found 10 subpopulations by diluting each culture 10-fold into 10 wells of a 96 well microplate containing KB media to a final volume of 200µl. Samples of these initial bacterial cultures were also frozen (20% glycerol, -80°C) to be used for replicates, and assigned the names PAO1_FT1, PAO1_FT2, PAO1_FT3.

For each ancestral replicate, we selected phage resistance against each of the 4 individual phage strains independently (1st step of sequential selection) and simultaneously against each possible phage pair (i.e. 6 different pairwise combinations) by exposing each of the 10 bacterial subpopulations to a different phage treatment. Bacterial subpopulations were diluted 100-fold into 600ul of phage stock solution (300ul of each phage for simultaneous selection) in deep-well 96 well plates, giving a multiplicity of infection of ~100 phage per bacteria at a density of ~10⁷ bacterial cells per ml, then plated out in 60ul volumes onto KB agar. For combinations with low expected mutation frequency, the complete mixture was plated (i.e. all 600ul in 60ul volumes). Following incubation at 37°C for 24h, single colonies were picked from each plate and re-streaked onto KB agar to remove phage particles and incubated overnight. If no colonies were present, the same plates were incubated for a further 24h at 37°C to allow slow-growing mutants time to produce colonies, which were then selected and re-streaked as before. Single colonies were selected from streak plates and grown overnight in 6ml KB, before glycerol stocks were prepared (20% glycerol, stored at -80°C) and characterised for phage-resistance by cross-streaking against pure stocks of each phage strain on KB agar. Any phage treatments for which no bacterial colonies could be selected, or where selected colonies lacked any phage resistance, the whole selection process was repeated using the same initial ancestral clone, inoculated directly from the glycerol stock to produce bacterial subpopulations. One clone per ancestral replicate was then chosen for further characterisation (i.e. resistance strength, fitness costs and sequence analysis), based on initial cross-streaking results. This produced a total of 12 resistant mutants selected against single phage strains (1st step sequential selection – 3 ancestral replicates x 4 phage strains), and 18 resistant mutants

selected against two phages simultaneously (i.e. 3 ancestral replicates x 6 pairwise phage combinations).

To complete sequential selection, we next exposed resistant bacteria selected against individual phages (i.e. 1st step sequential selection) to each additional phage strain (2nd step sequential selection). Clones selected in the first step of sequential selection were inoculated directly from glycerol stocks into 6ml KB and grown for 8h at 37°C, then diluted 10-fold into 3 wells of a 96 well plate to found 3 subpopulations per clone, which were used to select 2nd step sequential resistance against each of the other phage strains using the same protocol as above. This produced a further 36 resistant mutants (3 ancestral replicates x 4 1st-step phages x 3 2nd step phages). As before, any clones lacking phage-resistance, or phage treatments producing no viable colonies, were repeated. This was mainly an issue for combinations including phages PA5P2 and PT7 (both Type IV pilus binding): up to 75% of populations yielded no resistant mutants, further compounded by a lack of 'true' resistance in the selected colonies (up to 90% of selected colonies lacking quantitative resistance when selected against combinations including PT7 or PA5P2). Therefore, treatments containing phage PT7 (under both sequential and simultaneous selection) were later discarded due to extremely low mutation frequencies, lack of phage-resistance in selected colonies and high levels of bacterial contamination, indicating that true PT7 resistance is very difficult to acquire in combination with other phage strains.

4.2.3 *Quantitative resistance assays*

To determine the strength of resistance provided by mutations selected at each stage of sequential selection, and by simultaneous exposure to multiple phages, all spontaneous resistant mutants were assayed against all ancestral phage strains. Resistance assays were performed in 96 well microplates in KB media added to a final volume of 150µl. A ratio of approximately 10 phage per bacteria was used, giving densities of $\sim 10^7$ bacterial cells and $\sim 10^8$ phage particles per ml (i.e. multiplicity of infection of ~ 10). The strength of resistance was measured as Relative Bacterial Growth (RBG) in the presence of phage relative to in the absence of phage (Eq.1, where t denotes time and Abs for absorbance at 600 nm; Poullain et al., 2008), such that a value of 1 indicates complete resistance (i.e. equal growth in the presence and absence of phage). Differences in resistance strength between selection treatments, and stages of sequential

selection, were analysed using ANOVAs followed by post-hoc Tukey tests, on data blocked by ancestral replicate and phage pair identity.

For phage i , bacteria j :

$$RBG_{ij} = \frac{[Abs_{600}(t=8h) - Abs_{600}(t=0h)]_{ij}}{[Abs_{600}(t=8h) - Abs_{600}(t=0h)]_{controlj}} \quad (1)$$

4.2.4 Relative fitness of phage-resistant mutants

To assess the fitness costs imposed by different resistance mutations, we compared the growth of all resistant mutants to the ancestral PAO1 strain in the absence of phage. Bacterial cultures were inoculated into 150 μ l KB media in 96 well microtitre plates directly from glycerol stocks, and incubated at 37°C with a shaking cycle every 30mins when optical density was measured as absorbance at 600nm, for a total of 48h to produce a growth curve. The maximum growth rate was calculated for each resistant mutant and divided by the mean ancestral maximum growth rate (replicates matched within plates) to give relative fitness. A relative fitness of 1 indicates equal fitness with the ancestral strain, indicating that any resistance mutations present impose no fitness costs. The effect of selection treatment on bacterial fitness was determined using ANOVAs followed by post-hoc Tukey tests, on data blocked by ancestral replicate and phage pair identity.

4.2.5 Sequence analysis

All spontaneous phage-resistant mutants were sequenced using the Illumina MiSeq platform (performed by MicrobesNG, University of Birmingham), and resistance mutations were detected using the following bioinformatics analysis: short-reads were aligned to an annotated PAO1 reference using Burrows-Wheeler Aligner (Li and Durbin, 2009), GATK Haplotype Caller (McKenna et al., 2010) was used to identify SNPs and small indel variants, followed by annotation of gene information using SNPeff (Cingolani et al., 2012). Called variants were quality filtered by coverage (>20 reads per bp), and frequency of alternative allele (>80% of reads match alternative). Variants which occurred in all replicates were discarded as they represent differences between the annotated PAO1 reference genome (accession ID AE004091) and the ancestral genotype used in our experiments. All replicates evolved from ancestral clone PAO1_FT3 contained the same SNP in gene PA3676; therefore, because this mutation must have

arisen prior to the fluctuation test (i.e. when individual ancestral colonies were selected) and imposed no detectable fitness effect, it was ignored in subsequent analyses. Larger genetic variations, including deletions over 100bp and duplication events, were identified by analysing changes in coverage depth in R (R Core Team, 2016), and all variants were verified visually using an alignment viewer (Robinson et al., 2011). Variation in the number of mutations acquired under different selection regimes was assessed using an ANOVA with post-hoc Tukey tests, including a main effect of ancestral replicate. The relative fitness of mutants carrying either single or double resistance mutations were compared using post-hoc Tukey tests following an ANOVA.

4.3 Results

4.3.1 *Sequential resistance is rarely limited by a trade-off in resistance strength*

By exposing the bacterial host to different phages in a sequential manner, we were able to assess how the strength of resistance to each phage is influenced by the order of phage exposure. For a pair of phages targeting lipopolysaccharide (LPS) receptors (PA10P2 and 14/1), we typically found that the first-step resistance mutation provided resistance to both phages of approximately equivalent strength (Figure 4.1A, Tukey test on ANOVA interaction: $p > 0.99$ in 5 out of 6 replicates). Hence, sequential selection for second-step resistance to the alternate LPS-associated phage did not tend to increase resistance against this second phage (Figure 4.1A, Tukey test on ANOVA interaction: all $p > 0.1$). Moreover, following the second-step of sequential selection we observed only minimal trade-offs in resistance to the first phage (maximum decrease ~15%). Nonetheless the order of exposure to phages appeared to have an effect on the occurrence of trade-offs: whereas no trade-off was observed in 14/1 resistance following second-step sequential selection of PA10P2 resistance (Figure 4.1A, Tukey test on ANOVA interaction: all $p > 0.1$), PA10P2 resistance was slightly reduced following second-step sequential selection of 14/1 resistance in 2 out of 3 replicates (Figure 4.1A, Tukey test on ANOVA interaction: mean differences of -0.140 and -0.259, both $p < 0.001$).

By contrast, for pairs of phages that targeted different receptors, that is either the LPS or the Type-IV Pilus, the first-step resistance mutation rarely provided effective cross-resistance to the second-step phage. Whereas first-step resistance mutations against phage targeting LPS (PA10P2 or 14/1) provided

weak cross-resistance to the Type IV pilus-associated phage (PA5P2) in 2 out of 6 replicates (Figure 4.1B-C, Tukey test on ANOVA interactions: $p = 0.010$ and 0.001), first-step resistance mutations against PA5P2 provided no cross-resistance against the LPS-binding phages. This suggests that, unlike for the phage pair that shared the LPS receptor, multiple resistance mutations were required to protect against sequential phage pairs that targeted different receptors (Figure 4.1B-C, Tukey test on ANOVA interaction: resistance to second phage after 1st step c.f. 2nd step all $p < 0.001$). However, the strength of the first-step resistance was rarely reduced following sequential selection for the second-step resistance (1 out of 12 replicates). Indeed, we observed increases in the strength of the first-step resistance in half of the replicates following acquisition of the second-step resistance mutation (Figure 4.1B/C, Tukey test on ANOVA interaction: all $p < 0.001$). This implies that where phages target different receptors their resistances are additive when selected sequentially, and rarely impose trade-offs in the strength of resistance to phages which adsorb to different cell-surface receptors.

4.3.2 *Simultaneous phage selection results in weak resistance to both phages*

To determine if equivalent resistances against pairs of phages could be achieved in one-step rather than two sequential steps, we also selected resistant mutants against each phage pair simultaneously. Simultaneous selection by the phage pair targeting the LPS generally produced weak resistance against both phages, indeed these mutations provided weaker resistance than both the first step and second step resistance mutations observed during sequential selection with the same phages (Figure 4.1A; Tukey test on ANOVA interaction, simultaneous weaker than 1st-step sequential in 5/6 replicates $p < 0.05$; simultaneous weaker than 2nd-step sequential in 5/6 replicates, $p < 0.05$). Similarly, simultaneous selection for resistance against the phage pairs targeting different receptors consistently resulted in weaker resistance to both phages compared to sequential resistance (Figure 4.1B-C; Tukey test on ANOVA interactions: PA5P2 resistance - all replicates weaker with $p < 0.005$; PA10P2 resistance - 3/6 replicates weaker with $p < 0.05$; 14/1 resistance - all replicates weaker with $p < 0.05$). Together these results indicate that simultaneous exposure to multiple phages can reduce the strength of evolved resistance, even when the phage strains target the same receptor and promote reciprocal cross-resistance. Overall, this suggests that

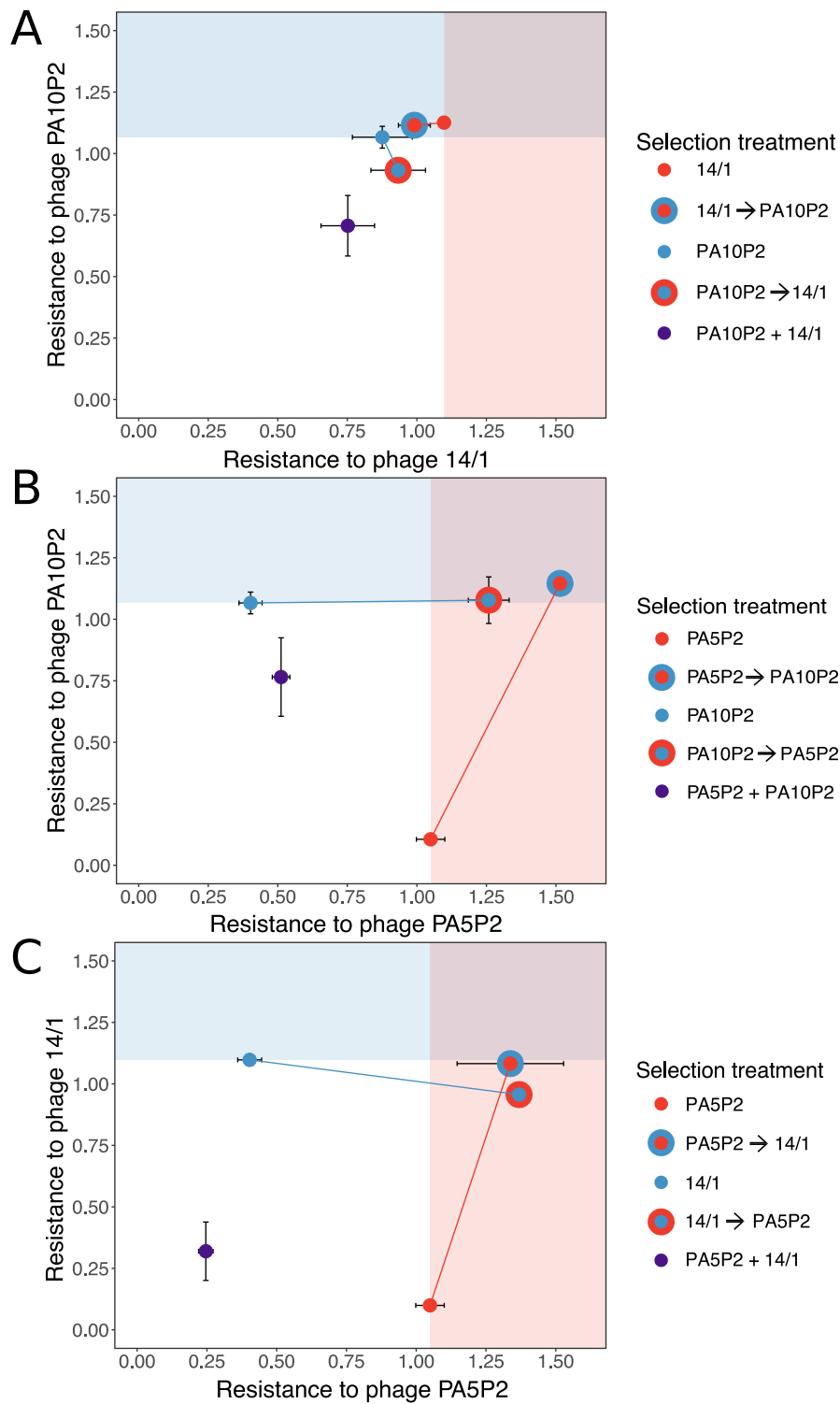


Figure 4.1 Trade-offs in the strength of resistance to each selection phage
 Strength of resistance, measured as reduction in bacterial growth (RBG), such that 1 indicates equal growth in the presence and absence of phage. Selection treatment for focal resistance is indicated by colour (see individual keys). Background shading indicates the mean resistance strength for the first step in sequential resistance treatments to highlight changes in resistance to the first-step phage in the second step of sequential selection treatments.

simultaneous exposure to multiple phages limits resistance evolution, but that this constraint can be overcome if the phages are encountered sequentially.

4.3.3 Cost of resistance against multiple phages can be determined by selection order

Sequential acquisition of resistance against multiple phages provided stronger resistance against both phages compared to mutants selected by simultaneous exposure, where in general only weak resistance against both phages was observed. The emergence of highly resistant bacteria could be limited if strong resistance against multiple phages arising from sequential acquisition of resistance mutations was associated with higher costs (i.e. lower relative fitness). Thus, we next compared the growth kinetics of the resistant mutants relative to the phage-susceptible ancestral bacterial genotype. Sequential resistance was more costly than simultaneous resistance in only less than half of replicates (Figure 4.2; Tukey test on ANOVA interactions: sequential resistance more costly in 6/13 replicates $p < 0.05$; sequential less costly in 2/13 replicates $p < 0.05$; no significant difference in 5/13 replicates). This suggests that strong resistance against multiple phages can often be acquired sequentially at no additional cost compared to weaker resistance acquired simultaneously. Nonetheless, order effects were important in determining the cost of resistance for some sequential resistances. When the first-step resistance was against a Type IV pilus binding phage followed by second-step resistance against a LPS-binding phage, we observed significant reductions in relative fitness following the second-step in half of the replicates (Figure 4.2B-C; Tukey test on ANOVA interaction: 3/6 replicates $p < 0.05$), whereas no significant change in fitness cost was observed in the opposite direction (i.e. exposure to first LPS-binding then type-IV pilus-binding phage). This suggests that the cost of resistance is mutation-specific, and fitness can be determined by order effects, suggesting that there may be epistatic interactions between specific resistance mutations.

4.3.4 The genetic basis of phage resistance after sequential versus simultaneous phage exposure

To assess how the genetic basis of resistance varied between treatments, we sequenced the whole genomes of three resistant mutants from each pairwise combination of the phages PA5P2, PA10P2 and 14/1 under both sequential and simultaneous selection regimes. Whereas single-phage resistance (i.e. first-step

of sequential selection) promoted acquisition of single mutations, selection of multiple phage-resistances was generally provided by multiple resistance mutations in both simultaneous and sequential selection regimes (Tukey test on ANOVA interaction: 2nd-step sequential v.s. 1st-step sequential, diff=1.20, p<0.0001; simultaneous v.s. 1st-step sequential, diff=1.18, p<0.001; simultaneous v.s. 2nd-step sequential, diff=-0.018, p=0.997).

For sequential resistance, we found that the first step resistance against all phages relied upon single variants in receptor-specific genes (Figure 4.3A; Table S4.1), with only one case of a secondary mutation which was likely due to hitchhiking. Most mutations conferring first-step resistance to LPS-binding phages (PA10P2 and 14/1) targeted the *wzy* gene, which encodes a polymerase involved in synthesis of the LPS B-band O-antigen (Table S4.1, see also Section 1.5.4 and Figure 1.4 for an overview of LPS structure). The LPS O-antigen forms a polysaccharide cap on the external bacterial membrane; this is variably expressed and one bacterial cell may display numerous LPS types with varying cap structure (Lam et al., 2011). All first-step resistance mutants selected using the type-IV pilus binding phage PA5P2 carried a single mutation affecting Type-IV pilus-associated genes (Figure 4.3A; Table S4.1; see also Section 1.5.4 and Figure 1.3 for an overview of Type IV pilus structure), including *pilB* (encoding a motor protein controlling pilus extension), *pilN* (encoding a product involved in pilus assembly), and *pilR* (encoding part of a two-component system regulating pilin production).

Sequential resistance against combinations of phages targeting different receptors required a combination of two mutations, each affecting a distinct receptor-specific target (Figure 4.3B; Table S4.1). Second-step resistance against the type-IV pilus binding phage PA5P2 required mutations targeting genes involved in pilus motility (*pilT* and *pilU*), extension and retraction (*pilB* and *pilY1* respectively), and structural pilins (*pilE*) (note however that for two replicates we were unable to identify the first-step mutations and therefore these sequences were discarded). Second-step resistance against an LPS-binding phage (PA10P2 or 14/1) commonly required secondary mutations in *wzy*, the same gene that provided first-step resistance against these phages. Interestingly, however, in two out of three replicates of sequential selection with PA5P2 followed by 14/1, we observed second-step mutations in a distinct target, *galU*, a

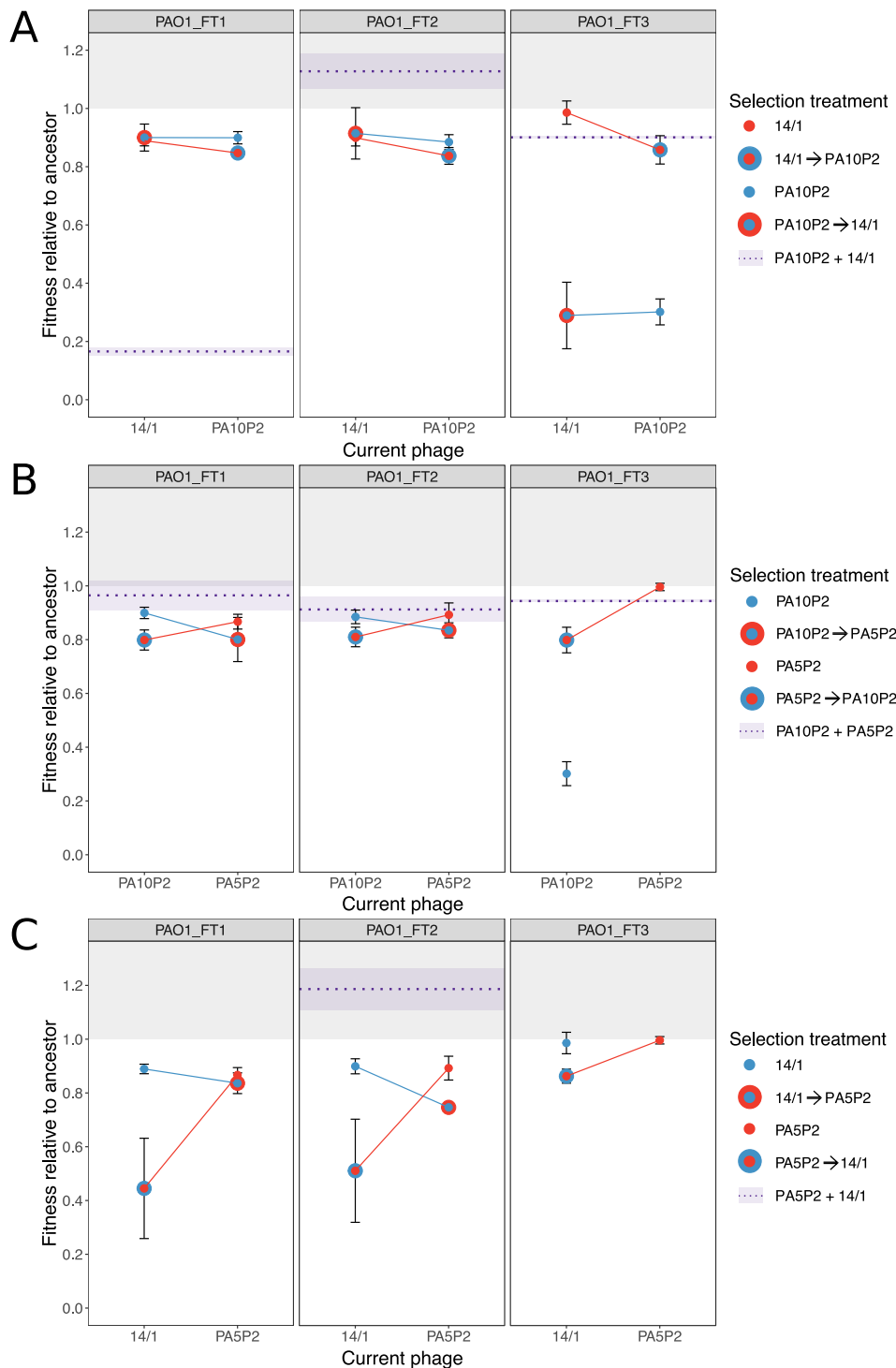


Figure 4.2 Relative fitness of resistant mutants is determined by selection regime

Fitness is measured as the maximum growth rate achieved during a 48h growth period and given relative to that of the ancestral genotype; a value above 1 (light grey background) indicates lack of fitness costs associated with resistance mutation(s). Selection treatment for focal resistances is indicated by colour (see individual keys). The mean relative fitness of simultaneous selection treatments is shown as a dashed purple line, with light purple shading to indicate standard error. Plot headings indicate which ancestral replicate was used in the fluctuation test.

uridylyltransferase involved in LPS biosynthesis. Additional mutations in non-receptor-specific genes were found in 3 out of 6 replicates where resistance to the Type IV pilus-associated phage was followed by sequential LPS-associated resistance, whilst no additional mutations were found in the reverse treatment order (i.e. LPS followed by Type IV pilus) (Figure 4.3B; Table S4.1). Taken together these genetic data confirm that trade-offs in resistance strength between combinations of phages which bind different receptors were uncommon when resistance was acquired sequentially because multiple receptor-specific mutations were acquired providing additive resistance.

For sequential resistance against pairs of phages targeting the same receptor we observed order effects for the number and targets of mutations observed. Only one mutation was detected per replicate following sequential selection with 14/1 followed by PA10P2, whereas for the reverse order we observed secondary mutations in the second-step mutants (Figure 4.3B; Table S4.1). For two replicates, we observed mutations in a gene of unknown function, PA0429, whilst the third replicate gained a second LPS-associated mutation (*wapH*, predicted glycosyl transferase; Table S4.1). It is unclear why parallel mutations in PA0429 would be selected because they provided no increase in resistance to 14/1 (in fact the first step resistance mutations in these replicates already provided strong cross-resistance to 14/1; Figure 4.1), nor any reduction of the associated fitness costs (Figure 4.4; Tukey test on ANOVA: *wzy-wzy+PA0429* $p=0.978$). By contrast, the *wapH* mutation did improve 14/1 resistance; here the first-step resistance mutation in the LPS biosynthesis gene *rml*, encoding a thymidylyltransferase, provided weak cross-resistance to 14/1 (Tukey test on ANOVA: strength of focal resistance vs. cross-resistance, $\text{diff} = -0.463$, $p<0.0001$), and furthermore, gaining the second-step resistance mutation was not associated with any increase in fitness costs (Figure 4.4; Tukey test on ANOVA: *rmlA-rmlA+wapH* $p=1$).

In striking contrast, whereas multiple receptor-specific mutations were accumulated during two-step sequential selection of resistance against phages targeting different receptors, this pattern was never observed under simultaneous selection (Figure 4.3C). Half of the resistant mutants resulting from simultaneous exposure to phage pairs with different receptor targets carried mutations in LPS-associated genes without any additional Type IV pilus-specific mutations (Figure 4.3C). Indeed, surprisingly, we were unable to identify any mutations in 2 out of

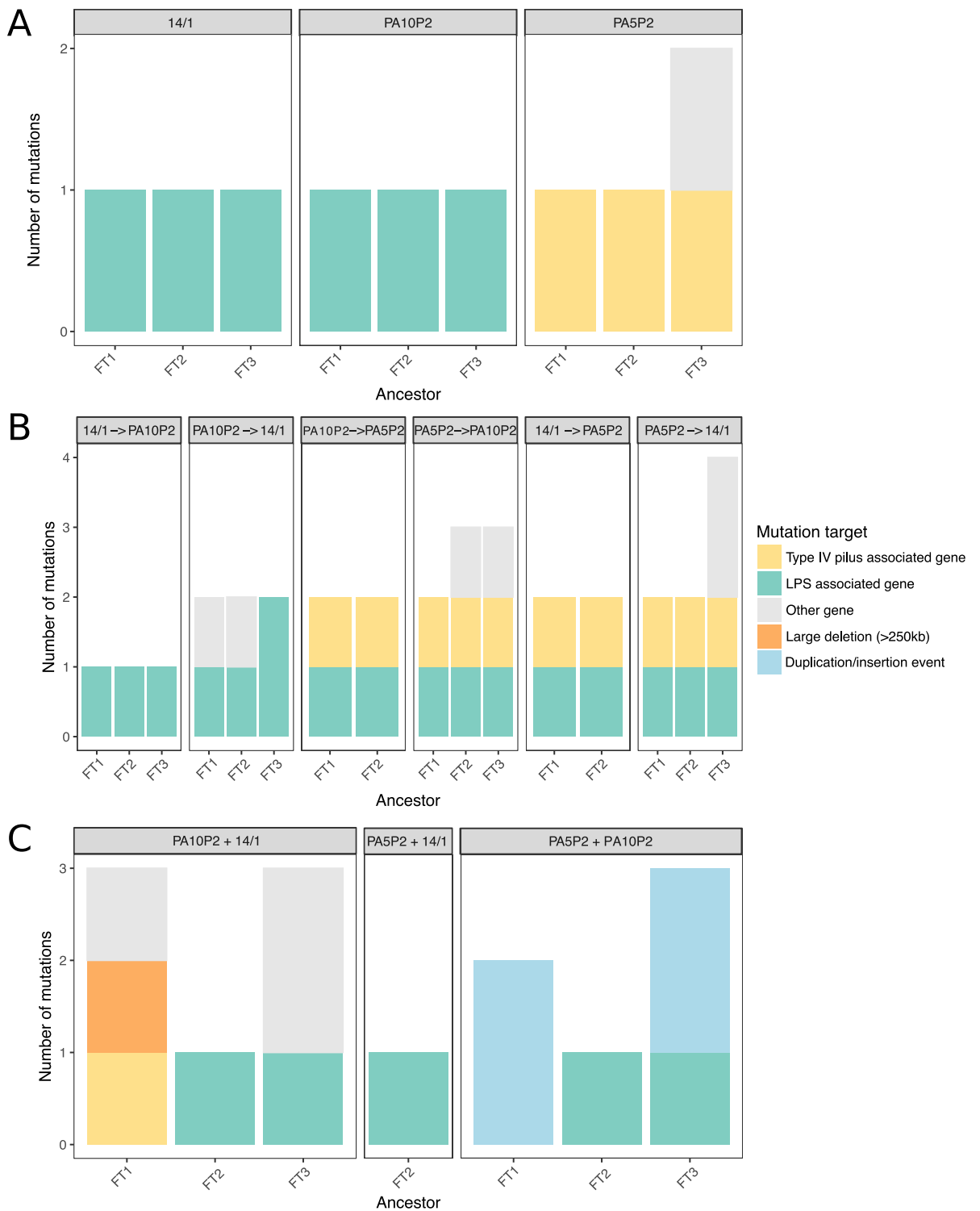


Figure 4.3 Treatment regimes determine the frequency and type of resistance mutations selected

Total number of identified mutations per resistant mutant across phage selection treatments (plot headings) under **A**) single **B**) sequential or **C**) simultaneous selection. Colours indicate category of mutational target (see key).

6 replicates, suggesting that these clones had either displayed phenotypic resistance or had subsequently undergone a reversion mutation to restore sensitivity. These potential alternative resistance strategies may also explain a high error rate in selection of resistant mutants against Type IV pilus-binding phages: up to 90% of clones selected against combinations containing Type IV pilus-binding phages were found to lack true resistance to the selection phages, indicating an alternative mechanism of resistance, or rapid reversion. Additionally the high level of failure to select any resistant colonies against these phages (up to 90% failure rate against certain combinations containing Type IV pilus-binding) indicates that true resistance mutations are potentially either very rare, or impose such high fitness costs that the bacteria cannot proliferate. In two simultaneous resistance mutants we observed duplication of the same two genes (approx. 1Mb apart) both with links to DNA recombination: one encoding a single-strand DNA binding protein (*ssb*) and the other a putative exonuclease (*PA3263*). However, what links this duplication to phage resistance is currently unclear.

Despite LPS binding phages promoting strong reciprocal cross-resistance, 2 out of 3 simultaneous resistance mutants selected against PA10P2 and 14/1 which target the LPS had secondary mutations in non-LPS genes. One had a large deletion of approx. 250 kbp (around 4% of the whole genome), affecting over 200 genes including *galU*, the LPS biosynthesis gene that was also mutated under sequential selection against PA5P2 and 14/1 (Figure 4.3C). This indicates that whilst PA10P2 and 14/1 both adsorb to the LPS, they probably target different sites, such that the strength of cross-resistance depends on specific effects of mutations on the LPS structure. Overall, this suggests that survival in the presence of two phages may be a stochastic process, where resistance against only one of the phages or a phenotypic resistance response may be sufficient to enable persistence of the bacterium.

4.3.5 *Fitness costs associated with specific resistance mutations*

Overall, mutants which acquired multiple resistance mutations were less fit than those with single resistance mutations (t-test, $t_{93,2}=4.63$, $p<0.0005$). Fitness costs were often additive for combinations of LPS and Type-IV pilus mutations, with pairs of resistance mutations imposing greater costs than single resistance mutations on their own (Figure 4.4). Second-step mutations in the LPS-associated gene *galU* increased fitness costs in combination with first-step mutations in Type IV pilus genes (Figure 4.4; Tukey test on ANOVA: pilN-

pilN+*galU* $p < 0.0001$; *pilR*-*pilR*+*galU* $p < 0.0001$), but this was not the case for *wzy* which imposed no additional cost (Figure 4.4; Tukey test on ANOVA: *pilR*-*pilR*+*wzy* $p = 0.826$). Similarly, for sequential resistance selected against the pair of LPS-binding phages, secondary mutations in both LPS and non-LPS targets were effectively cost-free (Figure 4.4; Tukey test on ANOVA: *wzy*-*wzy*+PA0429 $p = 0.978$; *rmlA*-*rmlA*+*wapH* $p = 1.00$). Whilst we were unable to calculate epistatic effects for most double mutants, as different loci were targeted in respective stages of sequential selection or multiple mutations were acquired concurrently, these results indicate that fitness costs of sequential resistance against multiple phages are likely to depend on epistatic interactions between multiple resistance mutations.

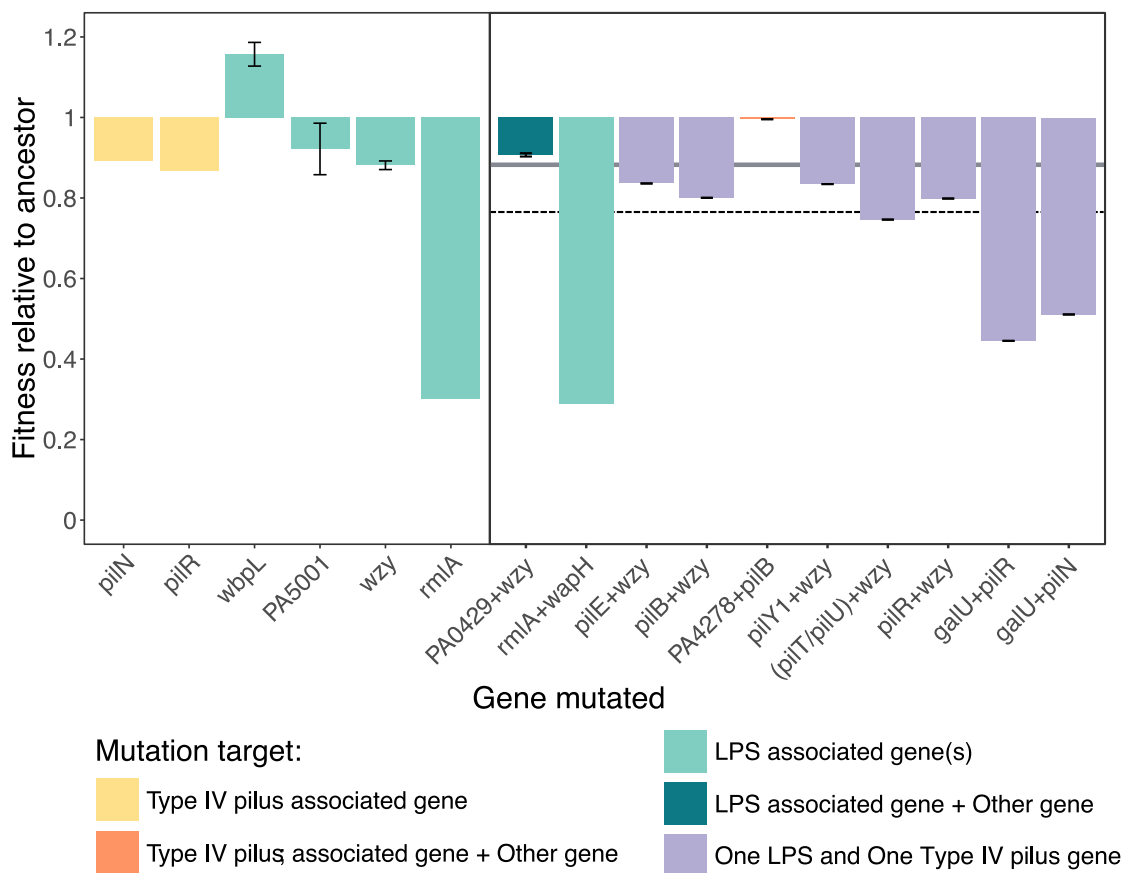


Figure 4.4 Contrasting fitness costs resulting from specific combinations of single and double mutations

Fitness relative to the ancestor, where a value of 1 indicates equal fitness and below 1 indicates a fitness cost associated with labelled single (left panel) or double (right panel) mutations. The dashed line indicates predicted additive cost of two mutations affecting different receptors, given as the sum of the mean cost of individual receptor-specific mutations (grey band; single LPS mutations = 0.886, single Type IV pilus specific mutations RF = 0.880).

4.4 Discussion

We compared the evolution of multi-phage resistance selected sequentially versus simultaneously against pairs of phage targeting either the same, or different cell-surface receptors for adsorption. Sequential resistance to phage combinations targeting different receptors was acquired by accumulation of multiple receptor-specific mutations which promoted strong additive resistance to both phage strains without trade-offs in the strength of resistance to each phage. In comparison, simultaneous exposure to multiple phages resulted in weaker resistance to both phage, through either single receptor-specific mutations, or other major genetic variations (i.e. deletion and duplication events) affecting a larger number of genes. Further, although sequentially-acquired resistance was generally much stronger, it often imposed no greater cost to host fitness than the corresponding (weaker) simultaneous resistance. This suggests that simultaneous phage exposure imposes far greater constraint on resistance evolution than sequential exposure, leading to weaker resistance at the same fitness cost.

However, when phages targeted distinct receptors, we did observe order-effects of sequential treatment in the costs of resistance. Sequential exposure to an LPS-binding phage following a Type IV pilus-binding phage decreased the relative fitness of the host, whereas there was no significant change in the cost between the two stages of sequential exposure in the opposite direction (i.e. Type IV pilus-binding phage after LPS-binding phage). Similar Type IV pilus mutations were selected in both sequential treatment orders, commonly affecting gene products involved in motility [e.g. *pilB*, *pilT* and *pilU* encode motor proteins and *pilY1* encodes an anti-retraction factor (Chiang et al., 2008; Johnson et al., 2011)]. The LPS biosynthesis gene *wzy* (Islam et al., 2010) was targeted in both sequential treatments, but imposed only modest increases in cost, whereas mutations in *galU*, a uridylyltransferase also involved in LPS biosynthesis (Dean and Goldberg, 2002), were selected twice under selection with the LPS-binding phage 14/1 following initial selection against the Type IV pilus-binding phage PA5P2 and caused severe decreases in bacterial fitness. Whereas mutations in *wzy* often affect only the B-band of LPS (Latino et al., 2016, 2017), *galU* mutations may cause broader structural changes, affecting both the LPS core and A-band (Choudhury et al., 2005; Dean and Goldberg, 2002), which may explain their more detrimental effect on bacterial fitness. Additionally, it is possible that some

primary mutations limit the acquisition of secondary mutations, for example, in second-step clones exposed to Type IV pilus-binding phage PA5P2 we were unable to detect the LPS-associated mutations in *rmlA* and *ssg* present in the first-step sequenced clone (Fernández et al., 2013; Rahim et al., 2000). Strong negative epistatic interactions between receptor-specific resistant mutations could limit or prevent the survival of bacteria carrying both mutations. Taken together these data suggest that sequential selection with Type IV pilus-binding phage followed by LPS-binding phage may both decrease the likelihood of multiple phage resistance genotypes arising, and impose substantial fitness costs upon those that do, which may be sufficient to allow eradication of the infection by antibiotic treatment, or even by the patient's own immune system.

Phages targeting the same receptor (LPS) provided strong cross-resistance to one another, such that the first-step of sequential resistance provided equally strong resistance to both LPS-binding phages through acquisition of a single mutation affecting LPS biosynthesis, irrespective of the focal LPS-binding phage used to select resistance. We therefore expected that simultaneous and second-step sequential selection against two-LPS binding phages would be equivalent to the first step of sequential selection. Consistent with this, under sequential selection resistance to both LPS-binding phages was provided by single mutations in LPS biosynthesis associated genes, and although second-step mutations were observed upon second-step exposure to 14/1 (in PA0429), this mutation neither affected resistance or fitness. By contrast, under simultaneous exposure, multiple resistance mutations were observed in two out of three replicates, one of which was a large deletion affecting approximately 4% of the host genome. This suggests that even when phages target the same receptor, subtle differences in their target sites may make it harder to resist both phages simultaneously through a single mutation, even-though single mutations providing resistance to both of the phages are available when encountered individually. This is conceptually similar to the synergy effect between phage strains, where combined killing is more effective than killing achieved by each phage single (Schmerer et al., 2014). Although our experiment did not permit phage-mediated regulation of bacterial density (as we selected spontaneous resistant mutants), this may influence the availability of resistance mutations during simultaneous phage treatments by limiting genetic variation, as slight differences in host range may permit a larger proportion of bacterial genotypes to be targeted by phage cocktails than by individual phages. Alternatively,

simultaneous exposure to multiple phages may induce host stress responses that alter the mutational landscape available to the host (e.g. through stress-induced mutagenesis; Foster, 2007), to promote adaptation. Phage DNA can trigger stress responses directed by phage shock proteins, which alter gene expression via σ^{54} the alternative sigma-factor RpoN (Weiner et al., 1991), affecting numerous systems including motility, iron uptake, protein secretion and cell envelope integrity (Darwin, 2013; Joly et al., 2010; Jovanovic et al., 2006). Further, the *P. aeruginosa bac* cluster, which contains proteins homologous to phage shock proteins, regulates cell mobility (via production of surfactants) and induces lifestyle switches to biofilm states via activation of σ^{54} the alternative sigma-factor RpoN (Macé et al., 2008). We have previously observed mutations in *rpoN* which provide cross-resistance to both LPS-binding and Type IV-pilus binding phages (Chapter 3). Therefore, whilst simultaneous exposure to multiple phages may reduce resistance evolution compared to sequential exposure due to the limited number of potential mutations which can provide resistance to both phages, they may also promote broader host adaptation responses.

Bacterial phenotypic responses to stressors may also explain why we were unable to identify resistance mutations in some hosts exposed simultaneously to multiple phage strains. Stochastic environmental changes which affect bacterial lifestyle traits can hinder phage infection in numerous ways and create heterogeneity in host phenotypes within a population (Lourenço et al., 2018): changes in temperature can affect the rigidity of the host cell membrane preventing phage infection (Labedan, 1984), and nutrient variability can reduce expression of phage receptors (Bull et al., 2014; Chapman-McQuiston and Wu, 2008; Levin et al., 2013). Changes in receptor expression levels could potentially limit phage adsorption sufficiently to enable survival of the host under simultaneous selection with multiple phage strains without leaving a genetic trace. Such resistances may be incidental to phage infection, or induced by phage products in the environment and/or products of cellular lysis, and may be considered as a phenotypic phage resistance (Bull et al., 2014; Lourenço et al., 2018). Alternatively, survival in the presence of multiple phages may require such costly resistance mutations that as soon as phage selection pressures are relieved reversion mutants restoring the original genotype rapidly outcompete the resistant genotype as the colony grows (Brockhurst et al., 2005; Chaudhry et al., 2018). Although reversion is often much less likely than acquisition of compensatory mutations (Levin et al., 2000), we saw little evidence of

compensatory mutations in our experiment, however, we did observe secondary mutations in genes of unknown function which arose concurrently with receptor-specific mutations suggesting that compensation may be occurring.

Compared to sequential selection of resistance, simultaneous exposure promoted acquisition of weaker resistance. Whereas sequential resistances in different receptor targets provide additive resistance, simultaneous exposure to multiple phages promoted a trade-off between phage resistances, often resulting in single receptor-specific mutations which promote relatively weak resistance to only one phage strain, or more complex mutational effects (e.g. duplication and deletion events) targeting many genes including those not known to be associated with LPS or Type IV pilus. Although large deletions are commonly found to provide phage resistance *in vitro* (Le et al., 2014; Pires et al., 2017), the loss of a large number of genes are likely to have broad reaching pleiotropic effects in more complex environments where bacteria must adapt to various environmental stressors (Folkesson et al., 2012; Smith et al., 2006) and may be influenced by the resident microflora (Duan et al., 2003). Additionally, single mutations which do not provide resistance to all phages present in the cocktail may not be sufficient to allow survival under sustained phage pressure (i.e. if phage propagate *in vivo*). Overall, this suggests that there are fewer mutational routes promoting bacterial survival in the presence of multiple phages simultaneously.

We found that fitness costs of multi-phage resistances could be maximised by promoting acquisition of multiple mutations in receptor genes in a particular order, specifically, by selecting resistance for Type IV pilus-associated resistance followed by LPS-associated resistance. As fitness costs are potentially exacerbated *in vivo*, due to more intense competition for resources and the requirement of expression of a broader range of traits (Cornforth et al., 2018; Rossi et al., 2018), maximising fitness costs associated with phage resistance could reduce the long-term success of resistant mutants. On the other hand, simultaneous exposure to multiple phage strains often imposed similar costs to sequential treatments, yet also promoted the evolution of weaker resistance to the phage combination. As phage treatment is a dynamic process, where as long as susceptible hosts remain, phage can propagate and potentially counter-adapt to bacterial resistance mechanisms, limiting the strength of evolved resistance may be just as beneficial as maximising host fitness costs. Further experiments

are warranted to determine the relative importance of these effects *in vivo*, as more complex environmental pressures may exacerbate fitness costs and buffer differences in resistance strength. Additionally, these results reflect the short-term evolution of resistance to a limited number of phage strains (only 3), targeting just 2 different bacterial receptors, with only 3 independent replicates. To determine whether these principles are consistently reproducible over a more diverse set of phage strains, future work is needed to incorporate the effects of both genetic and functional diversity of phages (i.e. variation in the functional phage binding receptor). Lastly, we selected resistant mutants over very short time scales (less than 48h), however, over longer time periods, the evolutionary landscape may be more complex (e.g. allowing for amelioration of fitness effects of resistance mutations).

These results highlight that the rational design of phage cocktails can limit the evolution of strong phage-resistance and determine the fitness cost of evolved resistance. Two strategies for rational design are proposed: simultaneous exposure to multiple phages targeting different bacterial receptors may limit the strength of evolved resistance, whilst maintaining relatively high resistance-associated fitness costs, providing an effective long-term therapeutic option which does not preclude additional applications. In contrast, sequential application of single phage strains may promote the evolution of strong phage-specific resistance mechanisms, but careful optimisation of phage combinations and order effects (i.e. Type IV pilus-binding phage followed by LPS-binding phage), may be the optimal way to impose the highest fitness effects and therefore promote the strongest suppression of bacterial growth. The choice of treatment strategy may be guided by the difference in relative benefits of these two strategies within the local context of disease (i.e. treatment of chronic versus acute infections), however, for both, it is clear that maximising the functional diversity of phage strains (i.e. targeting multiple bacterial receptors) is key to minimising the potential for resistance evolution.

Chapter Five

Functional diversity determines the efficacy of phage cocktails

5.1 Introduction

Bacterial killing by lytic phages regulates bacterial turnover in microbial communities, influencing bacterial community dynamics in both environmental and clinical settings (Harrison, 2007; Levin and Bull, 2004). Phages also represent a promising alternative to antibiotics for treating bacterial infection where rates of antibiotic resistance are rapidly rising (Chan et al., 2013; Pires et al., 2015; World Health Organisation, 2014). Phage cocktails for therapeutic use are commonly designed to maximise host range (e.g. Kelly et al., 2011), as communities of phages may better suppress bacterial growth and improve the efficacy of treatment if they target a larger proportion of pathogen genotypes. Surprisingly, however, the effect of phage diversity on the efficacy of phage combinations to suppress bacterial growth has not been explicitly tested. Phage diversity is predicted to exceed that of their hosts by up to 10 times (Clokier et al., 2011), and may vary between communities just metres apart (Frederickson et al., 2003). A survey of phages able to infect *Pseudomonas aeruginosa*, a commonly multi-drug resistant opportunistic pathogen (Breidenstein et al., 2011), across 4 continents identified 7 distinct phage groups with lytic activity against 87% of clinical bacterial strains tested (Ceysens et al., 2009), and novel phage taxa are continually being discovered (Amgarten et al., 2017; Sepúlveda-Robles et al., 2012). When designing a phage cocktail, is more diverse always better in terms of its efficacy?

Increasing species richness has been shown to improve the function of microbial communities by two distinct mechanisms (Bell et al., 2005; Evans et al., 2017). Firstly, if species perform different ecological roles, then higher diversity communities can deliver higher performance due to functional complementarity, through filling more of the available niche space (Bell et al., 2005; Salles et al., 2009). Secondly, more diverse communities are more likely to contain highly performing taxa simply by chance, leading to a positive relationship between diversity and function through the so-called selection effect (Bell et al., 2005;

Evans et al., 2017). Understanding the mechanisms of complementarity in community function and the roles performed by highly performing species are likely to aid the design of effective phage cocktails.

On the other hand, functional redundancy among species in a community leads to diminishing returns of further increasing species richness, resulting in a saturating relationship between diversity and function (Petchey and Gaston, 2006; Tilman et al., 1997; Yin et al., 2000). This suggests that if the functional diversity of phage combinations can be maximised at lower levels of species richness then simpler phage cocktails could achieve equivalent efficacy as more diverse cocktails, thus reducing the manufacturing and regulatory challenges (Brüssow, 2012; Merabishvili et al., 2018; Verbeken et al., 2012). For phages, a key functional trait is likely to be the bacterial cell-surface receptor used by the phage for adsorption during lytic infection. Thus phage combinations targeting higher numbers of receptors would be predicted to be more efficacious because they would limit the potential for bacteria to evolve resistance via cell surface modification since this would likely require multiple mutations (e.g. Betts et al., 2018; Gurney et al., 2017; Tanji et al., 2004), potentially imposing additive fitness costs (Koskella et al., 2011), and reduce the competition among phages for shared adsorption sites.

By applying the principles of biodiversity-ecosystem functioning to phage cocktails, we hope to determine the relative importance of species richness, functional diversity and phage identity effects on the efficacy of multi-phage treatments. We constructed 827 different phage combinations, ranging in species diversity from 1-phage to 12-phages, incorporating functionally diverse phages targeting either Type IV pilus or lipopolysaccharide (LPS) for adsorption. We show that phage diversity has a saturating relationship with efficacy (i.e., suppression of bacterial growth), such that low diversity phage combinations could provide high performance provided that they had high functional diversity (i.e., targeted multiple distinct adsorption receptors). Additionally, we developed a pathway analysis method to assess the influence of cross-resistance structure on phage combination performance and show that the addition of phage strains that do not promote cross-resistance to other members of the combination cause large improvements in the efficacy of the phage cocktail.

5.2 Materials and methods

5.2.1 Phage combination design and assembly

A set of 12 phages which were characterised in Chapter 3 were used to build phage combinations of varying diversity. Of these 12 phages, 4 were known to adsorb via the Type IV pilus, and 8 via LPS. In total, we assembled 827 different phage combinations, ranging from single phage (12), all possible 2- and 3-member communities (66 and 220 respectively), a random partition of 4- and 6-member communities (264 of each), and the full 12-member community. A random partition design was used to select 4 and 6-phage communities which equally represent all phage strains across both diversity levels, as described by Bell *et al.* (2009).

Phage stocks were propagated using the bacterial host *Pseudomonas aeruginosa* PAO1. Overnight bacterial cultures, grown in 6ml KB and incubated at 37°C with shaking at 180rpm, were diluted 100-fold into new media (6ml KB), then phage were added directly from glycerol stocks (stored in 20% glycerol at -80°C). Following overnight incubation phage cultures were filtered (0.22µm) to remove bacteria and stored at 4°C until use. To limit human error, triplicate master plates of phage communities were assembled in deep 96 well plates using a liquid handling robot (epMotion® 5070, Eppendorf, Germany). Equal volumes of each phage were added to give a final volume of 120µl per community.

5.2.2 Measuring the efficacy of phage combinations

Bacterial replicates were inoculated from three single colonies into 6ml KB and grown overnight at 37°C with shaking at 180rpm, before diluting 100-fold into assay plates containing 120µl of KB. Phage communities were transferred from the master plates (15µl per well) to give a multiplicity of infection of approximately 100 phage per bacterial cell (actual MOI $\sim 80.4 \pm 20.2$ with initial bacterial density of $\sim 9.6 \times 10^7 \pm 1.1 \times 10^7$). Optical density (absorbance at 600nm; Abs_{600}) was measured immediately, then after 24h incubation at 37°C, static. Cocktail efficacy was measured as reduction in bacterial growth (Eq 1, 1-RBG; Poullain *et al.*, 2008).

For phage i , bacteria j :

$$Reduction_{ij} = 1 - \frac{[Abs_{600}(t=8h) - Abs_{600}(t=0h)]_{ij}}{[Abs_{600}(t=8h) - Abs_{600}(t=0h)]_{controlj}} \quad (1)$$

5.2.3 Modelling the diversity-efficacy relationship

The relationship between phage diversity (i.e. strain richness) and reduction in bacterial growth was analysed using a linear model method designed to separate significant factors affecting biodiversity-ecosystem functioning (Bell et al., 2009). Phage diversity and functional diversity (i.e. number of different receptor targets) were included as interacting main effects, alongside other main effects of receptor targets (i.e. LPS and Type IV pilus), phage identity, non-linear phage diversity, and community ID. Due to the saturating relationship between phage diversity and reduction of bacterial growth, we also fitted a non-linear asymptotic exponential model to the data. Model parameters were determined using the nonlinear least squares function in R (R Core Team, 2016), and compared to equivalent linear models using Akaike Information Criterion (AIC).

5.2.4 Characterisation and pathway analysis of cross-resistance

To test the effect of cross-resistance (CR) structure on the efficacy of phage combinations, we determined stepwise changes in phage efficacy and cross-resistance structure between phage communities which are subsets of one another. By adding community members in a stepwise manner it is possible to form pathways of increasing diversity (i.e. starting with a 1-phage community and introducing additional phage strains in a stepwise manner to produce 2, 3, 4, 6 and 12 member communities; Figure 5.1). We identified 52,200 unique pathways based upon the 827 different phage communities in our experiment. For each community, we determined the cross-resistance structure of the phage combination based on previous characterisation of all pairwise cross-resistance interactions (Chapter 3). Some communities were composed of only one type of cross-resistance interaction (i.e. all symmetrical, or all asymmetrical), others had mixed symmetry (i.e. include both symmetrical and asymmetrical interactions), and communities containing any phage pairs which did not promote cross-resistance were categorised separately (as Include Non-CR). By characterising the unique stepwise changes between adjacent diversity levels within each pathway (4,288 in total), we were able to determine how transitions in cross-resistance structure influence the efficacy of phage combinations. Main effects of

existing cross-resistance structure and the introduction of phages to yield novel cross-resistance interactions on phage combination efficacy at different diversity levels were determined using an ANOVA with post-hoc Tukey tests to determine significant interactions.

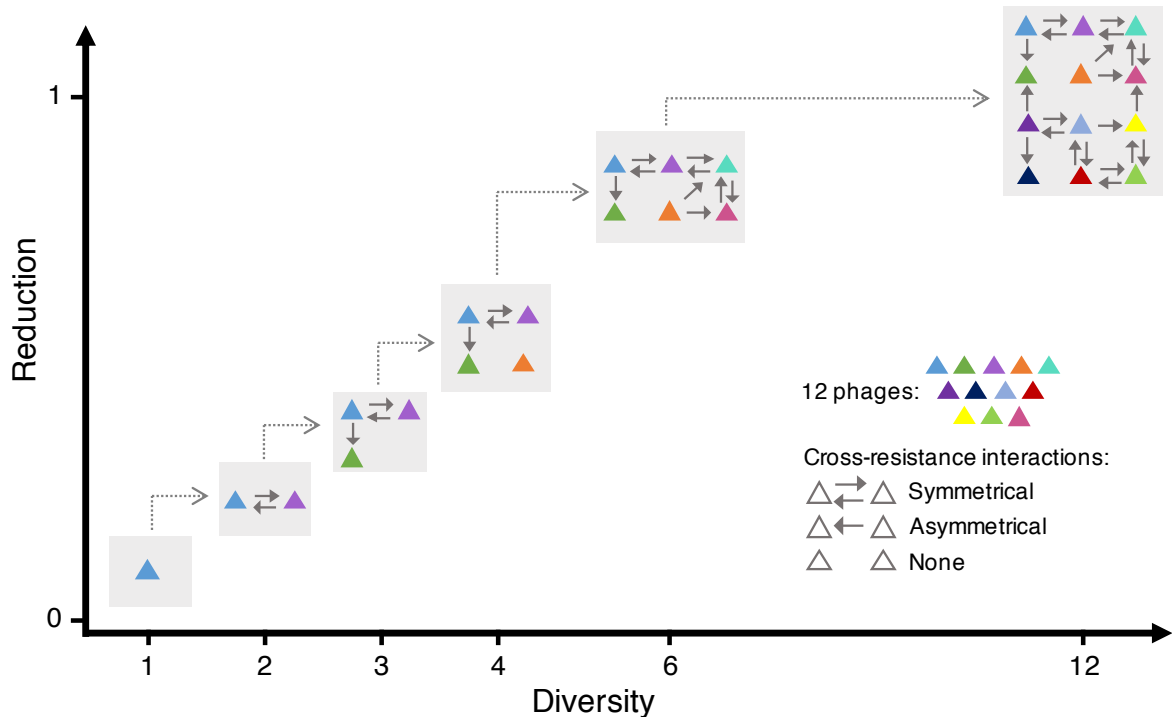


Figure 5.1 Illustration of the pathway analysis methodology

This illustrates one potential pathway out of 52,200 unique possibilities within the dataset. A pathway is built of stepwise increases in phage diversity, starting with a 1-phage community, and building up to the full 12-phage community. At each level, the cross-resistance structure of the community can be characterised (note that the interactions shown here are purely illustrative), and the Reduction value demonstrates the efficacy of the combination. By comparing the stepwise changes in these characteristics (grey dashed arrows) we can determine the key factors of cross-resistance which influence the effectiveness of phage combinations.

5.3 Results

5.3.1 Diminishing returns of increasing phage diversity on phage cocktail efficacy

To explore the effect of phage diversity on the suppression of bacterial growth, we constructed 827 different phage communities from a pool of 12 phages. This included all possible single, pairwise and tripartite phage combinations (12, 66 and 220 communities respectively), a randomly partitioned subset of 4- and 6-phage communities (264 of each), and the full 12-phage community. Phage diversity (i.e. number of strains) explained only 30% of variation in efficacy of

bacterial growth reduction (linear model: $F_{1,5740}=2497$, $p<0.0001$, $R^2=0.303$). Non-linear models explained a greater proportion of the variation: the relationship between diversity and reduction of bacterial growth was best explained by an asymptotic exponential model (Figure 5.2; $AIC_{\text{linear model}} = 205$; $AIC_{\text{asymptotic model}} = -1190$) where the asymptote was reached when bacterial growth was completely suppressed (i.e. reduction = 1). This suggests that low diversity phage combinations were capable of suppressing bacterial growth equally well compared to much more diverse phage combinations indicative of functional redundancy in phage efficacy to reduce bacterial growth among the constituent phage strains.

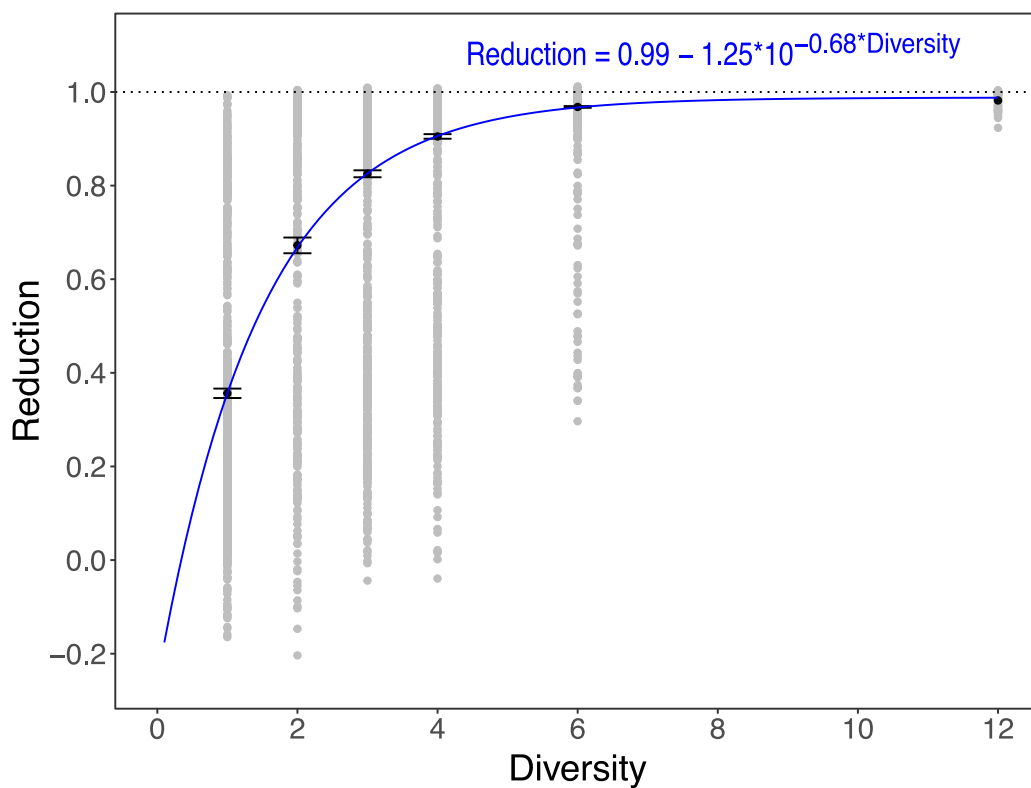


Figure 5.2 Saturating relationship between the efficacy and diversity of phage combinations

Mean reduction (\pm s.e.) of bacterial growth in the presence of phage relative to phage-free growth, where 1 indicates complete suppression of bacterial growth by the phage community, with raw data in grey to emphasise distribution. An asymptotic exponential with the equation shown was fit to the data using a non-linear least squares model.

5.3.2 Higher functional diversity of phages improves cocktail efficacy

Functional diversity can often explain variation in performance among communities better than species diversity, particularly where there is functional redundancy among the community members. In phages, one key functional trait

is the cell surface receptor used for adsorption. We have previously identified the cell-surface receptor targeted by each of the phages used here (see Chapter 3). Of these 12 phages, 4 phages adsorb to the Type IV pilus whilst the remaining 8 phages adsorb to the lipopolysaccharide (LPS). We found that phage functional diversity and strain diversity together explained ~70% of the variation in reduction in bacterial growth (linear model with main effects of phage diversity and functional diversity and their interaction: $F_{3,5738}=4476$, $p<0.0001$, $R^2=0.701$). Although phage combinations required both LPS- and Type IV pilus-binding phages to be highly performing, Type IV pilus binding phages contributed more to phage combination efficacy than LPS-binding phages (linear model coefficient of Type IV pilus-binding phages: $t=11.16$, $p<0.0001$; linear model coefficient of LPS-binding phages: $t=-24.57$, $p<0.001$). Consistent with this, for combinations of phages targeting only one surface receptor type (i.e. low functional diversity), Type IV pilus-binding phages outperform LPS-binding phages, although both types show linear increases in efficacy with increasing phage diversity (Figure 5.3A-B). By contrast, combinations containing both LPS- and type IV pilus-binding phages (i.e. high functional diversity) showed a saturating relationship between efficacy and phage diversity and were better able to completely suppress bacterial growth at lower levels of phage diversity (Figure 5.3C). Phage identity accounted for only ~3% of remaining variation (linear model: $F_{12,5730}=15.45$, $p<0.0001$), suggesting that although the presence of certain phage strains can influence phage combination efficacy (see Chapter 3), phage functionality (i.e. target receptor) is a much better predictor of its contribution to phage community function.

When the efficacy of phage combinations were compared to that of their best constituent (i.e. the community member with the highest reduction value when tested alone), these results are further supported. All combinations with high functional diversity performed significantly better than their best constituent alone [multiple one-sided t-tests on relative reduction ($\text{Reduction}_{\text{combination}} / \text{Reduction}_{\text{best constituent}}$); all p -values <0.005], whereas phage pairs binding to the same receptor (i.e. low diversity combinations with limited functional diversity), performed no better than their best constituent alone (multiple one-sided t-tests on relative reduction; all p -values >0.05). This suggests that phage combinations with low functional diversity depend more strongly on the selection effect, where the efficacy of the community is dependent on the presence of more effective individual constituents, than combinations with a higher functional diversity.

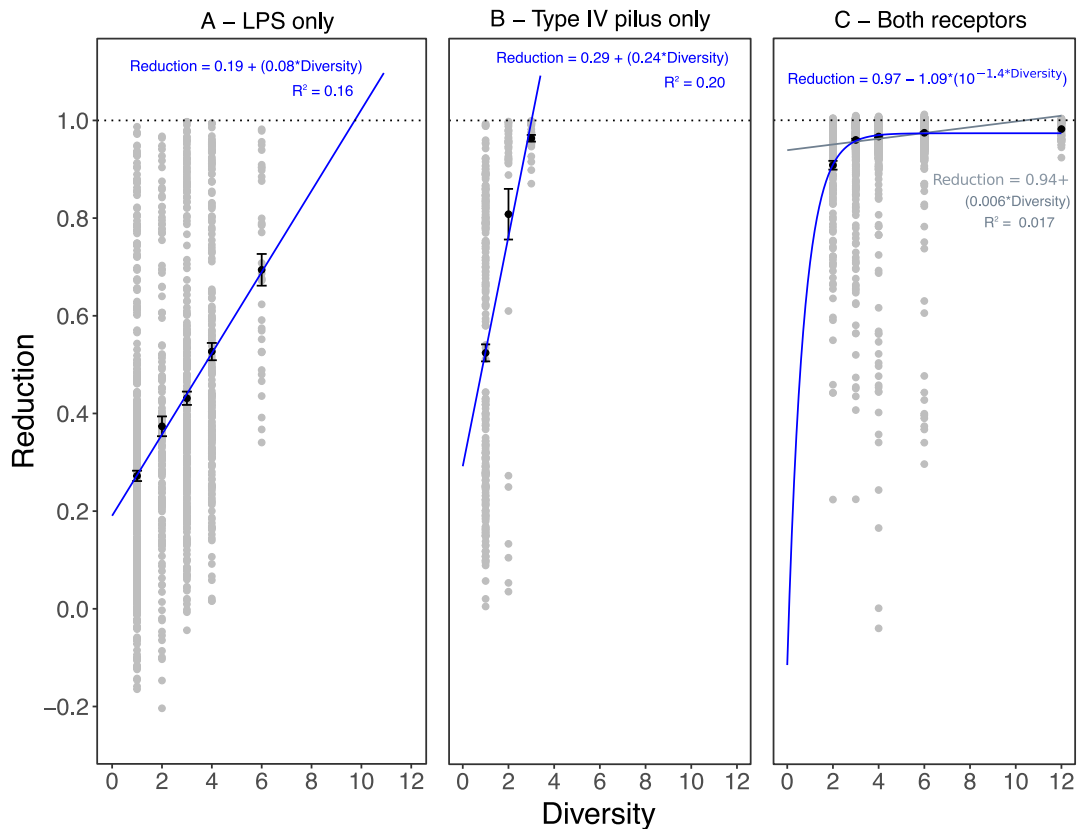


Figure 5.3 Receptor classification determines the linearity of the diversity-reduction relationship

Reduction in bacterial growth by phage combinations where all phage target (A) LPS, or (B) Type IV pilus, and by combinations with diverse phage targets (C). Mean reduction (\pm s.e.) at each diversity level is shown in black, with raw data in grey to show distribution of data points. Optimal models for the effect of diversity on reduction of bacterial growth, determined by Akaike information criterion (AIC), are shown in blue, either as asymptotic exponential or linear regression.

5.3.3 Addition of phages which minimise cross-resistance improves cocktail efficacy

One possible explanation for the higher efficacy of high functional diversity phage combinations targeting multiple cell surface receptors is that they minimise the probability of cross-resistance evolution. Cross-resistance occurs when evolution of resistance against one phage provides bacteria with concomitant resistance to another distinct phage, and this is most likely to occur for phages that adsorb to the same cell-surface receptor. Having previously characterised the network of cross-resistance interactions for the phages used here (Chapter 3), we next assessed the contribution of cross-resistance to the efficacy of phage combinations. Using a novel pathway analysis, we identified subsets of phage

communities linked by the stepwise addition of phages (Figure 5.1). We identified 52,200 unique pathways among the 827 different phage communities in our experiment, comprising 4,288 unique transitions in community composition. For each stepwise addition, we then determined the change in cross-resistance structure (Figure 5.1) and phage combination efficacy (i.e. reduction in bacterial growth; Figure 5.4).

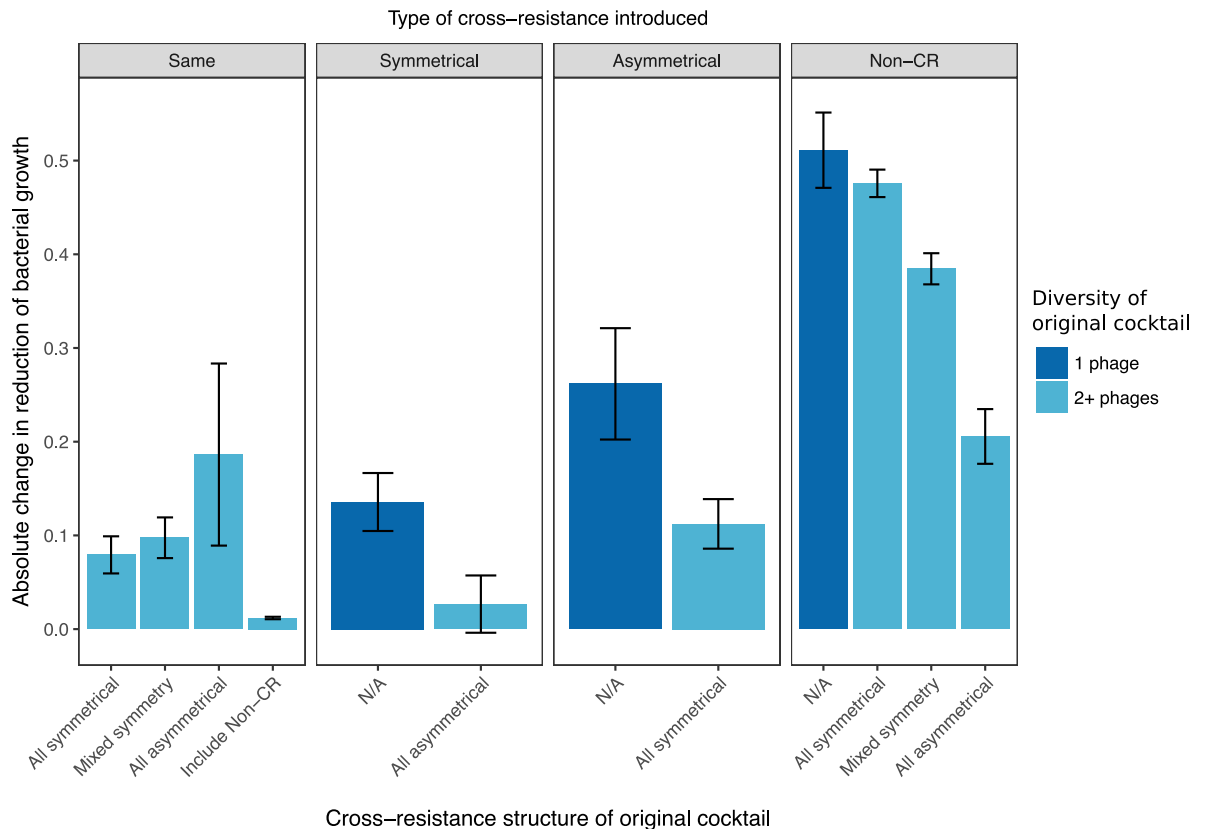


Figure 5.4 Stepwise changes in cross-resistance structure reveal key transitions in the efficacy of phage combinations

Pathways through adjacent diversity levels were broken down into 4,288 unique stepwise transitions. For each step, we characterised the cross-resistance structure of the original community (x-axis), with single-phage communities highlighted in dark blue, and classified the change in cross-resistance structure by the addition of novel interactions (panels). Improvements in cocktail efficacy were measured as the mean change in reduction of bacterial growth (\pm s.e.).

The greatest improvements in the efficacy of phage combinations were gained when a phage was added that promoted no cross resistance to the other phages already present in the combination (Figure 5.4; Tukey test on ANOVA interaction: Non-CR v.s. Asymmetrical diff=0.280 $p < 0.0001$; Non-CR v.s. Symmetrical diff=0.284 $p < 0.0001$). This effect was strongest for transitions from a 1-phage to

a 2-phage combination and for higher diversity combinations where the pre-existing structure of cross-resistance was symmetrical (Figure 5.4; Tukey test on ANOVA interaction: comparisons of single-phage treatments and symmetrically cross-resistant communities to communities with mixed symmetry or asymmetry only, all $p < 0.0001$). Additionally, greater increases in phage efficacy were gained when a phage that was added promoted asymmetrical cross-resistance compared to symmetrical cross-resistance (Figure 5.4; Tukey test on ANOVA interaction: $p = 0.035$) in transitions from 1-phage to 2-phage combinations. This pathway analysis suggests that adding phages that promote minimal cross-resistance to the other phages already present in the combination provided the greatest improvement in performance of phage cocktails.

5.4 Discussion

To enable rational design of phage therapy cocktails, it is important to understand the factors which determine the efficacy of phage combinations in suppressing bacterial growth. Applying concepts from the analysis of biodiversity-ecosystem function relationships, we determined the relative contributions of phage diversity, identity and functional diversity to phage cocktail efficacy. We observed a saturating relationship between phage richness and efficacy. Combinations with higher functional diversity in terms of the number of cell surface receptors targeted for phage adsorption were more effective at suppressing bacterial growth, and were able to do so completely at very low levels of diversity (2-3 phages). Large improvements in the performance of combinations were driven by the stepwise addition of phage that did not promote cross resistance to other phages already present in the combination. Together, these data suggest that effective phage combinations can be designed by choosing specific strains that target multiple distinct cell surface receptors and promote low rates of cross-resistance, both of which are properties that can be achieved at relatively low phage diversity levels.

The mean efficacies of phage combinations using multiple receptor targets were best described by an asymptotic exponential model, demonstrating a saturating effect of diversity whereby additional phages do not improve cocktail efficacy presumably due to their functional redundancy. This suggests strong complementarity among phages targeting distinct bacterial cell-surface receptors (i.e. a complementation effect; Salles et al., 2009), possibly by limiting the evolution of host resistance. In contrast, phage combinations with low functional

diversity (i.e. only targeting one cell-surface receptor) were influenced more strongly by phage identity and diversity than functionally diverse phage communities. This indicates a potential selection effect as more diverse communities are more likely to contain highly effective individuals (Bell et al., 2005; Evans et al., 2017). Additionally, we found that the efficacy of phage combinations with both low diversity and functional diversity were limited by the activity of their best constituent, which suggests a strong selection effect for these combinations. In contrast, combinations with a higher functional diversity, even with only 2 constituents, were able to outperform their best constituent, indicating complementation in the activity of phages which bind to different bacterial receptors. Whilst our phage combinations were assessed using one host genotype over a relatively short period of time, allowing higher host genotype diversity and extended time for resistance evolution to occur may reveal differences in the relative contribution of phage identity and richness compared to functional phage diversity. Functional diversity is likely to be important in chronic infections, where extensive diversification in bacterial genotype are typically observed during adaptation to the infection environment (Mowat et al., 2011; Smith et al., 2006) and competing microflora (Harrison, 2007). Such within-host adaptation frequently leads to highly heterogeneous bacterial populations that vary in expression of common phage receptor targets, including modification and even loss of LPS and Type IV pilus (Hancock et al., 1983; Huse et al., 2010; Mahenthalingam et al., 1994). Higher functional diversity could allow infection of a broader range of bacterial genotypes even following within host diversification (Friman et al., 2013; Mattila et al., 2015). Here we were limited to a functional diversity of 2 receptor binding types, but further increases in functional diversity for example by adding phages targeting additional distinct receptors such as outer membrane porins (Chan et al., 2016) and other membrane anchored proteins such as TonB, which is involved in iron-siderophore uptake (Betts et al., 2018; Poole et al., 1996), is likely to lead to further increases in efficacy. Additionally, if rare bacterial genotypes are particularly important in causing serious disease, then strong identity effects are expected to apply to as phage targeting these bacterial cells will contribute more than average to the efficacy of the phage cocktail, suggesting it is important that phage therapies are designed to target a broad range of patient-specific bacterial genotypes (Pirnay et al., 2010). By combining these concepts into rational design principles, phage cocktails could be optimised to both target a broad range of host genotypes and maximise

functional diversity to create highly effective phage cocktails, which minimise resistance evolution, with minimal phage richness.

A broader range of bacterial resistance mechanisms may be encountered *in vivo*, including adaptive resistance mechanisms such as CRISPR (Horvath and Barrangou, 2010). Unlike surface modification resistance mutations, CRISPR-mediated resistance is likely to promote different cross-resistance interactions between phages due to their genetic similarity rather than their functionality (i.e. receptor target for adsorption). Additionally, inducible resistance mechanisms may be preferentially selected *in vivo*, if they impose fewer fitness costs compared to surface modification (Westra et al., 2015). This suggests that whilst functional diversity of phage strains is necessary to limit the evolution of cross-resistance via surface modification, maximising genetic diversity could be important to limit cross-resistance via alternative resistance mechanisms.

Using a novel analysis method ('pathway analysis', see Figure 5.1) we determined how stepwise transitions in community structure changed phage cocktail efficacy. This analysis revealed that the largest improvements in cocktail efficacy were achieved by addition of phage strains which do not promote cross-resistance to other phages already present in the cocktail. However, it was not necessary to completely restrict cross-resistance interactions to improve community function, as novel asymmetrical interactions were also beneficial to the overall efficacy. As asymmetrical cross-resistance is more common between Type IV pilus-binding phage than between LPS-binding phage (Chapter 3), which are more likely to promote symmetrical cross-resistance to one another, this may explain why minimal communities of pilus-binding phage had high efficacy, whereas even 6-phage communities were unable to completely suppress bacterial growth for combinations of phages that all targeted the LPS. Receptor loss may impose much higher fitness costs *in vivo*, due to pleiotropic effects (Bohannan et al., 2002; Scanlan et al., 2015a) and the requirement of a wider range of traits for fitness in more complex environments (Skurnik et al., 2013; Smith et al., 2006; Winstanley et al., 2016). We may, therefore, expect to observe a higher frequency of asymmetrical cross-resistance in complex environments where complete loss of a receptor is associated with severe fitness costs in the bacterium.

Overall, we show that effective phage combinations maximise functional diversity in terms of receptors targeted for adsorption because this limits the evolution of

cross-resistance. We observed complementarity of phage combinations with high functional diversity, allowing them to outperform their best constituents even at low phage diversity, suggesting that highly effective combinations do not require high species diversity. Whilst other factors such as phylogenetic relatedness among phages and strong phage identity effects may play a role in determining efficacy *in vivo*, functional diversity provides a fundamental basis for phage cocktail design. Low diversity phage combinations which maximise functional diversity have the potential to simplify the design, manufacturing and regulatory requirements for therapeutic cocktails whilst optimising their efficacy and therefore warrant further investigation.

Chapter Six

Discussion

Lytic infection by phages regulates bacterial density and therefore phages shape the structure of microbial communities across a wide range of ecosystems, including within some clinical bacterial infections (James et al., 2015; Levin and Bull, 2004; Weinbauer and Rassoulzadegan, 2004). Phages may provide alternative or complementary therapies to replace or augment antibiotic treatments that are becoming less effective due to high rates of resistance (Chan et al., 2013; Torres-Barceló and Hochberg, 2016; World Health Organization, 2014). Like antibiotics, bacteria readily evolve resistance to phages, thus to ensure that phage therapies are sustainable in the face of resistance evolution we must understand the ecological and evolutionary processes governing the emergence of phage resistance in bacteria. In this thesis, I explored how bacteria-phage infection networks (BPINs) are influenced by environmental factors, and how the genetic mechanisms which promote cross-resistance underpin the structure of bacteria-phage communities and are likely to influence phage therapies. Imbalances in selection pressures at low resource levels, magnified by increased encounters in mixed environments, destabilised bacteria-phage co-evolution and drove phage to extinction, in *Pseudomonas fluorescens* SBW25-phage Φ 2 populations (Chapter 2). Network analysis of these populations through time revealed that phage populations were rescued by reinvasion of phage-susceptible bacterial genotypes that swept through the population to high frequency (Chapter 2). This demonstrates that BPIN structures are dynamic through time, shaped by coevolutionary dynamics, and significantly influenced by the abiotic environment. Next, I characterised the genetic interactions which underpin BPIN structure, by assessing the structure of cross-resistance evolution by *Pseudomonas aeruginosa* PAO1 against a panel of 27 lytic phage strains. Cross-resistance was common between phage strains which adsorb to the same bacterial receptors, creating a modular cross-resistance network defined by phage target receptors (Chapter 3). The genetic basis of resistance was further explored by comparing the evolution of resistance under sequential versus simultaneous exposure to multiple phages. Whilst sequential exposure allowed the accumulation of multiple receptor-specific mutations which promoted strong resistances against both phages, simultaneous exposure to phages results in

weaker resistances, but imposed similar fitness costs (Chapter 4). Finally, I assessed the influence of phage diversity on the efficacy of phage combinations to suppress bacterial growth and found that highly effective combinations are characterised by high functional diversity (i.e. target multiple different adsorption receptors) (Chapter 5). These data provide insight into the mechanisms which drive resistance evolution against combinations of multiple phages and may be exploited to aid the rational design of phage cocktails to improve the efficacy and durability of phage therapy.

6.1 Insights into community structure from network analysis

6.1.1 Community structure is determined by resistance interactions

We implemented two forms of network analysis to characterise the community structure of bacteria-phage interactions at the population level (Chapter 2), and at a genetic level, to show how cross-resistance evolution influences community structure (Chapter 3). Differences in connectance (i.e. the proportion of realised links) and the mean strength of interactions within bipartite bacteria phage-infection networks (BPINs) of *P. fluorescens* SBW25 and phage Φ 2, helped to reveal the mechanism of phage extinction in low resource communities; increased connectance with reduced interaction strengths indicate that highly phage susceptible bacterial genotypes sweep through the population to rescue phage from extinction (Chapter 2). To understand the more fundamental processes underlying phage resistance, and the mechanisms which promote cross-resistance in particular, we characterised the evolution of cross-resistance by *Pseudomonas aeruginosa* PAO1 against 27 different lytic phages, to produce a cross-resistance network (Chapter 3). This network elucidates the gene-gene interactions which underpin BPIN structure, specifically, how modification of bacterial cell-surface receptors has the potential to influence numerous interacting phage species. Therefore, a logical next step would be to investigate the genetic interactions between phage strains, and how this influences infectivity and host range, and gain a better understanding of how bacterial cross-resistance and phage cross-infectivity networks influence BPIN structure and bacteria-phage co-evolution at the community level.

6.1.2 Network parameters may be influenced by environmental context

The modular structure of the cross-resistance network characterised in Chapter 3 was determined by surface-modification based resistance evolution; cross-resistance was more likely between phages which adsorb to the same receptor

than between phages using different receptors, as resistance was acquired by mutations which resulted in modification or loss of the adsorption receptor. Therefore, bacteria which have alternative resistance mechanisms may promote changes in the modularity of cross-resistance. Further, as the expression of different resistance mechanisms may vary across ecological landscapes depending on the relative investment in constitutive versus inducible defences (Westra et al., 2015), modularity is likely to be dynamic, depending on the variability and expression of different phage-resistance mechanisms present in the population.

6.1.3 *Future directions for network analysis in bacteria-phage interactions*

Network analysis is a highly adaptable tool which has the potential to uncover key ecological and evolutionary dynamics within bacteria-phage interactions. Cross-resistance interactions are likely to be highly dependent on species diversity of both bacteria and phage. Multiple phages can interact synergistically (Schmerer et al., 2014), or may compete by interfering for lytic infection by exclusion (Dulbecco, 1952; Labrie et al., 2010) or by promoting phage lifestyle switches [e.g. choice between lytic and lysogenic infection, (Erez et al., 2017)]. Therefore, future experiments should consider variation in species diversity and adaptability as key factors which determine cross-resistance structure. Further, assessing the abiotic factors which influence connectance within BPINs and CR networks could improve our understanding of the structural dynamics of natural bacteria-phage populations, and how they remain robust to environmental and evolutionary changes. In relation to phage therapy, network analysis tools have the potential to identify key members of the pathogen community (i.e. hubs), which could be targeted to destabilise the bacterial community (e.g. Agler et al., 2016) and improve the chances of successful treatment. As many infections consist of communities of different species, creating a 'pathobiome' (Vayssier-Taussat et al., 2014), removing one species may destabilise the community sufficiently to allow the infection to be cleared by the patients' immune system, or by antibiotic treatment. Additionally, by identifying how bacterial diversity influences the modularity of cross-resistance networks, phage therapies could be optimised to limit the evolution of resistance in more complex environments.

6.2 Genetic basis of resistance determines network modularity

6.2.1 *Directional networks reveal cross-resistance asymmetry*

Previous studies have shown that cross-resistance, where resistance to a focal phage strain additionally protects the host from other phages, can result from the

modification of cell-surface receptors impeding phage adsorption (Betts et al., 2016a; Lenski, 1984, 1988), and even increase susceptibility to antibiotics (Chan et al., 2016). Using directional cross-resistance networks, we have shown that cross-resistance isn't always reciprocal, and asymmetrical interactions can frequently occur (Chapter 3). The evolution of asymmetry may simply be a product of the frequency at which different genes are mutated, and the strength of focal resistance they provide. If mutations in global regulators, such as RpoN (Lloyd et al., 2017; Totten et al., 1990), can provide the same degree of resistance as receptor-specific mutations, then a higher proportion of resistant genotypes may offer cross-resistance against phages targeting other receptors (Chapter 3). Resistance mutations targeting the same biosynthesis pathway, but at different positions, may determine the degree of cross-resistance provided to phage adsorbing to the same receptor. For Type IV pilus-binding phages, mutations near the end of the pathway, only affecting individual pilus components such as the motor proteins encoded by *pilB* and *pilT* (Chiang et al., 2008) provided weaker cross-resistance compared to mutations disrupting expression of pilus-specific genes, via RpoN and the two-component system which activates it (encoded by *pilS* and *pilR*; Hobbs et al., 1993) (Chapter 3). Although the specific mechanism is yet to be determined, we observed a similar effect for LPS-binding phages; whereas *wzy* mutations affecting biosynthesis of the LPS B-band (Islam et al., 2010) provide strong cross-resistance to multiple LPS phages (Chapters 3 and 4), mutations affecting *rmlA*, a thymidyltransferase involved in LPS production (Rahim et al., 2000), provided weaker cross-resistance to other LPS-binding phages (Chapter 4). Further work is necessary to fully characterise the phenomenon of asymmetrical cross-resistance and determine its influence on microbial community structure and the evolution of phage resistance.

6.2.2 *Local context may determine network structure*

If the likelihood of asymmetrical cross-resistance is determined by the mutational landscape available to the host, then the structure of cross-resistance is likely to be strongly influenced by the local environmental context. For example, increased population sizes at high resource levels increase the mutational supply available to both bacteria and phage populations, providing larger genetic reservoirs for adaptation (Lopez Pascua et al., 2014; Lopez-Pascua and Buckling, 2008). The rate of bacterial adaptation may increase in more complex environments, such as in the presence of multiple phages (Betts et al., 2018), which could potentially

drive rapid changes in the structure of bacteria-phage communities and influence the potential of cross-resistance evolution.

Conflicting selection pressures in complex environments are likely to constrain the evolution of cross-resistance where high fitness costs are incurred, for example if resistance mutations which provide cross-resistance negatively influence other traits such as nutrient uptake (Bohannan et al., 2002). Chronic bacterial infections provide an ideal study system for bacterial adaptation within a complex ecological setting, and can help us to assess the constraints upon resistance evolution *in vivo*: a diverse range of bacterial traits arise and coexist during adaptation to the abiotic environment (i.e. nutrient availability and spatial structures) (Winstanley et al., 2016), the local microbiota (Duan et al., 2003), co-infecting pathogens (Cox et al., 2010; Harrison, 2007), and attack by the host immune system and antibiotic treatments (Smith et al., 2006). Therefore, the fitness costs of phage resistance are likely to be inflated if they impose trade-offs in other expressed traits (Bohannan et al., 2002; Scanlan et al., 2015b). For example, this is likely to moderate the degree of surface modification; we commonly observed resistance genotypes with significantly impaired twitching motility, due to loss or significant modification of Type IV pilus (Chapter 3), however, if smaller structural changes can limit phage adsorption at lower cost, these are likely to be preferentially selected *in vivo*. Broader pleiotropic effects in complex environments, due to the requirement for bacterial expression of a greater number of traits, may also limit the evolution of between-module cross-resistance. The increased fitness costs imposed by mutations in global regulators compared to receptor-specific mutations (Chapter 3), suggest that the spread of broadly cross-resistant genotypes may be constrained *in vivo*. Specifically, we observed mutations in the gene encoding the alternative sigma factor RpoN, which regulates the expression of nearly 700 genes, and influences a broad range of traits including motility, biofilm formation and production of molecules which coordinate quorum sensing such as pyocyanin and pyoverdine (Lloyd et al., 2017). Therefore, mutations in *rpoN* are likely to have strongly negative pleiotropic effects *in vivo*, and may also moderate bacterial virulence (Lloyd et al., 2017). However, it is unclear how prolonged exposure to phages may influence this process, as more costly resistances may dominate if strong selection for phage resistance is sustained, and could potentially be ameliorated by the acquisition of compensatory mutations (Levin et al., 2000). Future experimental work is needed to understand how the fitness costs associated with phage resistance specifically

may be ameliorated, but there is a broad range of evidence demonstrating the occurrence of compensation mutations which ameliorate the fitness effects of antibiotic costs (Andersson and Hughes, 2010). Overall, this suggests that the evolution of cross-resistance may be more limited in more complex environments, promoting more modular network structures through prevalence of asymmetrical interactions. However, further work is necessary to determine how conflicting selection pressures may influence the fitness costs associated with phage resistance and alter the structure of cross-resistance within natural microbial communities.

6.3 Rational design of phage therapeutics

6.3.1 Maximising functional diversity limits the evolution of cross-resistance

The bacterial surface receptor to which a phage adsorbs determines its host range, and as such is a key determinant of phage function. We found that phage combinations which have high functional diversity (i.e. target multiple different adsorption receptors) promote the least cross resistance to one other (Chapter 3), and hence limit the evolution of resistance as multiple resistance mutations are required to provide strong specific resistance to each phage (Chapter 4). Both pairwise combinations (Chapter 3) and higher order phage combinations (Chapter 5) more effectively suppressed bacterial growth when functional diversity was maximised. Further, lower diversity phage combinations were required to achieve maximum suppression of bacterial growth when functional diversity was high. This suggests that phage cocktails can be rationally designed with fewer members targeting multiple distinct bacterial receptors, which would simplify the design and production of phage therapies making them easier to regulate (Sybesma et al., 2018).

6.3.2 Functional diversity as an important predictor of treatment success

In more complex systems, such as chronic infection of the cystic fibrosis lung, where adaptation to the local environment may influence expression and modification of cell-surface receptors resulting in diverse bacterial populations (Burns et al., 2001; Hancock et al., 1983; Harrison, 2007; Mahenthiralingam et al., 1994), phage functional diversity may be important to maximise the host range of phage cocktails. The pleiotropic effects of phage resistance mutations (Bohannan et al., 2002; Scanlan et al., 2015b) may result in inflated fitness costs within more complex environments, due to the broad range of traits required for survival and adaptation (Cornforth et al., 2018; Skurnik et al., 2013; Winstanley

et al., 2016). Hence, similarly to the concept of combinations therapies which combine antibiotics and phage to impose divergent selection pressures upon the bacterium thus limiting their capacity to adapt (Chan et al., 2016; Torres-Barceló and Hochberg, 2016), phage cocktails which target multiple adsorption receptors may limit the evolution of resistance even more strongly *in vivo* than we observed *in vitro* (Chapters 3 and 5). In these experiments, we observed complete suppression of bacterial growth by a phage combination with a functional diversity of 2 (i.e. targeting LPS and Type IV pilus only) (Chapter 5). Therefore, incorporating additional phage to increase functional diversity further [i.e. those targeting other membrane receptor such as TonB and OprM (Betts et al., 2018; Chan et al., 2016)], may further optimise phage combinations and help buffer any unforeseen adverse effects encountered *in vivo*. Overall, this suggests that phage combinations with high functional diversity may be even more effective *in vivo*, by targeting a broader range of hosts, and limiting the evolution of resistance, improving the evolutionary durability of the treatment.

Additionally, reduced virulence appears to be a common collateral effect associated with phage resistance (Castillo et al., 2014; Laanto et al., 2012; León and Bastías, 2015). Phage adsorption receptors commonly contribute towards bacterial virulence, therefore by promoting modification or loss of these targets, phage therapy may moderate bacterial virulence, providing an additional benefit compared to antibiotic treatments. Both LPS and Type IV pilus influence the virulence of *P. aeruginosa*: LPS is a major virulence factor which elicits host inflammatory responses (Pier, 2007), and Type IV pilus promotes attachment to epithelial cells to aid colonisation of the host (Hahn, 1997). We have observed accumulation of resistance mutations against both of these targets within the same bacterium (Chapter 4) in addition to mutations affecting the global regulator, RpoN, which influences a broad range of virulence associated traits including motility and biofilm formation (Chapter 3, Lloyd et al., 2017), suggesting that phage combinations can result in modification of multiple virulence traits. Therefore, by combining phages which target multiple receptors which contribute towards bacterial virulence, phage therapy may substantially attenuate virulence of the bacterial host.

6.3.3 *Sequential or simultaneous application?*

Imamovic and Sommer (2013) developed sequential antibiotic treatment pathways which can optimise antibiotic use by minimising collateral resistance and maximising collateral sensitivity. However, it is unclear if this would also work

for phage therapies. A previous study investigating the effect of sequential phage administration to treat *P. aeruginosa* infections found that sequential phage treatments could perform as effectively as simultaneous treatments *in vitro*, however, they found that simultaneous application of phages was more effective than sequential treatments in a waxmoth model (Hall et al., 2012). We found that sequential exposure to phage pairs provided stronger phage-specific resistances through acquisition of multiple receptor-modifying mutations, whereas simultaneous exposure to phages resulted in weaker resistance to both phages (Chapter 4). Surprisingly, however, simultaneously selected resistances imposed similar fitness costs on average compared to those acquired sequentially, although directional effects of sequential treatments could potentially be exploited to maximise fitness costs imposed upon multiply resistant genotypes (Chapter 4). Unfortunately, we were unable to measure collateral sensitivity within our system, as the ancestral PAO1 strain is already highly susceptible to all phages used in this thesis, therefore further investigation including a more diverse range of host resistances is necessary to determine whether phage resistances can promote sensitivity to other strains in a similar manner as increasing antibiotic sensitivity (Chan et al., 2016). Whilst this suggests that simultaneous exposure to phages may constrain the evolution of resistance more so than sequential exposure, a fuller understanding of the relative fitness costs of sequentially and simultaneously selected resistance *in vivo*, and the potential interactions between specific mutations which promote negative epistasis, are needed to assess the implications for phage therapy.

6.3.4 *Maximise genetic diversity or functional diversity?*

The range of phage resistance mechanisms available to the bacteria will likely determine the structure of cross-resistance, and may therefore alter the relative contribution of genetic and functional diversities towards phage cocktail efficacy. For example, CRISPR is a form of adaptive immunity, whereby the bacterial host can recognise and degrade phage DNA if it has previously been identified as 'foreign' and stored as a CRISPR spacer (Barrangou et al., 2007; Horvath and Barrangou, 2010). Whilst receptor-based cross-resistance has the potential to protect the host from genetically distant phage, only requiring similarity in receptor binding sites within tail-fibres, cross-resistance in a CRISPR context may be stronger between genetically similar phages. As such, a different modular network may be created, grouping phages by phylogeny. Therefore, for phage therapy in the context of a bacterial infection, the relative importance of genetic

diversity and functional diversity on treatment efficacy will be dependent on the diversity of available phage resistance mechanisms, and therefore both forms of diversity should be maximised to produce effective cocktails. It is also important that pathogen diversity within the patient is fully characterised to enable the rational design of personalised treatments (e.g. Pirnay et al., 2010). A better understanding of cross-resistance structure, and the relative cost of different resistance mechanisms, in complex environments is needed to determine principles of rational cocktail design which promote both functional and genetic diversity.

6.3.5 *Limiting the evolution of phage resistance*

Bacterial infections are complex, and may vary as much between patients as through time in a single patient. Therefore, to maximise the chance of successful treatment using phage therapeutics, we must design phage treatments to suit specific needs. One of the main considerations must be the potential for resistance evolution, which is influenced to a great extent by the genetic diversity of the pathogen, which in turn may be determined by the context of disease. In contrast to our experimentally derived resistant mutants, which are spontaneous mutants selected from a lab-adapted bacterial strain allowed to proliferate and develop population diversity over just 24-48h, chronic infections are established over long time periods (perhaps years) and as such can develop very high levels of genetic diversity as the pathogen adapts to the local ecological conditions (both biotic and abiotic; see section 6.2.2). Within this genetically diverse population, phage-resistant mutants likely already dwell, and may also have accumulated mutations which ameliorate their fitness (Andersson and Hughes, 2010). The results presented in this thesis provide a number of potential strategies which may limit the evolution of resistance in such circumstances. Maximising phage functional diversity to limit the potential for cross-resistance increases the chances that bacterial genotypes which have resistance to numerous phage strains within a combination treatment are present. However, this may be further optimised by strategic implementation of phage treatments. For example, simultaneous applications with numerous phage strains require either very high doses to be administered, or *in situ* propagation of the phage within the infection site to ensure that bacterial genotypes which are susceptible to a single phage (or subset of phages) within a diverse cocktail actually encounter phage strains to which they are susceptible. Although these same factors would also influence the efficacy of single phage treatments, our data has indicated that sequential

exposure to single phage strains may select for stronger phage-specific resistance mutations which impose greater fitness costs, and therefore sequential treatments with phages which are functionally diverse, permitting time for phage *in situ* propagation between treatments, may be better able to treat infections where the pathogen community is highly diverse. However, future experimental work and clinical trials are necessary to determine the extent of phage propagation within an infection site and to optimise dosing strategies for phage application.

6.3.6 *Practical implementation of phage therapy – future directions*

Phage therapy is not a new idea, but more work is necessary to develop a broadly implementable methodology which meets the regulatory requirements of the western world. As a priority we must start to assess the practical application of single phage strains within clinical settings, focussing on the treatment of acute single species infections would allow optimisation of dosage and assessment of safety. Whilst phage therapies implemented in Eastern Europe are often under-documented and lack the rigorous clinical trials required in the UK, we can learn from their success: broad range cocktails, such as those commercially produced by the Eliava Institute in Georgia (see Section 1.6.1), are regularly updated by testing newly isolated phages against pathogenic bacterial strains in current circulation. This type of rapid and recurrent adaptation of therapeutic cocktails would not be possible under our current Good Manufacturing Practices which are applied to pharmaceutical products, and can retain novel products within the development pipeline for many years. Several options are available to overcome these issues. We can either adopt an alternative regulatory framework for phage treatments (see section 1.5.4 for a successful example of this in Belgium), or develop phage treatments which are more durable to the inevitable evolution of phage resistance. One way in which we can do this is to minimise the number of phage required to optimise the efficacy of phage treatments by maximising functional diversity of phage strains. The results presented in Chapters 5 demonstrate that phages which target different bacterial receptors have a complementary effect, primarily by limiting the evolution of cross-resistance, meaning that cocktails with a low species diversity can have high efficacy. However, much further work is needed to fully understand the complexities of these interactions, for example, whilst it seems clear that combinations which do not promote cross-resistance should be favoured, we do not fully understand the mechanistic basis of asymmetrical cross-resistance.

6.4 Conclusions

Bacteria-phage interactions shape microbial communities in both ecological and clinical scenarios. As such, it is important that we determine the factors which influence community structures, and their resilience to perturbations, to better understand how microbial communities function and how bacterial infections can be sustainably treated with phages. This work highlights the power of network analyses to characterise community structures and uncover the mechanisms which drive the evolution of resistance to multiple phages. Further, an understanding of these fundamental processes can aid the rational design of phage treatments, to both maximise the efficacy with which bacterial growth is suppressed and limiting the evolution of phage resistance to improve their evolutionary robustness.

Whilst we have determined a number of useful concepts to aid the rational design of phage therapies, further work is required to assess how these mechanisms may be influenced within complex *in vivo* environments. The simplest of these concepts to implement in cocktail design is maximisation of functional diversity; by combining phage strains which target different adsorption receptors, phage cocktails can be optimised with fewer members. Additionally, our work suggests that simultaneous application of phages may better constrain resistance evolution compared to sequential treatments. Both of these outcomes simplify the design of phage cocktails, which would hopefully minimise the regulatory hurdles facing phage therapy legislation and shorten the timeframe for phage therapy implementation in the EU. A more complete picture of cross-resistance evolution *in vivo* is necessary to determine the relative importance of each mechanism in the design of phage cocktails, but this work suggests that there are fundamental processes which can be harnessed to limit the evolution of resistance and optimise phage treatments.

Appendix A (Chapter Three)

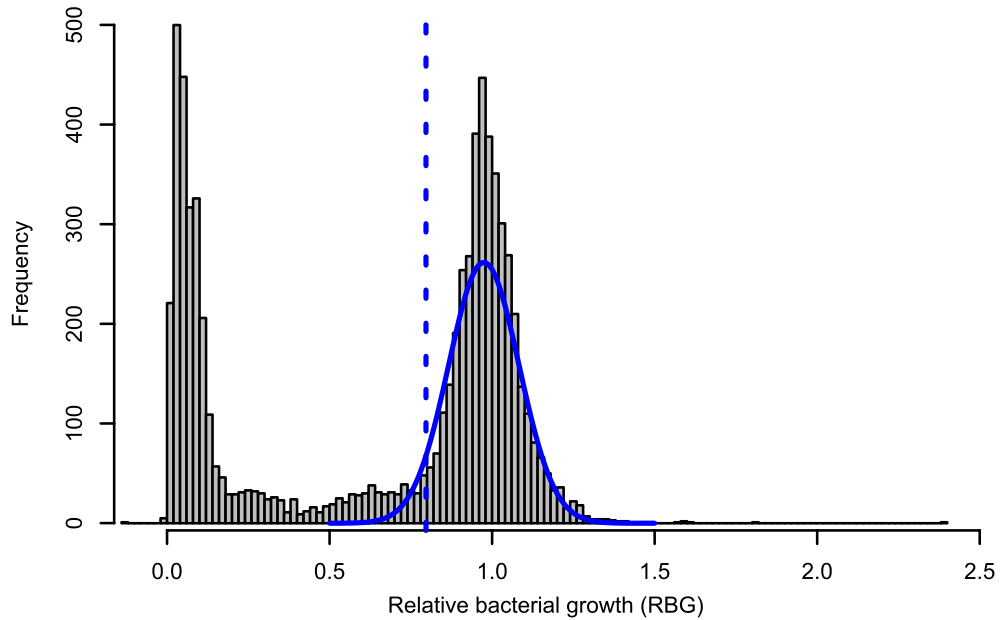


Figure S3.1. Relative bacterial growth (RBG) distributions and binary resistance threshold. The frequency histogram shows the relative bacterial growth values for 263 resistant mutants against all 27 phages. The blue curve shows the normal distribution of the resistance peak (RBG=1). The threshold of binary resistance was calculated as the 95% confidence interval of the normal distribution (blue dashed line; RBG=0.798).

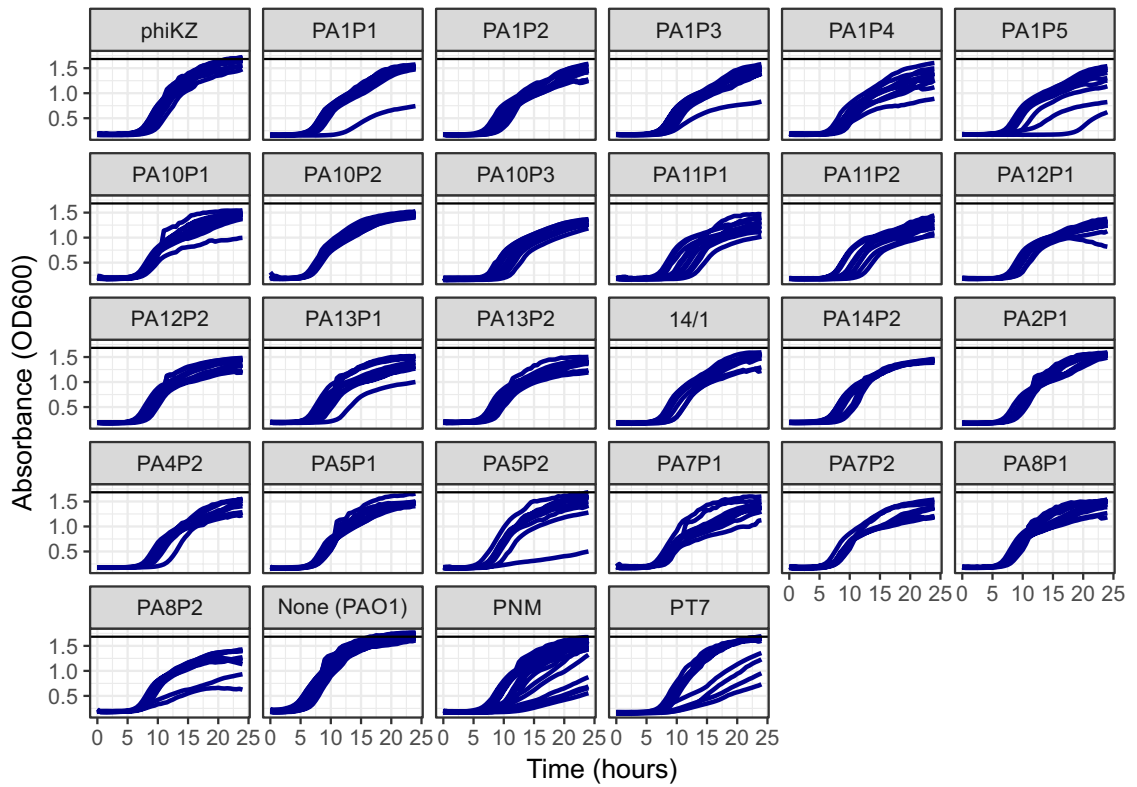


Figure S3.2. Growth curves showing the fitness impact of resistance mutations. Growth curves of all 263 spontaneous resistant mutants grouped by focal phage resistance (up to 10 mutants per focal phage), and the wild type ancestor (PAO1).

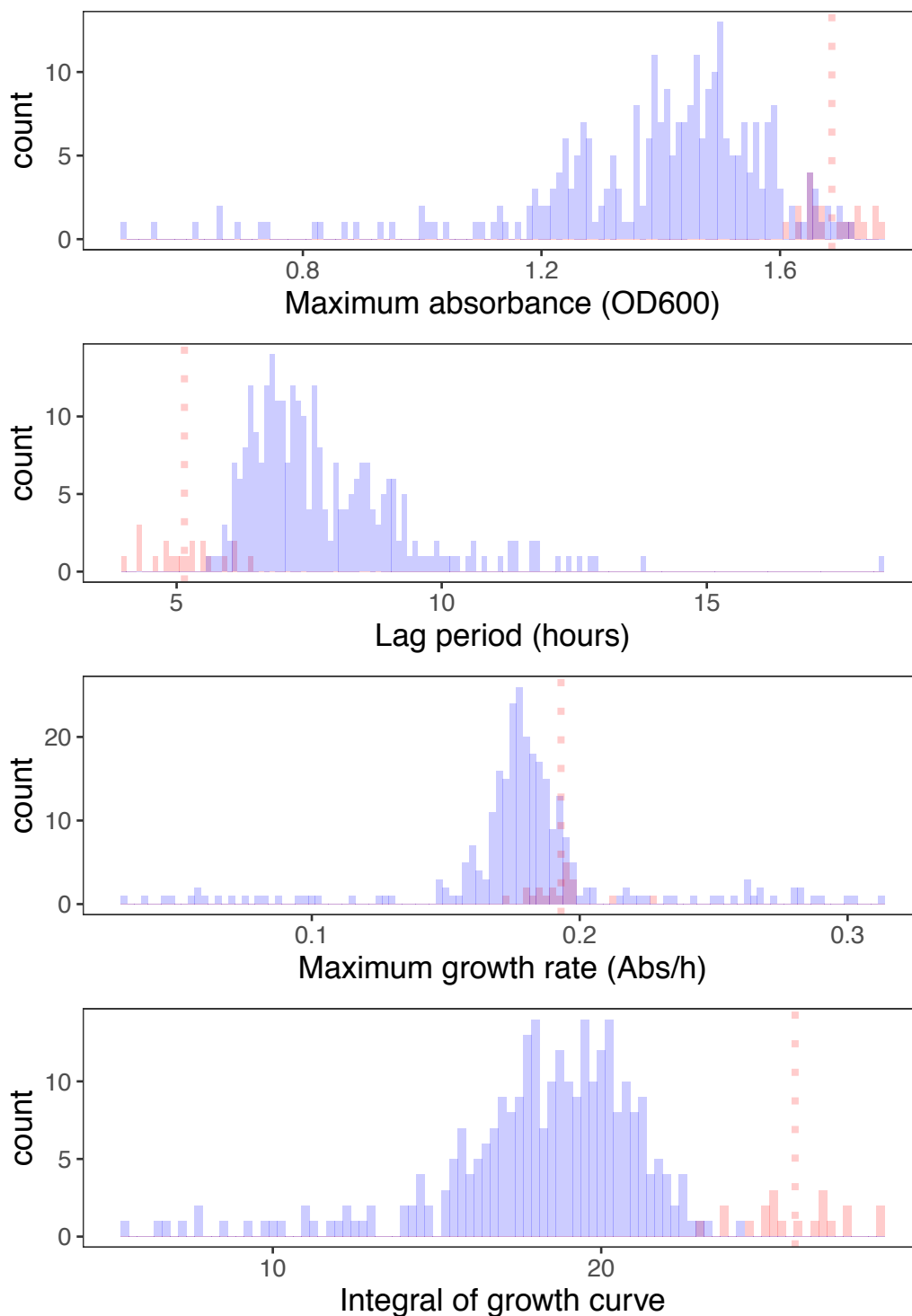


Figure S3.3. Frequency histograms of growth parameters for PAO1 and resistant mutants. Frequency histograms of growth parameters extracted from the bacterial growth curves (S10 Fig): maximum absorbance reached in 24 hours (OD600), lag period calculated as x-axis intercept (time, hours) of a tangent to the growth curve at the point of maximum growth rate, maximum growth rate, and integral of growth curve. Red histogram shows the wild type PAO1 ancestor, and blue shows 263 spontaneous resistant mutants.

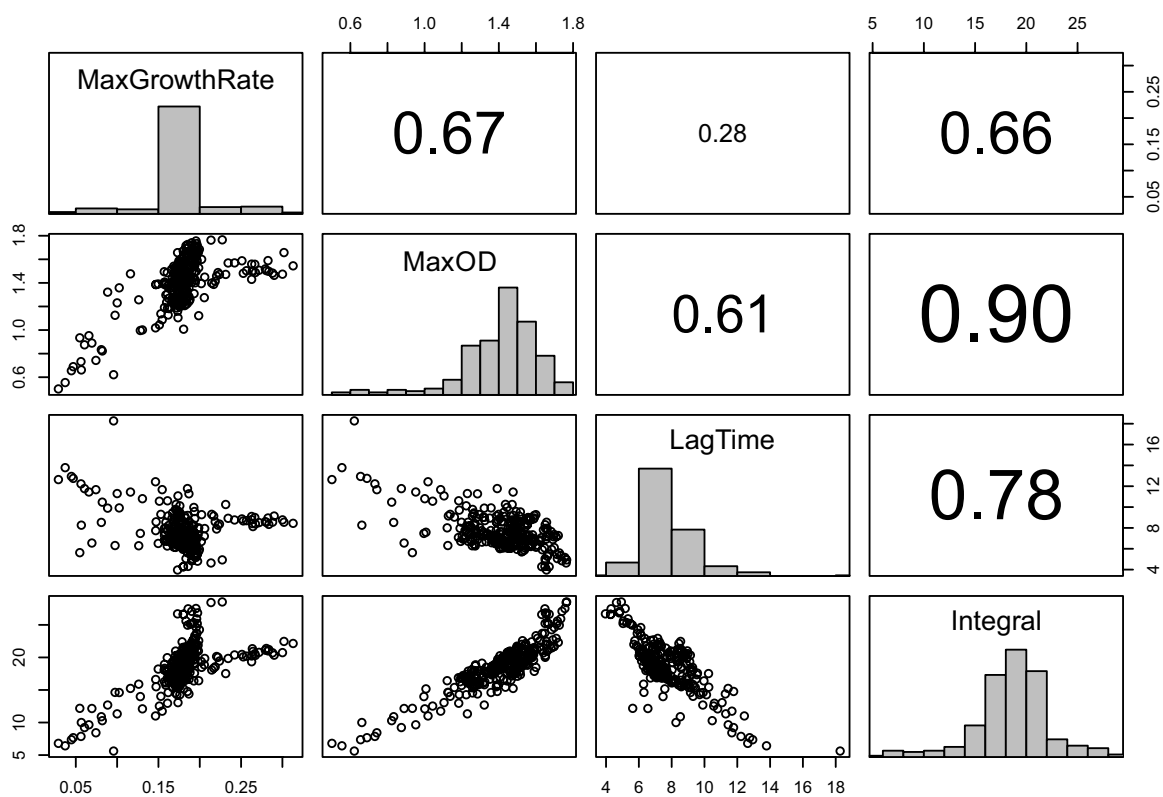


Figure S3.4. Correlation of growth parameters. Multiple linear regression of growth parameters for 263 spontaneous resistant mutants (S11 Fig): the diagonal shows the distribution of each growth parameter, the bottom quadrant plots correlations for each pair of growth parameters, and the top quadrant gives corresponding R^2 values.

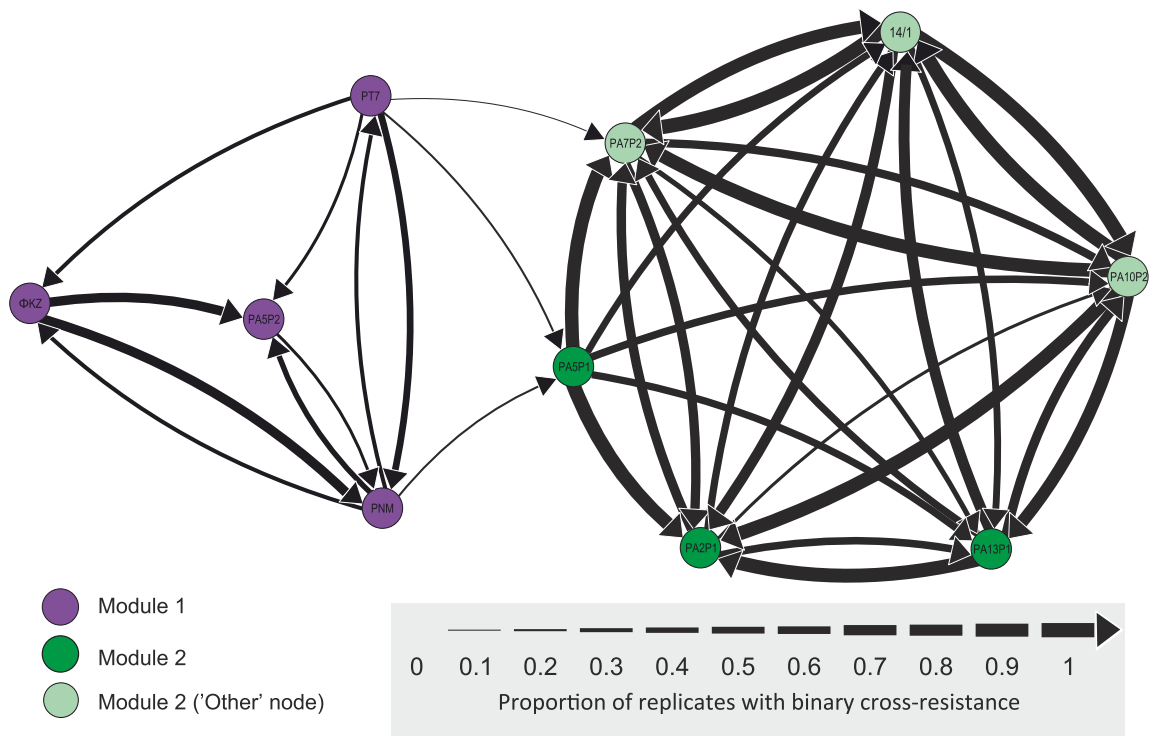


Figure S3.5. Cross-resistance subnetwork. A subset of the cross-resistance network showing all pairwise cross-resistance interactions between the ten phage strains used in the mutational frequency experiment and the suppression of bacterial growth assays.

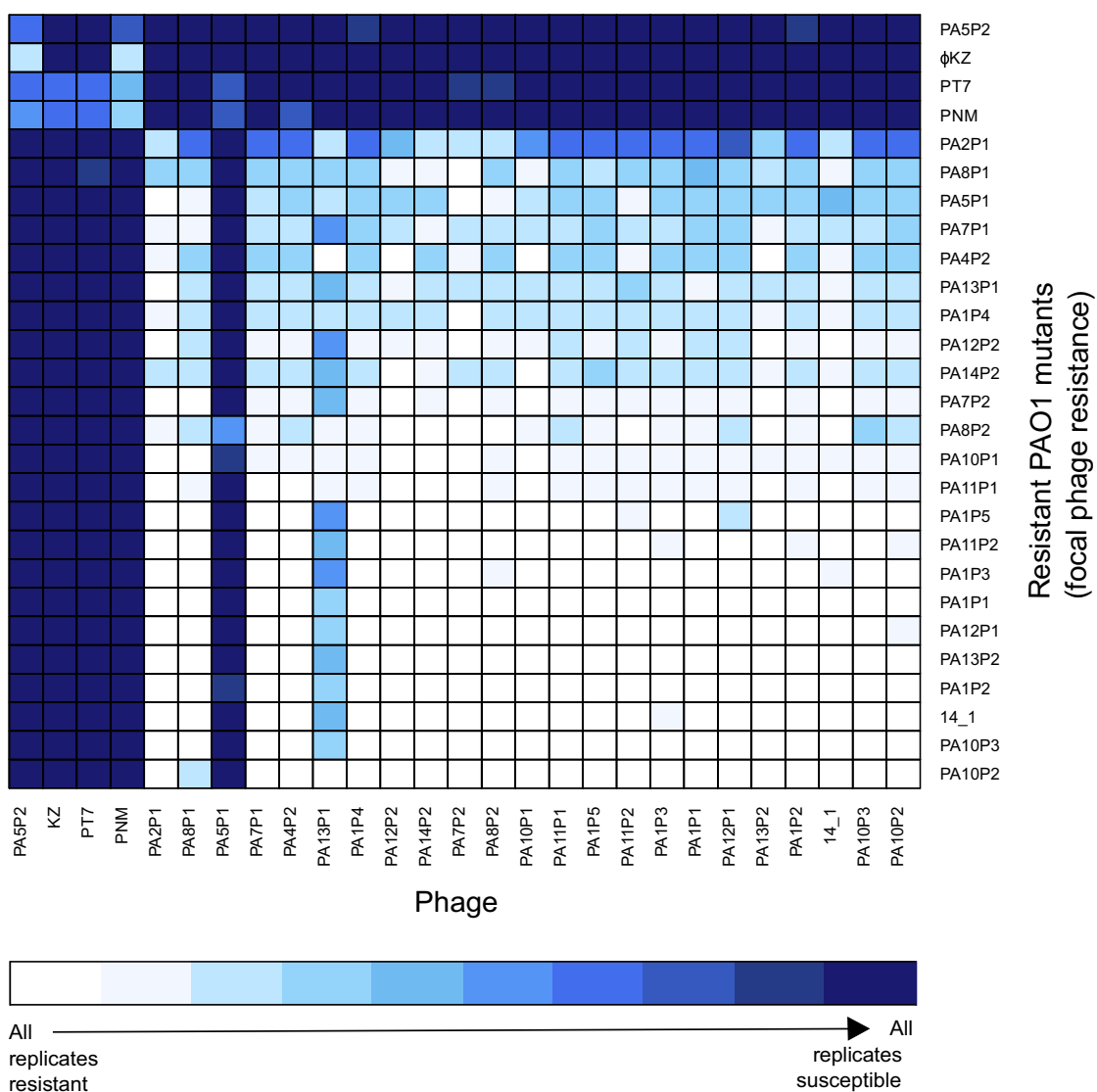


Figure S3.6. Bacteria phage infection network. Infection network showing resistance profiles of spontaneous mutants selected against individual phage. Spontaneous PA01 mutants are grouped so that each row represents up to 10 replicates selected against the same phage. Each column denotes individual phage strains which mutants were individually challenged against. Colour shading corresponds to the proportion of replicates which were susceptible to the corresponding phage (see key).

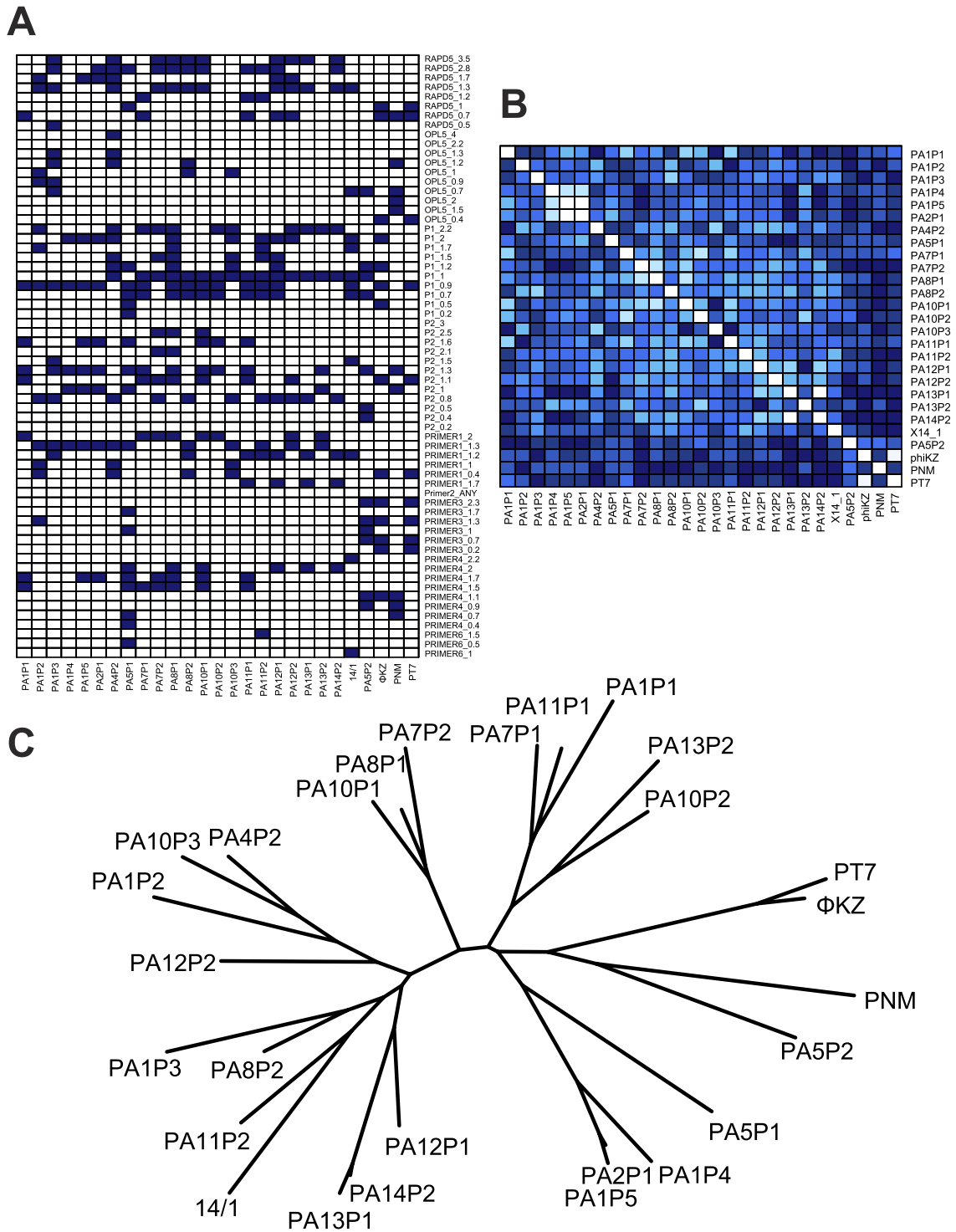


Figure S3.7. Characterisation of phage genetic diversity. **A**) Banding patterns produced by RAPD PCR (random amplified polymorphic DNA) analysis of 27 phages (columns) by the molecular weight of PCR products from 9 different primers (rows; S3 Table). **B**) Difference matrix summarising the dissimilarity of banding patterns between phages (i.e. 1 - proportion of bands in common). **C**) Neighbour-joining tree produced from the phage dissimilarity matrix.

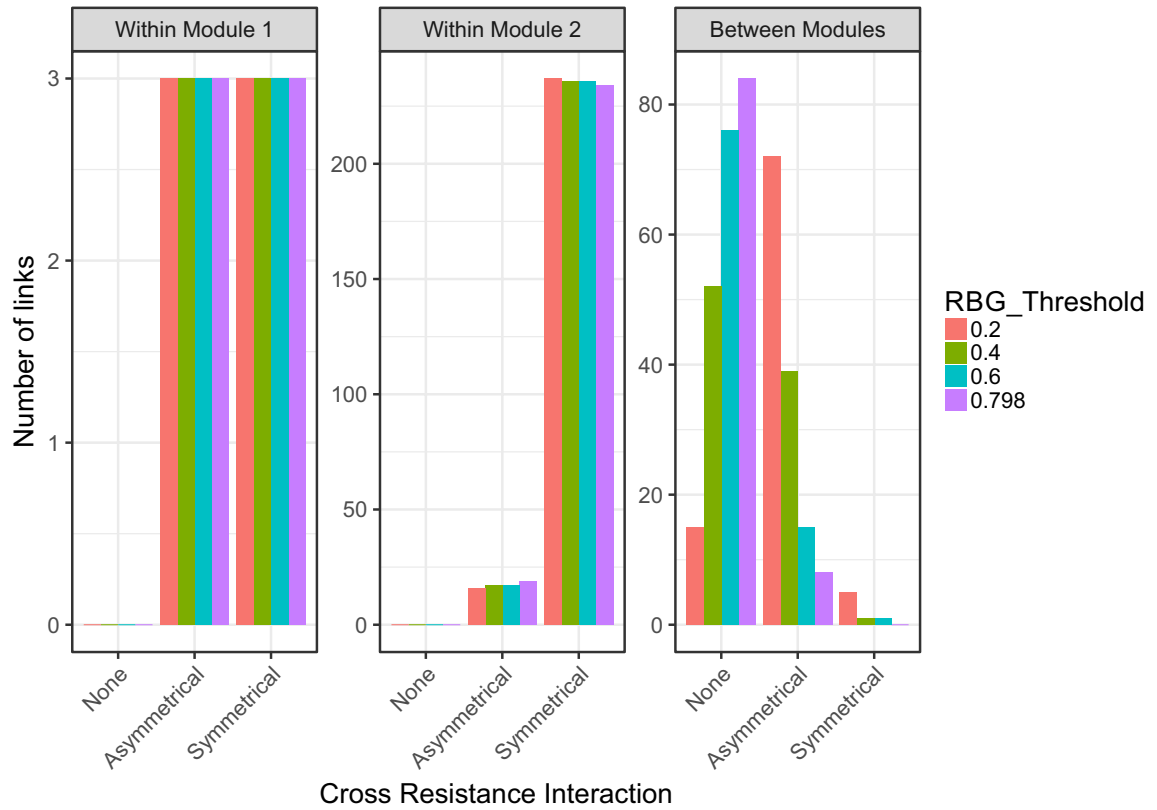


Figure S3.8. Cross-resistance network structure at different resistance thresholds. Number and type of links between phage pairs within and between each cross-resistance module for different values of the binary threshold of resistance.

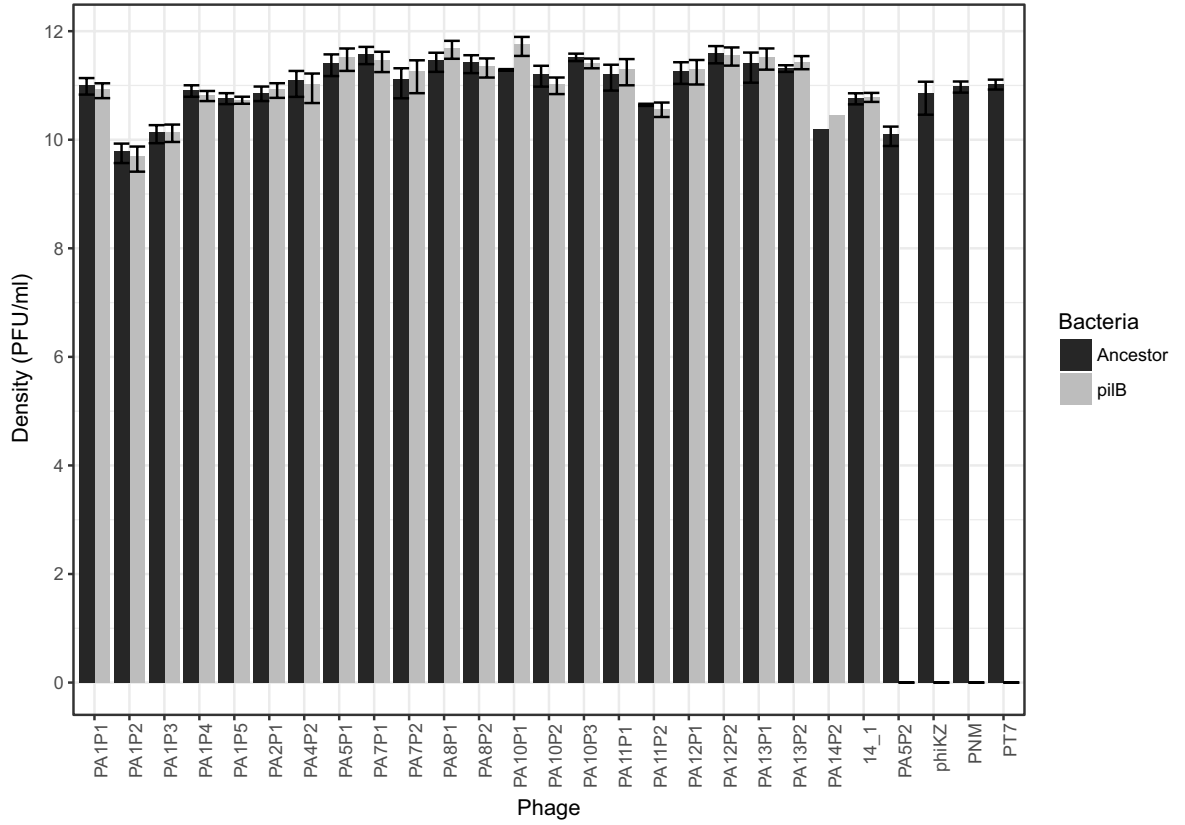


Figure S3.9. Phage infection of PAO1 versus a *pilB* transposon mutant. Plaque forming units per ml when plated on the pilated wildtype (Black; 'Ancestor') and the unpiliated *pilB* transposon mutant (Grey).

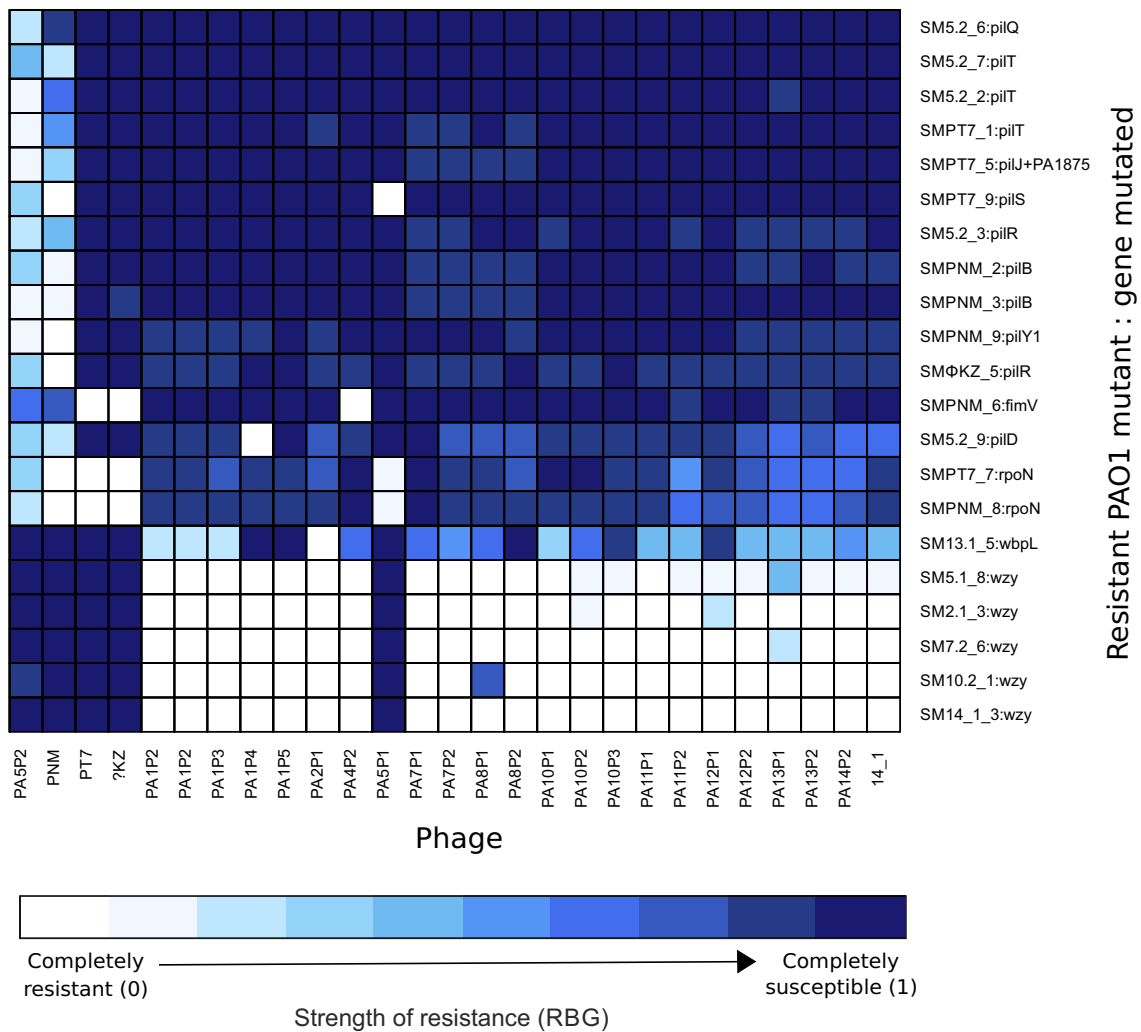


Figure S3.10. Cross-resistance profiles of sequenced resistant mutants. Bacteria phage infection network showing sequenced resistant mutants where gene location of SNPs are identified (rows), against 27 phage strains (columns). Strength of resistance (RBG) scales from complete resistance (white) to complete susceptibility (dark blue).

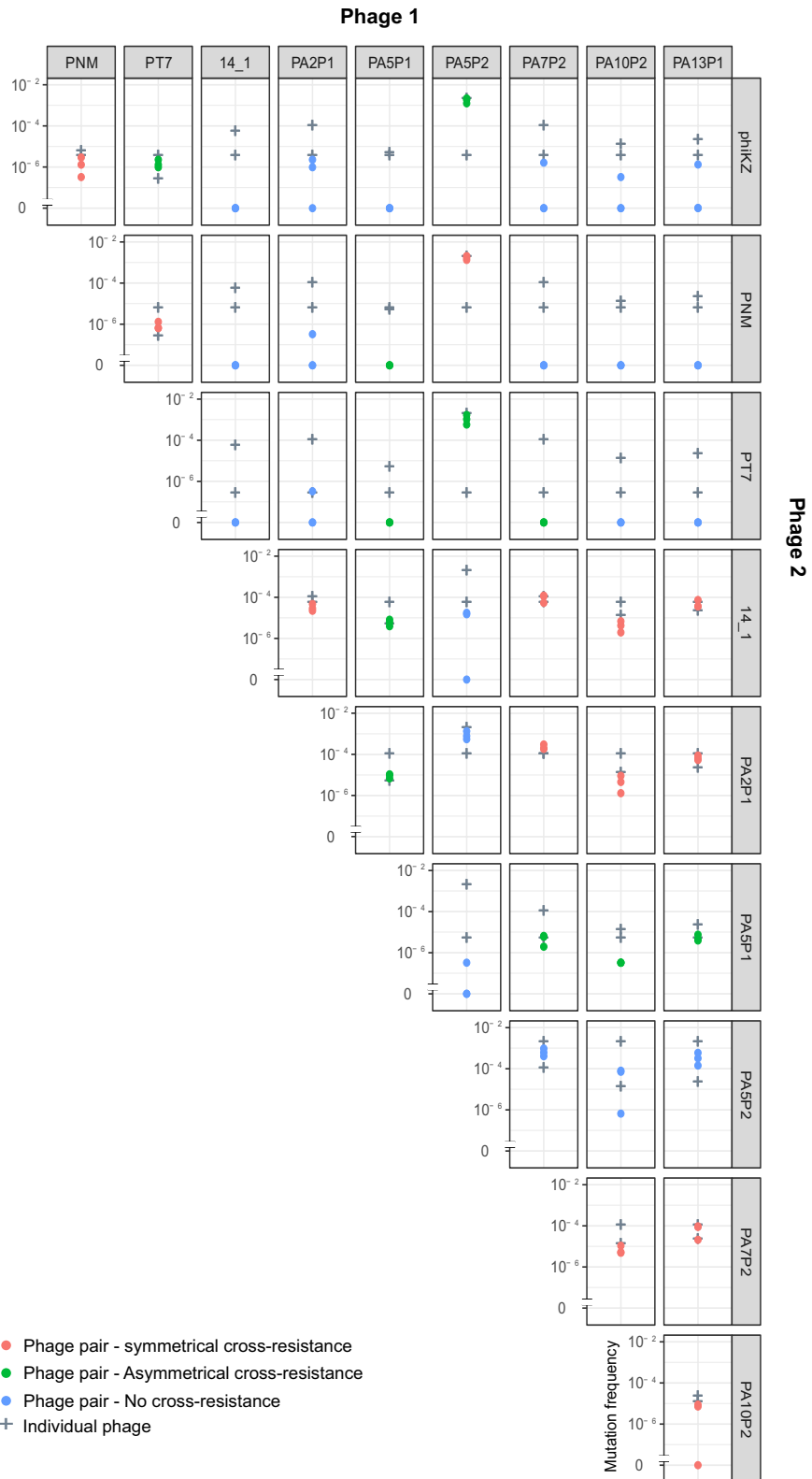


Figure S3.11. Absolute frequencies of resistance mutations against phage pairs. Frequency of resistance mutations against single phage (+) and phage pairs coloured by cross-resistance type associated with each phage pair (blue - no cross resistance; green - asymmetrical cross-resistance; red - symmetrical cross-resistance).

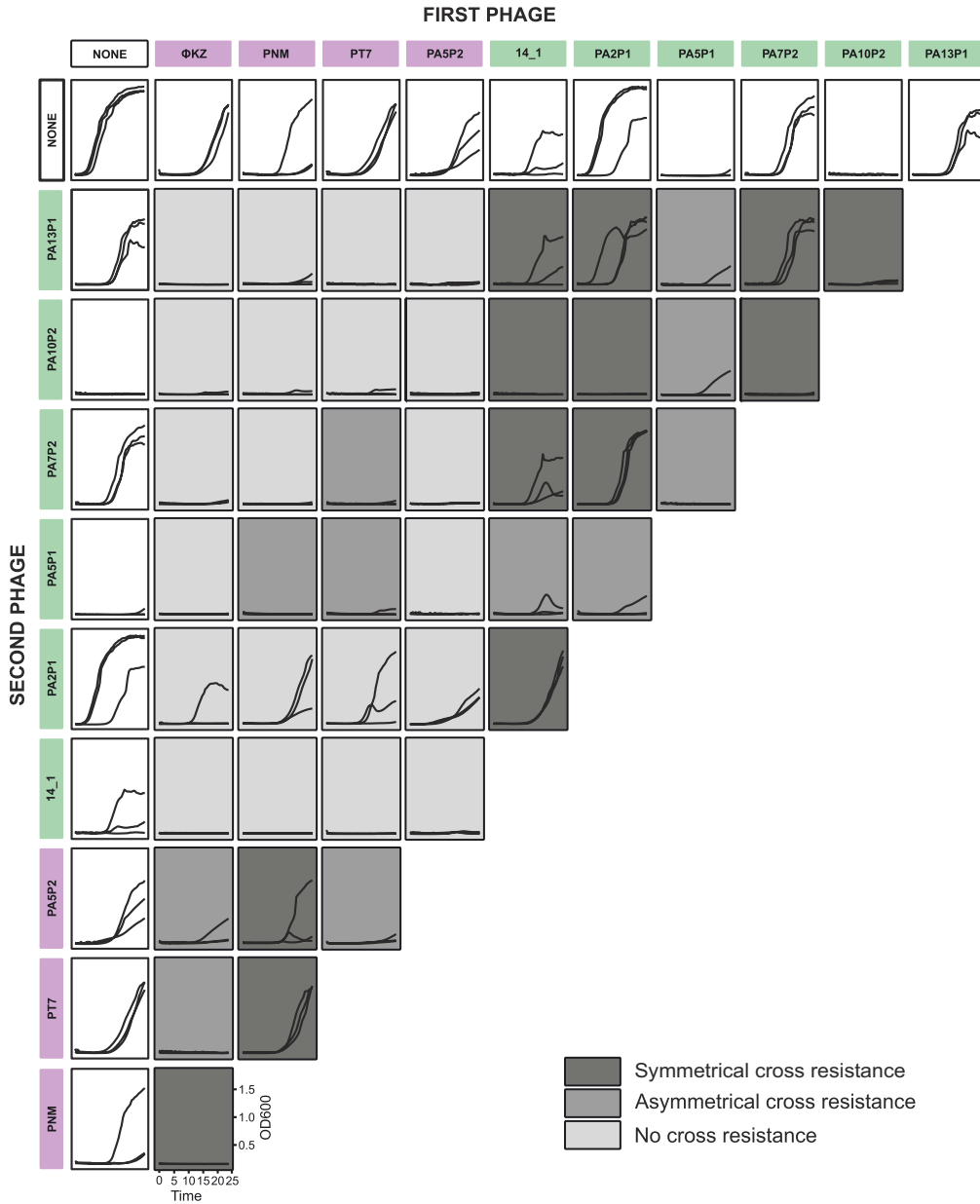


Figure S3.12. Suppression of bacterial growth by phage monocultures and pairwise phage combinations. Bacterial density was measured as OD (600nm, y-axis) over 24 hours (x-axis) in the presence of single phages (white background), or two phages (grey backgrounds). Dark grey background denotes phage pairs that exert symmetric cross-resistance, mid grey for phage pairs that show asymmetric cross-resistance, and light grey for no observed cross-resistance.

Strain	Source	Date first isolated	Isolation Host	Morphotype	Genome size (kb)	Accession number
ΦKZ	Sewage water, Kazakhstan	1975		Myoviridae	280.33	NC_004629.1
PNM	Mtkvari River, Tbilisi, Georgia	1999		Podoviridae	42.72	-
PT7	Lake Ku, Tbilisi, Georgia	1999		Myoviridae	58.2	-
14/1	Sewage water, Regensburg, Germany	2000		Myoviridae	66.23	NC_011703.1
PA1P1	Sewage water, Jyväskylä, Finland	2015	<i>Pseudomonas aeruginosa</i> 61841	-	-	-
PA1P2			<i>Pseudomonas aeruginosa</i> 61841	-	-	-
PA1P3			<i>Pseudomonas aeruginosa</i> 61841	-	66.46	-
PA1P4			<i>Pseudomonas aeruginosa</i> 61841	-	-	-
PA1P5			<i>Pseudomonas aeruginosa</i> 61841	-	-	-
PA2P1			<i>Pseudomonas aeruginosa</i> 61823	-	-	-
PA4P2			<i>Pseudomonas aeruginosa</i> 61432	-	-	-
PA5P1			<i>Pseudomonas aeruginosa</i> 11AN03663	-	-	-
PA5P2			<i>Pseudomonas aeruginosa</i> 11AN03663	-	-	-
PA7P1			<i>Pseudomonas aeruginosa</i> 62314	-	-	-
PA7P2			<i>Pseudomonas aeruginosa</i> 62314	-	-	-
PA8P1			<i>Pseudomonas aeruginosa</i> 62263	-	-	-
PA8P2			<i>Pseudomonas aeruginosa</i> 62263	-	-	-
PA10P1			<i>Pseudomonas aeruginosa</i> 62206	-	-	-
PA10P2	<i>Pseudomonas aeruginosa</i> 62206	-	-	-		
PA10P3	<i>Pseudomonas aeruginosa</i> 62206	-	-	-		
PA11P1	<i>Pseudomonas aeruginosa</i> 62180	-	66.06	-		
PA11P2	<i>Pseudomonas aeruginosa</i> 62180	-	-	-		
PA12P1	<i>Pseudomonas aeruginosa</i> 62181	-	-	-		
PA12P2	<i>Pseudomonas aeruginosa</i> 62181	-	-	-		
PA13P1	<i>Pseudomonas aeruginosa</i> 62172	-	-	-		
PA13P2	<i>Pseudomonas aeruginosa</i> 62172	-	-	-		
PA14P2	<i>Pseudomonas aeruginosa</i> 62109	-	-	-		

Table S3.1. Overview of phage strains. Details of the isolation and characterisation of the phage collection.

Name	Sequence	Reference
RAPD5/Primer5 ⁱⁱ	5'AACGCGCAAC3'	ⁱ : [1] ⁱⁱ : [2]
P1	5'CCGCAGCCAA3'	[1]
P2	5'AACGGGCAGA3'	[1]
OPL5	5'ACGCAGGCAC3'	[1]
Primer1	5'GGTGC GGGAA3'	[2]
Primer2	5'GTTTCGCTCC3'	[2]
Primer3	5'GTAGACCCGT3'	[2]
Primer4	5'AAGAGCCCGT3'	[2]
Primer6	5'CCCGTCAGCA3'	[2]

1. AzizianR, NasserA, AskariH, TaheriKalaniM, SadeghifardN, PakzadI, et al. Sewage as a rich source of phage study against *Pseudomonas aeruginosa* PAO. *Biologicals*. 2015; 43: 238–241. doi:10.1016/j.biologicals.2015.05.004
2. KumariS, HarjaiK, ChhibberS. Isolation and characterization of *Klebsiella pneumoniae* specific bacteriophages from sewage samples. *Folia Microbiol (Praha)*. 2010; 55: 221 – 227. doi:10.1007/s12223-010-0032-7

Table S3.2. RAPD PCR primers

Primers used in the RAPD-PCR analysis of phage genetic relatedness.

Function	Gene mutated	Operon/Cluster	Gene product activity	Chromosome position (bp)	Effect type	Putative impact	Clone	Focal phage resistance	Cross-resistance provided
Lipopolysaccharide biosynthesis	wbpL	wbp cluster	Glycosyl transferase required for LPS A- and B-band biosynthesis	3529218	frameshift (1bp insertion)	HIGH	SM13.1_5	PA13P1	within module 2
	wzy	wbp cluster	LPS B-band O-antigen polymerase	3538988	frameshift (1bp insertion)	HIGH	SM10.2_1	PA10P2	within module 2
Type IV pilus motility				3538988	frameshift (1bp insertion)	HIGH	SM14/1_3	14/1	within module 2
				3538988	frameshift (1bp insertion)	HIGH	SM2.1_3	PA2P1	within module 2
				3538988	frameshift (1bp insertion)	HIGH	SM5.1_8	PA5P1	within module 2
				3538988	frameshift (1bp insertion)	HIGH	SM7.2_6	PAP7P2	within module 2
				5071434	stop gained	HIGH	SMPNM_2	PNM	within module 1
				5070526	frameshift (4bp deletion)	HIGH	SMPNM_3	PNM	within module 1
				437147	missense variant	MODERATE	SM5.2_2	PA5P2	within module 1
				437058-438250	deletion (1,192bp)	HIGH	SM5.2_7	PA5P2	within module 1
				437130	disruptive inframe deletion (12bp)	MODERATE	SMP7_1	PT7	within module 1
				5101300	frameshift (1bp deletion)	HIGH	SMPNM_9	PNM	within module 1
Type IV pilus biosynthesis				453128	missense variant	MODERATE	SMP7_5	PT7	within module 1
Signaling and global regulation				5073276	stop gained	HIGH	SM5.2_9	PA5P2	between modules
Other				5676479-5676662	deletion (183bp)	HIGH	SM5.2_6	PA5P2	within module 1
				3497951-3497986	frameshift (35bp deletion)	HIGH	SMPNM_6	PNM	within module 1
				4993096	frameshift (1bp deletion)	HIGH	SMPNM_8	PNM	between modules
				4994077	missensevariant	MODERATE	SMP7_7	PT7	between modules
				5096180	frameshift(1bpdeletion)	HIGH	SM5.2_3	PA5P2	within module 1
				5096282	missensevariant	MODERATE	SMphikZ_5	φ KZ	within module 1
				5094532	stoppained	HIGH	SMP7_9	PT7	between modules
				2045090	missensevariant	MODERATE	SMP7_5	PT7	within module 1

Table S3.3. Mutations identified by whole genome sequencing. Blue highlighting indicates between-module cross-resistance.

Appendix B (Chapter Four)

Category	Gene name	Operon/cluster	Gene product activity	Chromosome position (bp)	Effect type	Putative impact	Treatment	Ancestor
LPS biosynthesis	galU		UTP-glucose-1-phosphate uridylyltransferase	2215599-2215679	deletion (80bp)	HIGH	PA5P2->14/1	PAO1_FT2
				2215816	stop gained	HIGH	PA5P2->14/1	PAO1_FT1
	PA5001 (Ssg)	PA5005-PA5004-PA5003-PA5002-PA5001	cell-surface sugar biosynthetic glycosyltransferase	5618765	frameshift	HIGH	14/1	PAO1_FT3
							14/1->PA10P2	PAO1_FT3
	PA5004 (wapH)	PA5005-PA5004-PA5003-PA5002-PA5001	probable glycosyl transferase	5622353-5622444	deletion (91bp)	HIGH	PA10P2->14/1	PAO1_FT3
	rmlA	rmlB-rmlD-rmlA-rmlC	glucose-1-phosphate thymidyltransferase	5812961	missense variant	MODERATE	PA10P2 PA10P2->14/1	PAO1_FT3 PAO1_FT3
	wbpL	wbp cluster	glycosyltransferase	3529218	frameshift	HIGH	PA10P2+14/1 PASP2+14/1	PAO1_FT2 PAO1_FT2
	wzy	wbp cluster	LPS B-band O-antigen polymerase	3538031	frameshift	HIGH	PA10P2 PA10P2->14/1	PAO1_FT2 PAO1_FT2
				3538428	stop gained	HIGH	14/1->PA5P2 14/1->PA10P2	PAO1_FT1 PAO1_FT1
				3538499	frameshift	HIGH	14/1 14/1->PA5P2 14/1->PA10P2	PAO1_FT2 PAO1_FT2 PAO1_FT2
			3538988	frameshift	HIGH	PASP2->PA10P2 PA10P2 PA10P2+14/1 PA5P2->14/1 PASP2->PA10P2 PASP2->PA10P2 PASP2+PA10P2 PASP2+PA10P2 PA10P2->14/1 PA10P2->PA5P2	PAO1_FT1 PAO1_FT1 PAO1_FT3 PAO1_FT3 PAO1_FT2 PAO1_FT3 PAO1_FT3 PAO1_FT2 PAO1_FT1 PAO1_FT1	
Type IV pilus biosynthesis	pilB		motor protein - pilus extension	5070925	missense variant	MODERATE	PA5P2 PA5P2->14/1 PA5P2->PA10P2 PA10P2->PA5P2	PAO1_FT3 PAO1_FT3 PAO1_FT3 PAO1_FT1
	pilE	fimU-pilV-pilW-pilX-pilY1-pilY2-pilE	minor pilin	5104842	conservative inframe insertion (12bp)	MODERATE	14/1->PA5P2	PAO1_FT1
	pilN	pilM-pilN-pilO-pilP-pilQ	type IV pilus assembly protein	5679190	missense variant	MODERATE	PA5P2 PA5P2->14/1 PA5P2->PA10P2	PAO1_FT2 PAO1_FT2 PAO1_FT2
	pilR	pilS-pilR	two-component response regulator	5095672	missense variant	MODERATE	PA5P2 PA5P2->14/1 PA5P2->PA10P2	PAO1_FT1 PAO1_FT1 PAO1_FT1
	pilT+pilU		twitching motility proteins	437058-438250	deletion (1,192bp)	HIGH	14/1->PA5P2	PAO1_FT2
	pilY1	fimU-pilV-pilW-pilX-pilY1-pilY2-pilE	putative anti-retraction factor	5101958 5103165	stop gained frameshift	HIGH HIGH	PA10P2->PA5P2 PA10P2+14/1	PAO1_FT2 PAO1_FT1
Other gene variations	PA0142-nuh			163275	intergenic	MODIFIER	PA10P2+14/1	PAO1_FT3
	PA0429		predicted Nucleotide-diphospho-sugar transferase	480379	missense variant	MODERATE	PA10P2->14/1	PAO1_FT2
				480952	stop gained	HIGH	PA10P2->14/1	PAO1_FT1
	PA0845-PA0846		intergenic	923945	intergenic	MODIFIER	PA5P2->PA10P2	PAO1_FT2
	PA1065		unknown	1151442	missense variant	MODERATE	PA10P2+14/1	PAO1_FT3
	PA1567		predicted oxidation-reduction activity	1709197	conservative inframe insertion (6bp)	MODERATE	PA5P2->14/1	PAO1_FT3
	PA3722-PA3723			4167572	intergenic	MODIFIER	PA10P2+14/1	PAO1_FT1
	birA-PA4279-PA4278	inferred sporulation-related domain	4786538	missense variant	MODERATE	PA5P2 PA5P2->14/1 PA5P2->PA10P2	PAO1_FT3 PAO1_FT3 PAO1_FT3	
Other				3651299-3651424	Duplication and insertion		PA5P2+PA10P2 PA5P2+PA10P2	PAO1_FT3 PAO1_FT1
				4746797-4747035	Duplication and insertion		PA5P2+PA10P2 PA5P2+PA10P2	PAO1_FT3 PAO1_FT1
				2194891-2445323	large deletion (>250 kb)		PA10P2+14/1	PAO1_FT1

Table S4.1. Identity and function of genes where mutations were identified

Abbreviations

Abi	Abortive infection
Abs	Absorbance
AIC	Akaike information criterion
ANOVA	Analysis of variation
ARD	Arms race dynamics
bp	Base pair
BPIN	Bacteria-phage infection network
BREX	Bacteriophage exclusion
CF	Cystic fibrosis
CFU	Colony forming units
CR	Cross-resistance
CRF	Cross-resistance frequency
CRI	Cross-resistance index
CRISPR	Clustered regularly interspaced short palindromic repeats
DNA	Deoxyribose nucleic acid
ERQ	Escalating Red Queen
EU	European Union
FRQ	Fluctuating Red Queen
FSD	Fluctuating selection dynamics
GATK	Genome analysis toolkit
GLS	Generalised least squares
kb	Kilobase
KB	King's Media B
LB	Luria broth
LPS	Lipopolysaccharide
LS	Link strength
mb	Megabase
MF	Mutation frequency
PCR	Polymerase chain reaction
PDR	Pandrug resistance
PFU	Plaque forming units
PRI	Proportion of realised interactions
RAPD	Random amplification of polymorphic DNA
RBG	Relative bacterial growth
RM	Restriction modification
RMF	Relative mutation frequency
SE	Standard error
SNP	Single nucleotide polymorphism

Bibliography

- Abedon, S.T. (2014). Phage Therapy: Eco-Physiological Pharmacology. *Scientifica* 2014, 581639.
- Abedon, S.T., and Thomas-Abedon, C. (2010). Phage therapy pharmacology. *Curr. Pharm. Biotechnol.* 11, 28–47.
- Ackermann, H.-W. (2007). 5500 Phages examined in the electron microscope. *Arch. Virol.* 152, 227–243.
- Agler, M.T., Ruhe, J., Kroll, S., Morhenn, C., Kim, S.-T., Weigel, D., and Kemen, E.M. (2016). Microbial Hub Taxa Link Host and Abiotic Factors to Plant Microbiome Variation. *PLOS Biol.* 14, e1002352.
- Alekshun, M.N., and Levy, S.B. (2007). Molecular Mechanisms of Antibacterial Multidrug Resistance. *Cell* 128, 1037–1050.
- Alemayehu, D., Casey, P.G., McAuliffe, O., Guinane, C.M., Martin, J.G., Shanahan, F., Coffey, A., Ross, R.P., and Hill, C. (2012). Bacteriophages ϕ MR299-2 and ϕ NH-4 Can Eliminate *Pseudomonas aeruginosa* in the Murine Lung and on Cystic Fibrosis Lung Airway Cells. *MBio* 3, e00029-12.
- Amgarten, D., Martins, L.F., Lombardi, K.C., Antunes, L.P., de Souza, A.P.S., Nicastro, G.G., Kitajima, E.W., Quaggio, R.B., Upton, C., Setubal, J.C., et al. (2017). Three novel *Pseudomonas* phages isolated from composting provide insights into the evolution and diversity of tailed phages. *BMC Genomics* 18, 346.
- Andersson, D.I., and Hughes, D. (2010). Antibiotic resistance and its cost: is it possible to reverse resistance? *Nat. Rev. Microbiol.* 8, 260–271.
- Barbosa, C., Venail, P., Holguin, A.V., and Vives, M.J. (2013). Co-Evolutionary Dynamics of the Bacteria *Vibrio* sp. CV1 and Phages V1G, V1P1, and V1P2: Implications for Phage Therapy. *Microb. Ecol.* 66, 897–905.
- Barracough, T.G. (2015). How Do Species Interactions Affect Evolutionary Dynamics Across Whole Communities? *Annu. Rev. Ecol. Evol. Syst.* 46, 25–48.
- Barrangou, R., Fremaux, C., Deveau, H., Richards, M., Boyaval, P., Moineau, S., Romero, D.A., and Horvath, P. (2007). CRISPR Provides Acquired Resistance Against Viruses in Prokaryotes. *Science* 315, 1709–1712.
- Bascompte, J. (2010). Structure and Dynamics of Ecological Networks. *Science* 329, 765–766.
- Baym, M., Stone, L.K., and Kishony, R. (2016). Multidrug evolutionary strategies to reverse antibiotic resistance. *Science* 351, aad3292.
- Beckett, S.J. (2015). Nestedness and Modularity in Bipartite Networks. University of Exeter.

- Beckett, S.J., and Williams, H.T.P. (2013). Coevolutionary diversification creates nested-modular structure in phage–bacteria interaction networks. *Interface Focus* 3, 20130033.
- Bell, T., Newman, J.A., Silverman, B.W., Turner, S.L., and Lilley, A.K. (2005). The contribution of species richness and composition to bacterial services. *Nature* 436, 1157–1160.
- Bell, T., Lilley, A.K., Hector, A., Schmid, B., King, L., Newman, J.A., Morin, A.E.P.J., and DeAngelis, E.D.L. (2009). A Linear Model Method for Biodiversity–Ecosystem Functioning Experiments. *Am. Nat.* 174, 836–849.
- Bennett, P.M. (2008). Plasmid encoded antibiotic resistance: acquisition and transfer of antibiotic resistance genes in bacteria. *Br. J. Pharmacol.* 153, S347–S357.
- Bertozzi Silva, J., Storms, Z., and Sauvageau, D. (2016). Host receptors for bacteriophage adsorption. *FEMS Microbiol. Lett.* 363.
- Betts, A., Vasse, M., Kaltz, O., and Hochberg, M.E. (2013). Back to the future: evolving bacteriophages to increase their effectiveness against the pathogen *Pseudomonas aeruginosa* PAO1. *Evol. Appl.* 6, 1054–1063.
- Betts, A., Gifford, D.R., MacLean, R.C., and King, K.C. (2016a). Parasite diversity drives rapid host dynamics and evolution of resistance in a bacteria–phage system. *Evolution* 70, 969–978.
- Betts, A., Rafaluk, C., and King, K.C. (2016b). Host and Parasite Evolution in a Tangled Bank. *Trends Parasitol.* 32, 863–873.
- Betts, A., Gray, C., Zelek, M., MacLean, R.C., and King, K.C. (2018). High parasite diversity accelerates host adaptation and diversification. *Science* 360, 907–911.
- Bittner, M., Saldías, S., Estévez, C., Zaldívar, M., Marolda, C.L., Valvano, M.A., and Contreras, I. (2002). O-antigen expression in *Salmonella enterica* serovar Typhi is regulated by nitrogen availability through RpoN-mediated transcriptional control of the *rfaH* gene. *Microbiology* 148, 3789–3799.
- Bittner, M., Saldías, S., Altamirano, F., Valvano, M.A., and Contreras, I. (2004). RpoS and RpoN are involved in the growth-dependent regulation of *rfaH* transcription and O antigen expression in *Salmonella enterica* serovar Typhi. *Microb. Pathog.* 36, 19–24.
- Bjarnsholt, T., Jensen, P.Ø., Fiandaca, M.J., Pedersen, J., Hansen, C.R., Andersen, C.B., Pressler, T., Givskov, M., and Høiby, N. (2009). *Pseudomonas aeruginosa* biofilms in the respiratory tract of cystic fibrosis patients. *Pediatr. Pulmonol.* 44, 547–558.
- Blair, J.M.A., Webber, M.A., Baylay, A.J., Ogbolu, D.O., and Piddock, L.J.V. (2015). Molecular mechanisms of antibiotic resistance | *Nature Reviews Microbiology*. *Nat. Rev. Microbiol.* 13, 42–51.

- Bohannan, B.J.M., Travisano, M., and Lenski, R.E. (1999). Epistatic Interactions Can Lower the Cost of Resistance to Multiple Consumers. *Evolution* 53, 292–295.
- Bohannan, B.J.M., Kerr, B., Jessup, C.M., Hughes, J.B., and Sandvik, G. (2002). Trade-offs and coexistence in microbial microcosms. *Antonie Van Leeuwenhoek* 81, 107–115.
- Bondy-Denomy, J., Garcia, B., Strum, S., Du, M., Rollins, M.F., Hidalgo-Reyes, Y., Wiedenheft, B., Maxwell, K.L., and Davidson, A.R. (2015). Multiple mechanisms for CRISPR–Cas inhibition by anti-CRISPR proteins. *Nature* 526, 136–139.
- Boots, M. (2011). The Evolution of Resistance to a Parasite Is Determined by Resources. *Am. Nat.* 178, 214–220.
- Bottery, M.J., Wood, A.J., and Brockhurst, M.A. (2016). Selective Conditions for a Multidrug Resistance Plasmid Depend on the Sociality of Antibiotic Resistance. *Antimicrob. Agents Chemother.* 60, 2524–2527.
- Breidenstein, E.B.M., de la Fuente-Núñez, C., and Hancock, R.E.W. (2011). *Pseudomonas aeruginosa*: all roads lead to resistance. *Trends Microbiol.* 19, 419–426.
- Brockhurst, M.A., Morgan, A.D., Rainey, P.B., and Buckling, A. (2003). Population mixing accelerates coevolution. *Ecol. Lett.* 6, 975–979.
- Brockhurst, M.A., Rainey, P.B., and Buckling, A. (2004). The effect of spatial heterogeneity and parasites on the evolution of host diversity. *Proc. R. Soc. B Biol. Sci.* 271, 107–111.
- Brockhurst, M.A., Buckling, A., and Rainey, P.B. (2005). The effect of a bacteriophage on diversification of the opportunistic bacterial pathogen, *Pseudomonas aeruginosa*. *Proc. R. Soc. Lond. B Biol. Sci.* 272, 1385–1391.
- Brockhurst, M.A., Buckling, A., and Rainey, P.B. (2006). Spatial heterogeneity and the stability of host-parasite coexistence. *J. Evol. Biol.* 19, 374–379.
- Brockhurst, M.A., Morgan, A.D., Fenton, A., and Buckling, A. (2007). Experimental coevolution with bacteria and phage: The *Pseudomonas fluorescens*— Φ 2 model system. *Infect. Genet. Evol.* 7, 547–552.
- Brockhurst, M.A., Chapman, T., King, K.C., Mank, J.E., Paterson, S., and Hurst, G.D.D. (2014). Running with the Red Queen: the role of biotic conflicts in evolution. *Proc. R. Soc. Lond. B Biol. Sci.* 281, 20141382.
- Brüssow, H. (2012). What is needed for phage therapy to become a reality in Western medicine? *Virology* 434, 138–142.
- Buckling, A., and Brockhurst, M. (2012). Bacteria–Virus Coevolution. *Adv. Exp. Med. Biol.* 751, 347–370.
- Buckling, A., and Rainey, P.B. (2002). Antagonistic coevolution between a bacterium and a bacteriophage. *Proc. R. Soc. B Biol. Sci.* 269, 931–936.

- Bull, J.J., Vegge, C.S., Schmerer, M., Chaudhry, W.N., and Levin, B.R. (2014). Phenotypic Resistance and the Dynamics of Bacterial Escape from Phage Control. *PLOS ONE* 9, e94690.
- Burns, J.L., Gibson, R.L., McNamara, S., Yim, D., Emerson, J., Rosenfeld, M., Hiatt, P., McCoy, K., Castile, R., Smith, A.L., et al. (2001). Longitudinal Assessment of *Pseudomonas aeruginosa* in Young Children with Cystic Fibrosis. *J. Infect. Dis.* 183, 444–452.
- Burrows, L.L. (2012). *Pseudomonas aeruginosa* Twitching Motility: Type IV Pili in Action. *Annu. Rev. Microbiol.* 66, 493–520.
- Carlton, R.M. (1999). Phage therapy: past history and future prospects. *Arch. Immunol. Ther. Exp. (Warsz.)* 47, 267–274.
- Castillo, D., Christiansen, R.H., Dalsgaard, I., Madsen, L., and Middelboe, M. (2014). Bacteriophage resistance mechanisms in the fish pathogen *Flavobacterium psychrophilum*: Linking genomic mutations to changes in bacterial virulence factors. *Appl. Environ. Microbiol.* 80, 03699–14.
- Ceyssens, P.-J., and Lavigne, R. (2010). Bacteriophages of *Pseudomonas*. *Future Microbiol. Lond.* 5, 1041–1055.
- Ceyssens, P.-J., Noben, J.-P., Ackermann, H.-W., Verhaegen, J., Vos, D.D., Pirnay, J.-P., Merabishvili, M., Vanechoutte, M., Chibeu, A., Volckaert, G., et al. (2009). Survey of *Pseudomonas aeruginosa* and its phages: de novo peptide sequencing as a novel tool to assess the diversity of worldwide collected viruses. *Environ. Microbiol.* 11, 1303–1313.
- Chan, B.K., Abedon, S.T., and Loc-Carrillo, C. (2013). Phage cocktails and the future of phage therapy. *Future Microbiol.* 8, 769–783.
- Chan, B.K., Sistro, M., Wertz, J.E., Kortright, K.E., Narayan, D., and Turner, P.E. (2016). Phage selection restores antibiotic sensitivity in MDR *Pseudomonas aeruginosa*. *Sci. Rep.* 6, 26717.
- Chapman-McQuiston, E., and Wu, X.L. (2008). Stochastic Receptor Expression Allows Sensitive Bacteria to Evade Phage Attack. Part I: Experiments. *Biophys. J.* 94, 4525–4536.
- Chaudhry, W.N., Concepción-Acevedo, J., Park, T., Andleeb, S., Bull, J.J., and Levin, B.R. (2017). Synergy and Order Effects of Antibiotics and Phages in Killing *Pseudomonas aeruginosa* Biofilms. *PLOS ONE* 12, e0168615.
- Chaudhry, W.N., Pleška, M., Shah, N.N., Weiss, H., McCall, I.C., Meyer, J.R., Gupta, A., Guet, C.C., and Levin, B.R. (2018). Leaky resistance and the conditions for the existence of lytic bacteriophage. *PLOS Biol.* 16, e2005971.
- Chiang, P., and Burrows, L.L. (2003). Biofilm formation by hyperpiliated mutants of *Pseudomonas aeruginosa*. *J. Bacteriol.* 185, 2374–2378.
- Chiang, P., Sampaleanu, L.M., Ayers, M., Pahuta, M., Howell, P.L., and Burrows, L.L. (2008). Functional role of conserved residues in the characteristic secretion NTPase motifs of the *Pseudomonas aeruginosa* type IV pilus motor proteins PilB, PilT and PilU. *Microbiology* 154, 114–126.

- Choudhury, B., Carlson, R.W., and Goldberg, J.B. (2005). The structure of the lipopolysaccharide from a galU mutant of *Pseudomonas aeruginosa* serogroup-O11. *Carbohydr. Res.* *340*, 2761–2772.
- Cingolani, P., Platts, A., Wang, L.L., Coon, M., Nguyen, T., Wang, L., Land, S.J., Lu, X., and Ruden, D.M. (2012). A program for annotating and predicting the effects of single nucleotide polymorphisms, SnpEff. *Fly (Austin)* *6*, 80–92.
- Clokier, M.R., Millard, A.D., Letarov, A.V., and Heaphy, S. (2011). Phages in nature. *Bacteriophage* *1*, 31–45.
- Conrad, D., Haynes, M., Salamon, P., Rainey, P.B., Youle, M., and Rohwer, F. (2013). Cystic Fibrosis Therapy: A Community Ecology Perspective. *Am. J. Respir. Cell Mol. Biol.* *48*, 150–156.
- Cornforth, D.M., Dees, J.L., Ibberson, C.B., Huse, H.K., Mathiesen, I.H., Kirketerp-Møller, K., Wolcott, R.D., Rumbaugh, K.P., Bjarnsholt, T., and Whiteley, M. (2018). *Pseudomonas aeruginosa* transcriptome during human infection. *Proc. Natl. Acad. Sci.* 201717525.
- Cox, M.J., Allgaier, M., Taylor, B., Baek, M.S., Huang, Y.J., Daly, R.A., Karaoz, U., Andersen, G.L., Brown, R., Fujimura, K.E., et al. (2010). Airway Microbiota and Pathogen Abundance in Age-Stratified Cystic Fibrosis Patients. *PLOS ONE* *5*, e11044.
- Cryz, S.J., Pitt, T.L., Fürer, E., and Germanier, R. (1984). Role of lipopolysaccharide in virulence of *Pseudomonas aeruginosa*. *Infect. Immun.* *44*, 508–513.
- Csardi, G., and Nepusz, T. (2006). The igraph software package for complex network research. *InterJournal Complex Systems*, 1695.
- Dallas, T., and Cornelius, E. (2015). Co-extinction in a host-parasite network: identifying key hosts for network stability. *Sci. Rep.* *5*, 13185.
- Darwin, A.J. (2013). Stress Relief during Host Infection: The Phage Shock Protein Response Supports Bacterial Virulence in Various Ways. *PLOS Pathog.* *9*, e1003388.
- Davidson, I.W., Lawson, C.J., and Sutherland, I.W. (1977). An alginate lysate from *Azotobacter vinelandii* phage. *J. Gen. Microbiol.* *98*, 223–229.
- Dean, C.R., and Goldberg, J.B. (2002). *Pseudomonas aeruginosa* galU is required for a complete lipopolysaccharide core and repairs a secondary mutation in a PA103 (serogroup O11) wbpM mutant. *FEMS Microbiol. Lett.* *210*, 277–283.
- DeLong, E.F., Pace, N.R., and Kane, M. (2001). Environmental Diversity of Bacteria and Archaea. *Syst. Biol.* *50*, 470–478.
- Deredjian, A., Colinon, C., Brothier, E., Favre-Bonté, S., Cournoyer, B., and Nazaret, S. (2011). Antibiotic and metal resistance among hospital and outdoor strains of *Pseudomonas aeruginosa*. *Res. Microbiol.* *162*, 689–700.

- Deveau, H., Barrangou, R., Garneau, J.E., Labonté, J., Fremaux, C., Boyaval, P., Romero, D.A., Horvath, P., and Moineau, S. (2008). Phage Response to CRISPR-Encoded Resistance in *Streptococcus thermophilus*. *J. Bacteriol.* *190*, 1390–1400.
- Dormann, C.F., Gruber, B., and Freund, J. (2008). Introducing the bipartite Package: Analysing Ecological Networks. *R News* *8*, 8–11.
- Dormann, C.F., Freund, J., Bluethgen, N., and Gruber, B. (2009). Indices, graphs and null models: analyzing bipartite ecological networks. *Open Ecol. J.* *2*, 7–24.
- Doron, S., Melamed, S., Ofir, G., Leavitt, A., Lopatina, A., Keren, M., Amitai, G., and Sorek, R. (2018). Systematic discovery of antiphage defense systems in the microbial pangenome. *Science* *359*.
- Driscoll, J.A., Brody, S.L., and Kollef, M.H. (2007). The Epidemiology, Pathogenesis and Treatment of *Pseudomonas aeruginosa* Infections. *Drugs* *67*, 351–368.
- Duan, K., Dammel, C., Stein, J., Rabin, H., and Surette, M.G. (2003). Modulation of *Pseudomonas aeruginosa* gene expression by host microflora through interspecies communication. *Mol. Microbiol.* *50*, 1477–1491.
- Duckworth, D.H. (1976). “Who discovered bacteriophage?”. *Bacteriol. Rev.* *40*, 793–802.
- Duffy, S., Turner, P.E., and Burch, C.L. (2006). Pleiotropic Costs of Niche Expansion in the RNA Bacteriophage $\Phi 6$. *Genetics* *172*, 751–757.
- Dulbecco, R. (1952). MUTUAL EXCLUSION BETWEEN RELATED PHAGES1. *J. Bacteriol.* *63*, 209–217.
- Dy, R.L., Przybilski, R., Semeijn, K., Salmond, G.P.C., and Fineran, P.C. (2014). A widespread bacteriophage abortive infection system functions through a Type IV toxin–antitoxin mechanism. *Nucleic Acids Res.* *42*, 4590–4605.
- Erez, Z., Steinberger-Levy, I., Shamir, M., Doron, S., Stokar-Avihail, A., Peleg, Y., Melamed, S., Leavitt, A., Savidor, A., Albeck, S., et al. (2017). Communication between viruses guides lysis–lysogeny decisions. *Nature advance online publication*.
- Evans, R., Alessi, A.M., Bird, S., McQueen-Mason, S.J., Bruce, N.C., and Brockhurst, M.A. (2017). Defining the functional traits that drive bacterial decomposer community productivity. *ISME J.*
- Fernández, L., Álvarez-Ortega, C., Wiegand, I., Olivares, J., Kocíncová, D., Lam, J.S., Martínez, J.L., and Hancock, R.E.W. (2013). Characterization of the Polymyxin B Resistome of *Pseudomonas aeruginosa*. *Antimicrob. Agents Chemother.* *57*, 110–119.
- Filippov, A.A., Sergueev, K.V., He, Y., Huang, X.-Z., Gnade, B.T., Mueller, A.J., Fernandez-Prada, C.M., and Nikolich, M.P. (2011). Bacteriophage-Resistant Mutants in *Yersinia pestis*: Identification of Phage Receptors and Attenuation for Mice. *PLoS ONE* *6*.

- Fischer, S., Kittler, S., Klein, G., and Glünder, G. (2013). Impact of a Single Phage and a Phage Cocktail Application in Broilers on Reduction of *Campylobacter jejuni* and Development of Resistance. *PLOS ONE* 8, e78543.
- Flores, C.O., Meyer, J.R., Valverde, S., Farr, L., and Weitz, J.S. (2011). Statistical structure of host–phage interactions | *PNAS. Proc. Natl. Acad. Sci.* 108, E288–E297.
- Flores, C.O., Valverde, S., and Weitz, J.S. (2013). Multi-scale structure and geographic drivers of cross-infection within marine bacteria and phages. *ISME J.* 7, 520–532.
- Fokine, A., and Rossmann, M.G. (2014). Molecular architecture of tailed double-stranded DNA phages. *Bacteriophage* 4.
- Folkesson, A., Jelsbak, L., Yang, L., Johansen, H.K., Ciofu, O., Høiby, N., and Molin, S. (2012). Adaptation of *Pseudomonas aeruginosa* to the cystic fibrosis airway: an evolutionary perspective. *Nat. Rev. Microbiol.* 10, 841–851.
- Foster, P.L. (2007). Stress-Induced Mutagenesis in Bacteria. *Crit. Rev. Biochem. Mol. Biol.* 42, 373–397.
- Frederickson, C.M., Short, S.M., and Suttle, C.A. (2003). The Physical Environment Affects Cyanophage Communities in British Columbia Inlets. *Microb. Ecol.* 46, 348–357.
- Frederiksen, B., Koch, C., and Høiby, N. (1997). Antibiotic treatment of initial colonization with *Pseudomonas aeruginosa* postpones chronic infection and prevents deterioration of pulmonary function in cystic fibrosis. *Pediatr. Pulmonol.* 23, 330–335.
- Friman, V.-P., and Buckling, A. (2013). Effects of predation on real-time host–parasite coevolutionary dynamics. *Ecol. Lett.* 16, 39–46.
- Friman, V.-P., Lindstedt, C., Hiltunen, T., Laakso, J., and Mappes, J. (2009). Predation on Multiple Trophic Levels Shapes the Evolution of Pathogen Virulence. *PLOS ONE* 4, e6761.
- Friman, V.-P., Ghoul, M., Molin, S., Johansen, H.K., and Buckling, A. (2013). *Pseudomonas aeruginosa* Adaptation to Lungs of Cystic Fibrosis Patients Leads to Lowered Resistance to Phage and Protist Enemies. *PLoS ONE* 8, e75380.
- Friman, V.-P., Soanes-Brown, D., Sierocinski, P., Molin, S., Johansen, H.K., Merabishvili, M., Pirnay, J.-P., De Vos, D., and Buckling, A. (2016). Pre-adapting parasitic phages to a pathogen leads to increased pathogen clearance and lowered resistance evolution with *Pseudomonas aeruginosa* cystic fibrosis bacterial isolates. *J. Evol. Biol.* 29, 188–198.
- Fu, W., Forster, T., Mayer, O., Curtin, J.J., Lehman, S.M., and Donlan, R.M. (2010). Bacteriophage Cocktail for the Prevention of Biofilm Formation by *Pseudomonas aeruginosa* on Catheters in an In Vitro Model System. *Antimicrob. Agents Chemother.* 54, 397–404.

- Fuhrman, J.A. (1999). Marine viruses and their biogeochemical and ecological effects. *Nature* 399, 541–548.
- Gandon, S., and Michalakis, Y. (2002). Local adaptation, evolutionary potential and host–parasite coevolution: interactions between migration, mutation, population size and generation time. *J. Evol. Biol.* 15, 451–462.
- Gandon, S., Buckling, A., Decaestecker, E., and Day, T. (2008). Host–parasite coevolution and patterns of adaptation across time and space. *J. Evol. Biol.* 21, 1861–1866.
- Girvan, M., and Newman, M.E.J. (2002). Community structure in social and biological networks. *PNAS* 99, 7821–7826.
- Goldfarb, T., Sberro, H., Weinstock, E., Cohen, O., Doron, S., Charpak-Amikam, Y., Afik, S., Ofir, G., and Sorek, R. (2015). BREX is a novel phage resistance system widespread in microbial genomes. *EMBO J.* 34, 169–183.
- Gómez, P., and Buckling, A. (2011). Bacteria-Phage Antagonistic Coevolution in Soil. *Science* 332, 106–109.
- Gómez, P., Ashby, B., and Buckling, A. (2015a). Population mixing promotes arms race host–parasite coevolution. *Proc. R. Soc. B Biol. Sci.* 282, 20142297.
- Gómez, P., Bennie, J., Gaston, K.J., and Buckling, A. (2015b). The Impact of Resource Availability on Bacterial Resistance to Phages in Soil. *PLoS ONE* 10, e0123752.
- Gurney, J., Aldakak, L., Betts, A., Gougat-Barbera, C., Poisot, T., Kaltz, O., and Hochberg, M.E. (2017). Network structure and local adaptation in coevolving bacteria-phage interactions. *Mol. Ecol.*
- Hahn, H.P. (1997). The type-4 pilus is the major virulence-associated adhesin of *Pseudomonas aeruginosa*--a review. *Gene* 192, 99–108.
- Hall, A.R., Scanlan, P.D., and Buckling, A. (2011a). Bacteria-Phage Coevolution and the Emergence of Generalist Pathogens. *Am. Nat.* 177, 44–53.
- Hall, A.R., Scanlan, P.D., Morgan, A.D., and Buckling, A. (2011b). Host–parasite coevolutionary arms races give way to fluctuating selection. *Ecol. Lett.* 14, 635–642.
- Hall, A.R., Vos, D.D., Friman, V.-P., Pirnay, J.-P., and Buckling, A. (2012). Effects of Sequential and Simultaneous Applications of Bacteriophages on Populations of *Pseudomonas aeruginosa* In Vitro and in Wax Moth Larvae. *Appl. Environ. Microbiol.* 78, 5646–5652.
- Hambly, E., and Suttle, C.A. (2005). The virosphere, diversity, and genetic exchange within phage communities. *Curr. Opin. Microbiol.* 8, 444–450.
- Hancock, R.E., Mutharia, L.M., Chan, L., Darveau, R.P., Speert, D.P., and Pier, G.B. (1983). *Pseudomonas aeruginosa* isolates from patients with cystic fibrosis: a class of serum-sensitive, nontypable strains deficient in lipopolysaccharide O side chains. *Infect. Immun.* 42, 170–177.

- Hanlon, G.W., Denyer, S.P., Olliff, C.J., and Ibrahim, L.J. (2001). Reduction in Exopolysaccharide Viscosity as an Aid to Bacteriophage Penetration through *Pseudomonas aeruginosa* Biofilms. *Appl. Environ. Microbiol.* *67*, 2746–2753.
- Haraguchi, Y., and Sasaki, A. (2000). The Evolution of Parasite Virulence and Transmission Rate in a Spatially Structured Population. *J. Theor. Biol.* *203*, 85–96.
- Harrison, F. (2007). Microbial ecology of the cystic fibrosis lung. *Microbiology* *153*, 917–923.
- Harrison, E., Laine, A.-L., Hietala, M., and Brockhurst, M.A. (2013). Rapidly fluctuating environments constrain coevolutionary arms races by impeding selective sweeps. *Proc. R. Soc. B Biol. Sci.* *280*, 20130937–20130937.
- Harrison, E., Wood, A.J., Dytham, C., Pitchford, J.W., Truman, J., Spiers, A., Paterson, S., and Brockhurst, M.A. (2015). Bacteriophages Limit the Existence Conditions for Conjugative Plasmids. *MBio* *6*, e00586-15.
- Harvey, H., Bondy-Denomy, J., Marquis, H., Sztanko, K.M., Davidson, A.R., and Burrows, L.L. (2018). *Pseudomonas aeruginosa* defends against phages through type IV pilus glycosylation. *Nat. Microbiol.* *3*, 47.
- Heilmann, S., Sneppen, K., and Krishna, S. (2012). Coexistence of phage and bacteria on the boundary of self-organized refuges. *Proc. Natl. Acad. Sci.* *109*, 12828–12833.
- Hentzer, M., Teitzel, G.M., Balzer, G.J., Heydorn, A., Molin, S., Givskov, M., and Parsek, M.R. (2001). Alginate Overproduction Affects *Pseudomonas aeruginosa* Biofilm Structure and Function. *J. Bacteriol.* *183*, 5395–5401.
- d’Herelle, F. (1917). Sur un microbe invisible antagoniste des bacilles dysentériques. *CR Acad Sci Paris*.
- Hertveldt, K., Lavigne, R., Pleteneva, E., Sernova, N., Kurochkina, L., Korchevskii, R., Robben, J., Mesyanzhinov, V., Krylov, V.N., and Volckaert, G. (2005). Genome comparison of *Pseudomonas aeruginosa* large phages. *J. Mol. Biol.* *354*, 536–545.
- Hesse, E., and Buckling, A. (2015). Host population bottlenecks drive parasite extinction during antagonistic coevolution. *Evolution* *70*, 235–240.
- Hobbs, M., Collie, E.S., Free, P.D., Livingston, S.P., and Mattick, J.S. (1993). PilS and PilR, a two-component transcriptional regulatory system controlling expression of type 4 fimbriae in *Pseudomonas aeruginosa*. *Mol. Microbiol.* *7*, 669–682.
- Horvath, P., and Barrangou, R. (2010). CRISPR/Cas, the Immune System of Bacteria and Archaea. *Science* *327*, 167–170.
- Hoskisson, P.A., and Smith, M.C. (2007). Hypervariation and phase variation in the bacteriophage ‘resistome.’ *Curr. Opin. Microbiol.* *10*, 396–400.

Huse, H.K., Kwon, T., Zlosnik, J.E.A., Speert, D.P., Marcotte, E.M., and Whiteley, M. (2010). Parallel Evolution in *Pseudomonas aeruginosa* over 39,000 Generations In Vivo. *MBio* 1, e00199-10.

Imamovic, L., and Sommer, M.O.A. (2013). Use of Collateral Sensitivity Networks to Design Drug Cycling Protocols That Avoid Resistance Development. *Sci. Transl. Med.* 5, 204ra132-204ra132.

Islam, S.T., Taylor, V.L., Qi, M., and Lam, J.S. (2010). Membrane Topology Mapping of the O-Antigen Flippase (Wzx), Polymerase (Wzy), and Ligase (WaaL) from *Pseudomonas aeruginosa* PAO1 Reveals Novel Domain Architectures. *MBio* 1, e00189-10.

James, C.E., Davies, E.V., Fothergill, J.L., Walshaw, M.J., Beale, C.M., Brockhurst, M.A., and Winstanley, C. (2015). Lytic activity by temperate phages of *Pseudomonas aeruginosa* in long-term cystic fibrosis chronic lung infections. *ISME J.* 9, 1391–1398.

Jensen, E.C., Schrader, H.S., Rieland, B., Thompson, T.L., Lee, K.W., Nickerson, K.W., and Kokjohn, T.A. (1998). Prevalence of Broad-Host-Range Lytic Bacteriophages of *Sphaerotilus natans*, *Escherichia coli*, and *Pseudomonas aeruginosa*. *Appl. Environ. Microbiol.* 64, 575–580.

Jessup, C.M., and Forde, S.E. (2008). Ecology and evolution in microbial systems: the generation and maintenance of diversity in phage–host interactions. *Res. Microbiol.* 159, 382–389.

Johnson, M.D.L., Garrett, C.K., Bond, J.E., Coggan, K.A., Wolfgang, M.C., and Redinbo, M.R. (2011). *Pseudomonas aeruginosa* PilY1 binds integrin in an RGD- and calcium-dependent manner. *PLoS One* 6, e29629.

Joly, N., Engl, C., Jovanovic, G., Huvet, M., Toni, T., Sheng, X., Stumpf, M.P.H., and Buck, M. (2010). Managing membrane stress: the phage shock protein (Psp) response, from molecular mechanisms to physiology. *FEMS Microbiol. Rev.* 34, 797–827.

Jovanovic, G., Lloyd, L.J., Stumpf, M.P.H., Mayhew, A.J., and Buck, M. (2006). Induction and Function of the Phage Shock Protein Extracytoplasmic Stress Response in *Escherichia coli*. *J. Biol. Chem.* 281, 21147–21161.

Jurczak-Kurek, A., Gaşior, T., Nejman-Faleńczyk, B., Bloch, S., Dydecka, A., Topka, G., Necel, A., Jakubowska-Deredas, M., Narajczyk, M., Richert, M., et al. (2016). Biodiversity of bacteriophages: morphological and biological properties of a large group of phages isolated from urban sewage. *Sci. Rep.* 6, 34338.

Kassen, R., Buckling, A., Bell, G., and Rainey, P.B. (2000). Diversity peaks at intermediate productivity in a laboratory microcosm. *Nature* 406, 508–512.

Kelly, D., McAuliffe, O., O'Mahony, J., and Coffey, A. (2011). Development of a broad-host-range phage cocktail for biocontrol. *Bioeng. Bugs* 2, 31–37.

King, J.D., Kocíncová, D., Westman, E.L., and Lam, J.S. (2009). Review: Lipopolysaccharide biosynthesis in *Pseudomonas aeruginosa*. *Innate Immun.* 15, 261–312.

- Kirby, A.E. (2012). Synergistic Action of Gentamicin and Bacteriophage in a Continuous Culture Population of *Staphylococcus aureus*. *PLOS ONE* 7, e51017.
- Koonin, E.V., Makarova, K.S., and Wolf, Y.I. (2017). Evolutionary Genomics of Defense Systems in Archaea and Bacteria. *Annu. Rev. Microbiol.* 71, 233–261.
- Koskella, B., and Brockhurst, M.A. (2014). Bacteria–phage coevolution as a driver of ecological and evolutionary processes in microbial communities. *FEMS Microbiol. Rev.* 38, 916–931.
- Koskella, B., Lin, D.M., Buckling, A., and Thompson, J.N. (2011). The costs of evolving resistance in heterogeneous parasite environments. *Proc. R. Soc. Lond. B Biol. Sci.* rspb20112259.
- Kumaran, D., Taha, M., Yi, Q., Ramirez-Arcos, S., Diallo, J.-S., Carli, A., and Abdelbary, H. (2018). Does Treatment Order Matter? Investigating the Ability of Bacteriophage to Augment Antibiotic Activity against *Staphylococcus aureus* Biofilms. *Front. Microbiol.* 9.
- Kutter, E., De Vos, D., Gvasalia, G., Alavidze, Z., Gogokhia, L., Kuhl, S., and Abedon, S.T. (2010). Phage Therapy in Clinical Practice: Treatment of Human Infections. *Curr. Pharm. Biotechnol.* 11, 69–86.
- Kuznetsova, A., Brockhoff, P.B., and Christensen, R.H.B. (2017). ImerTest Package: Tests in Linear Mixed Effects Models. *J. Stat. Softw.* 82, 1–26.
- Laanto, E., Bamford, J.K.H., Laakso, J., and Sundberg, L.-R. (2012). Phage-Driven Loss of Virulence in a Fish Pathogenic Bacterium. *PLOS ONE* 7, e53157.
- Labedan, B. (1984). Requirement for a fluid host cell membrane in injection of coliphage T5 DNA. *J Virol* 49, 273–275.
- Labrie, S.J., Samson, J.E., and Moineau, S. (2010). Bacteriophage resistance mechanisms. *Nat. Rev. Microbiol.* 8, 317–327.
- Lam, J.S., Taylor, V.L., Islam, S.T., Hao, Y., and Kocíncová, D. (2011). Genetic and Functional Diversity of *Pseudomonas aeruginosa* Lipopolysaccharide. *Front. Microbiol.* 2.
- Latino, L., Midoux, C., Hauck, Y., Vergnaud, G., and Pourcel, C. (2016). Pseudolysogeny and sequential mutations build multiresistance to virulent bacteriophages in *Pseudomonas aeruginosa*. *Microbiology* 162, 748–763.
- Latino, L., Caroff, M., and Pourcel, C. (2017). Fine structure analysis of lipopolysaccharides in bacteriophage-resistant *Pseudomonas aeruginosa* PAO1 mutants. *Microbiol. Read. Engl.* 163, 848–855.
- Le, S., Yao, X., Lu, S., Tan, Y., Rao, X., Li, M., Jin, X., Wang, J., Zhao, Y., Wu, N.C., et al. (2014). Chromosomal DNA deletion confers phage resistance to *Pseudomonas aeruginosa*. *Sci. Rep.* 4, 4738.
- Leid, J.G., Willson, C.J., Shirtliff, M.E., Hassett, D.J., Parsek, M.R., and Jeffers, A.K. (2005). The Exopolysaccharide Alginate Protects *Pseudomonas*

- aeruginosa Biofilm Bacteria from IFN- γ -Mediated Macrophage Killing. *J. Immunol.* *175*, 7512–7518.
- Lenski, R.E. (1984). Two-Step Resistance by *Escherichia Coli* B to Bacteriophage T2. *Genetics* *107*, 1–7.
- Lenski, R.E. (1988). Experimental Studies of Pleiotropy and Epistasis in *Escherichia coli*. I. Variation in Competitive Fitness Among Mutants Resistant to Virus T4. *Evolution* *42*, 425–432.
- Lenski, R.E., and Levin, B.R. (1985). Constraints on the Coevolution of Bacteria and Virulent Phage: A Model, Some Experiments, and Predictions for Natural Communities. *Am. Nat.* *125*, 585–602.
- León, M., and Bastías, R. (2015). Virulence reduction in bacteriophage resistant bacteria. *Front. Microbiol.* *6*.
- Levin, B.R., and Bull, J.J. (1996). Phage Therapy Revisited: The Population Biology of a Bacterial Infection and Its Treatment with Bacteriophage and Antibiotics. *Am. Nat.* *147*, 881–898.
- Levin, B.R., and Bull, J.J. (2004). Population and evolutionary dynamics of phage therapy. *Nat. Rev. Microbiol.* *2*, 166–173.
- Levin, B.R., Antonovics, J., and Sharma, H. (1988). Frequency-Dependent Selection in Bacterial Populations. *Philos. Trans. R. Soc. B Biol. Sci.* *319*, 459–472.
- Levin, B.R., Perrot, V., and Walker, N. (2000). Compensatory mutations, antibiotic resistance and the population genetics of adaptive evolution in bacteria. *Genetics* *154*, 985–997.
- Levin, B.R., Moineau, S., Bushman, M., and Barrangou, R. (2013). The Population and Evolutionary Dynamics of Phage and Bacteria with CRISPR-Mediated Immunity. *PLOS Genet.* *9*, e1003312.
- Li, H., and Durbin, R. (2009). Fast and accurate short read alignment with Burrows–Wheeler transform. *Bioinformatics* *25*, 1754–1760.
- Lister, P.D., Wolter, D.J., and Hanson, N.D. (2009). Antibacterial-Resistant *Pseudomonas aeruginosa*: Clinical Impact and Complex Regulation of Chromosomally Encoded Resistance Mechanisms. *Clin. Microbiol. Rev.* *22*, 582.
- Lively, C.M. (2010). The Effect of Host Genetic Diversity on Disease Spread. *Am. Nat.* *175*, E149–E152.
- Livermore, D.M. (2002). Multiple Mechanisms of Antimicrobial Resistance in *Pseudomonas aeruginosa*: Our Worst Nightmare? *Clin. Infect. Dis.* *34*, 634–640.
- Lloyd, M.G., Lundgren, B.R., Hall, C.W., Gagnon, L.B.-P., Mah, T.-F., Moffat, J.F., and Nomura, C.T. (2017). Targeting the alternative sigma factor RpoN to combat virulence in *Pseudomonas aeruginosa*. *Sci. Rep.* *7*, 12615.

- Loc-Carrillo, C., and Abedon, S.T. (2011). Pros and cons of phage therapy. *Bacteriophage* 1, 111–114.
- Lopez Pascua, L., Hall, A.R., Best, A., Morgan, A.D., Boots, M., and Buckling, A. (2014). Higher resources decrease fluctuating selection during host–parasite coevolution. *Ecol. Lett.* 17, 1380–1388.
- Lopez-Pascua, L.D.C., and Buckling, A. (2008). Increasing productivity accelerates host–parasite coevolution. *J. Evol. Biol.* 21, 853–860.
- Lourenço, M., De Sordi, L., and Debarbieux, L. (2018). The Diversity of Bacterial Lifestyles Hampers Bacteriophage Tenacity. *Viruses* 10.
- Macé, C., Seyer, D., Chemani, C., Cosette, P., Di-Martino, P., Guery, B., Filloux, A., Fontaine, M., Molle, V., Junter, G.-A., et al. (2008). Identification of Biofilm-Associated Cluster (bac) in *Pseudomonas aeruginosa* Involved in Biofilm Formation and Virulence. *PLOS ONE* 3, e3897.
- Mahenthalingam, E., Campbell, M.E., and Speert, D.P. (1994). Nonmotility and phagocytic resistance of *Pseudomonas aeruginosa* isolates from chronically colonized patients with cystic fibrosis. *Infect. Immun.* 62, 596–605.
- Maier, B., and Wong, G.C.L. (2015). How Bacteria Use Type IV Pili Machinery on Surfaces. *Trends Microbiol.* 23, 775–788.
- Marraffini, L.A. (2015). CRISPR-Cas immunity in prokaryotes. *Nature* 526, 55–61.
- Martin, P.R., Hobbs, M., Free, P.D., Jeske, Y., and Mattick, J.S. (1993). Characterization of pilQ, a new gene required for the biogenesis of type 4 fimbriae in *Pseudomonas aeruginosa*. *Mol. Microbiol.* 9, 857–868.
- Mattick, J.S., Whitchurch, C.B., and Alm, R.A. (1996). The molecular genetics of type-4 fimbriae in *Pseudomonas aeruginosa* - a review. *Gene* 179, 147–155.
- Mattila, S., Ruotsalainen, P., and Jalasvuori, M. (2015). On-Demand Isolation of Bacteriophages Against Drug-Resistant Bacteria for Personalized Phage Therapy. *Front. Microbiol.* 6.
- McCallin, S., Alam Sarker, S., Barretto, C., Sultana, S., Berger, B., Huq, S., Krause, L., Bibiloni, R., Schmitt, B., Reuteler, G., et al. (2013). Safety analysis of a Russian phage cocktail: From MetaGenomic analysis to oral application in healthy human subjects. *Virology* 443, 187–196.
- McKenna, A., Hanna, M., Banks, E., Sivachenko, A., Cibulskis, K., Kernytsky, A., Garimella, K., Altshuler, D., Gabriel, S., Daly, M., et al. (2010). The Genome Analysis Toolkit: A MapReduce framework for analyzing next-generation DNA sequencing data. *Genome Res.* 20, 1297–1303.
- McVay, C.S., Velásquez, M., and Fraclick, J.A. (2007). Phage Therapy of *Pseudomonas aeruginosa* Infection in a Mouse Burn Wound Model. *Antimicrob. Agents Chemother.* 51, 1934–1938.
- Merabishvili, M., Verhelst, R., Glonti, T., Chanishvili, N., Krylov, V., Cuvelier, C., Tediashvili, M., and Vanechoutte, M. (2007). Digitized fluorescent RFLP

- analysis (fRFLP) as a universal method for comparing genomes of culturable dsDNA viruses: application to bacteriophages. *Res. Microbiol.* *158*, 572–581.
- Merabishvili, M., Pirnay, J.-P., Verbeken, G., Chanishvili, N., Tediashvili, M., Lashkhi, N., Glonti, T., Krylov, V., Mast, J., Van Parys, L., et al. (2009). Quality-Controlled Small-Scale Production of a Well-Defined Bacteriophage Cocktail for Use in Human Clinical Trials. *PLoS ONE* *4*, e4944.
- Merabishvili, M., Pirnay, J.-P., and De Vos, D. (2018). Guidelines to Compose an Ideal Bacteriophage Cocktail. In *Bacteriophage Therapy: From Lab to Clinical Practice*, J. Azeredo, and S. Sillankorva, eds. (New York, NY: Springer New York), pp. 99–110.
- Meyer, J.R., Dobias, D.T., Weitz, J.S., Barrick, J.E., Quick, R.T., and Lenski, R.E. (2012). Repeatability and Contingency in the Evolution of a Key Innovation in Phage Lambda. *Science* *335*, 428–432.
- Middelboe, M., Holmfeldt, K., Riemann, L., Nybroe, O., and Haaber, J. (2009). Bacteriophages drive strain diversification in a marine Flavobacterium: implications for phage resistance and physiological properties. *Environ. Microbiol.* *11*, 1971–1982.
- Monk, A.B., Rees, C.D., Barrow, P., Hagens, S., and Harper, D.R. (2010). Bacteriophage applications: where are we now? *Lett. Appl. Microbiol.* *51*, 363–369.
- Morello, E., Sausseureau, E., Maura, D., Huerre, M., Touqui, L., and Debarbieux, L. (2011). Pulmonary Bacteriophage Therapy on *Pseudomonas aeruginosa* Cystic Fibrosis Strains: First Steps Towards Treatment and Prevention. *PLOS ONE* *6*, e16963.
- Mowat, E., Paterson, S., Fothergill, J.L., Wright, E.A., Ledson, M.J., Walshaw, M.J., Brockhurst, M.A., and Winstanley, C. (2011). *Pseudomonas aeruginosa* Population Diversity and Turnover in Cystic Fibrosis Chronic Infections. *Am. J. Respir. Crit. Care Med.* *183*, 1674–1679.
- Newman, M.E.J., and Girvan, M. (2004). Finding and evaluating community structure in networks. *Phys Rev E* *69*.
- Nunn, D.N., and Lory, S. (1991). Product of the *Pseudomonas aeruginosa* gene *pilD* is a prepilin leader peptidase. *Proc. Natl. Acad. Sci.* *88*, 3281–3285.
- O’Driscoll, J., Glynn, F., Fitzgerald, G.F., and Sinderen, D. van (2006). Sequence Analysis of the Lactococcal Plasmid pNP40: a Mobile Replicon for Coping with Environmental Hazards. *J. Bacteriol.* *188*, 6629–6639.
- Ofir, G., and Sorek, R. (2018). Contemporary Phage Biology: From Classic Models to New Insights. *Cell* *172*, 1260–1270.
- Oliveira, P.H., Touchon, M., and Rocha, E.P.C. (2016). Regulation of genetic flux between bacteria by restriction–modification systems. *Proc. Natl. Acad. Sci.* *113*, 5658–5663.
- O’Neill, J. (2014). Antimicrobial Resistance: Tackling a crisis for the health and wealth of nations. *Rev. Antimicrob. Resist.*

- Pál, C., Papp, B., and Lázár, V. (2015). Collateral sensitivity of antibiotic-resistant microbes. *Trends Microbiol.* 23, 401–407.
- Paradis, E., Claude, J., and Strimmer, K. (2004). APE: Analyses of Phylogenetics and Evolution in R language. *Bioinforma. Oxf. Engl.* 20, 289–290.
- Paterson, S., Vogwill, T., Buckling, A., Benmayor, R., Spiers, A.J., Thomson, N.R., Quail, M., Smith, F., Walker, D., Libberton, B., et al. (2010). Antagonistic coevolution accelerates molecular evolution. *Nature* 464, 275–278.
- Persat, A., Inclan, Y.F., Engel, J.N., Stone, H.A., and Gitai, Z. (2015). Type IV pili mechanochemically regulate virulence factors in *Pseudomonas aeruginosa*. *Proc. Natl. Acad. Sci.* 112, 7563–7568.
- Petchey, O.L., and Gaston, K.J. (2006). Functional diversity: back to basics and looking forward. *Ecol. Lett.* 9, 741–758.
- Phagoburn: Evaluation of phage therapy for the treatment of burn wound infections.
- Pier, G.B. (2007). *Pseudomonas aeruginosa* lipopolysaccharide: A major virulence factor, initiator of inflammation and target for effective immunity. *Int. J. Med. Microbiol.* 297, 277–295.
- Pires, D.P., Boas, D.V., Sillankorva, S., and Azeredo, J. (2015). Phage therapy: a step forward in the treatment of *Pseudomonas aeruginosa* infections. *J. Virol.* JVI.00385-15.
- Pires, D.P., Dötsch, A., Anderson, E.M., Hao, Y., Khursigara, C.M., Lam, J.S., Sillankorva, S., and Azeredo, J. (2017). A Genotypic Analysis of Five *P. aeruginosa* Strains after Biofilm Infection by Phages Targeting Different Cell Surface Receptors. *Front. Microbiol.* 8.
- Pirnay, J.-P., Vos, D.D., Cochez, C., Bilocq, F., Pirson, J., Struelens, M., Duinslaeger, L., Cornelis, P., Zizi, M., and Vanderkelen, A. (2003). Molecular Epidemiology of *Pseudomonas aeruginosa* Colonization in a Burn Unit: Persistence of a Multidrug-Resistant Clone and a Silver Sulfadiazine-Resistant Clone. *J. Clin. Microbiol.* 41, 1192–1202.
- Pirnay, J.-P., Vos, D.D., Verbeken, G., Merabishvili, M., Chanishvili, N., Vaneechoutte, M., Zizi, M., Laire, G., Lavigne, R., Huys, I., et al. (2010). The Phage Therapy Paradigm: Prêt-à-Porter or Sur-mesure? *Pharm. Res.* 28, 934–937.
- Pirnay, J.-P., Verbeken, G., Rose, T., Jennes, S., Zizi, M., Huys, I., Lavigne, R., Merabishvili, M., Vaneechoutte, M., Buckling, A., et al. (2012). Introducing yesterday's phage therapy in today's medicine. *Future Virol.* 7, 379–390.
- Pirnay, J.-P., Blasdel, B.G., Bretaudeau, L., Buckling, A., Chanishvili, N., Clark, J.R., Corte-Real, S., Debarbieux, L., Dublanquet, A., Vos, D.D., et al. (2015). Quality and Safety Requirements for Sustainable Phage Therapy Products. *Pharm. Res.* 32, 2173–2179.

- Pirnay, J.-P., Verbeken, G., Ceysens, P.-J., Huys, I., De Vos, D., Ameloot, C., Fauconnier, A., Pirnay, J.-P., Verbeken, G., Ceysens, P.-J., et al. (2018). The Magistral Phage. *Viruses* *10*, 64.
- Poisot, T., Lepennetier, G., Martinez, E., Ramsayer, J., and Hochberg, M.E. (2011). Resource availability affects the structure of a natural bacteria–bacteriophage community. *Biol. Lett.* *7*, 201–204.
- Poole, K., Zhao, Q., Neshat, S., Heinrichs, D.E., and Dean, C.R. (1996). The *Pseudomonas aeruginosa* tonB gene encodes a novel TonB protein. *Microbiol. Read. Engl.* *142* (Pt 6), 1449–1458.
- Poullain, V., Gandon, S., Brockhurst, M.A., Buckling, A., and Hochberg, M.E. (2008). The evolution of specificity in evolving and coevolving antagonistic interactions between a bacteria and its phage. *Evolution* *62*, 1–11.
- R Core Team (2016). R: A Language and Environment for Statistical Computing (Vienna, Austria: R Foundation for Statistical Computing).
- Rafaluk, C., Gildenhard, M., Mitschke, A., Telschow, A., Schulenburg, H., and Joop, G. (2015). Rapid evolution of virulence leading to host extinction under host-parasite coevolution. *BMC Evol. Biol.* *15*, 112.
- Rahim, R., Burrows, L.L., Monteiro, M.A., Perry, M.B., and Lam, J.S. (2000). Involvement of the rml locus in core oligosaccharide and O polysaccharide assembly in *Pseudomonas aeruginosa*. *Microbiology* *146*, 2803–2814.
- Rakhuba, D.V., Kolomiets, E.I., Dey, E.S., and Novik, G.I. (2010). Bacteriophage receptors, mechanisms of phage adsorption and penetration into host cell. *Pol. J. Microbiol.* *59*, 145–155.
- Reece, K.S., and Phillips, G.J. (1995). New plasmids carrying antibiotic-resistance cassettes. *Gene* *165*, 141–142.
- Roach, D.R., and Debarbieux, L. (2017). Phage therapy: awakening a sleeping giant. *Emerg. Top. Life Sci.* *1*, 93–103.
- Roach, D.R., Leung, C.Y., Henry, M., Morello, E., Singh, D., Di Santo, J.P., Weitz, J.S., and Debarbieux, L. (2017). Synergy between the Host Immune System and Bacteriophage Is Essential for Successful Phage Therapy against an Acute Respiratory Pathogen. *Cell Host Microbe* *22*, 38-47.e4.
- Robinson, J.T., Thorvaldsdóttir, H., Winckler, W., Guttman, M., Lander, E.S., Getz, G., and Mesirov, J.P. (2011). Integrative genomics viewer. *Nat. Biotechnol.* *29*, 24–26.
- Rogues, A.-M., Boulestreau, H., Lashéras, A., Boyer, A., Gruson, D., Merle, C., Castaing, Y., Bébear, C.M., and Gachie, J.-P. (2007). Contribution of tap water to patient colonisation with *Pseudomonas aeruginosa* in a medical intensive care unit. *J. Hosp. Infect.* *67*, 72–78.
- Rohde, C., Resch, G., Pirnay, J.-P., Blasdel, B., Debarbieux, L., Gelman, D., Górski, A., Hazan, R., Huys, I., Kakabadze, E., et al. (2018). Expert Opinion on Three Phage Therapy Related Topics: Bacterial Phage Resistance, Phage Training and Prophages in Bacterial Production Strains. *Viruses* *10*, 178.

Rose, T., Verbeken, G., Vos, D.D., Merabishvili, M., Vaneechoutte, M., Lavigne, R., Jennes, S., Zizi, M., and Pirnay, J.-P. (2014). Experimental phage therapy of burn wound infection: difficult first steps. *Int. J. Burns Trauma* 4, 66–73.

Ross, A., Ward, S., and Hyman, P. (2016). More Is Better: Selecting for Broad Host Range Bacteriophages. *Front. Microbiol.* 7.

Rossi, E., Falcone, M., Molin, S., and Johansen, H.K. (2018). High-resolution in situ transcriptomics of *Pseudomonas aeruginosa* unveils genotype independent patho-phenotypes in cystic fibrosis lungs. *Nat. Commun.* 9, 3459.

Salles, J.F., Poly, F., Schmid, B., and Roux, X.L. (2009). Community niche predicts the functioning of denitrifying bacterial assemblages. *Ecology* 90, 3324–3332.

Samson, J.E., Magadán, A.H., Sabri, M., and Moineau, S. (2013). Revenge of the phages: defeating bacterial defences. *Nat. Rev. Microbiol.* 11, 675–687.

Sasaki, A. (2000). Host-parasite coevolution in a multilocus gene-for-gene system. *Proc. R. Soc. Lond. B Biol. Sci.* 267, 2183–2188.

Scanlan, P.D., and Buckling, A. (2012). Co-evolution with lytic phage selects for the mucoid phenotype of *Pseudomonas fluorescens* SBW25. *ISME J.* 6, 1148–1158.

Scanlan, P.D., Hall, A.R., Blackshields, G., Friman, V.-P., Davis, M.R., Goldberg, J.B., and Buckling, A. (2015a). Coevolution with bacteriophages drives genome-wide host evolution and constrains the acquisition of abiotic-beneficial mutations. *Mol. Biol. Evol.* 32, 1425–1435.

Scanlan, P.D., Buckling, A., and Hall, A.R. (2015b). Experimental evolution and bacterial resistance: (co)evolutionary costs and trade-offs as opportunities in phage therapy research. *Bacteriophage* 5, e1050153.

Schmerer, M., Molineux, I.J., and Bull, J.J. (2014). Synergy as a rationale for phage therapy using phage cocktails. *PeerJ* 2, e590.

Schrag, S.J., and Mittler, J.E. (1996). Host-Parasite Coexistence: The Role of Spatial Refuges in Stabilizing Bacteria-Phage Interactions. *Am. Nat.* 148, 348–377.

Sepúlveda-Robles, O., Kameyama, L., and Guarneros, G. (2012). High Diversity and Novel Species of *Pseudomonas aeruginosa* Bacteriophages. *Appl. Environ. Microbiol.* 78, 4510–4515.

Servick, K. (2016). Beleaguered phage therapy trial presses on. *Science* 352, 1506–1506.

Sivera Marza, J., Soothill, J., Boydell, P., and Collyns, T. (2006). Multiplication of therapeutically administered bacteriophages in *Pseudomonas aeruginosa* infected patients. *Burns* 32, 644–646.

Skurnik, D., Roux, D., Aschard, H., Cattoir, V., Yoder-Himes, D., Lory, S., and Pier, G.B. (2013). A Comprehensive Analysis of In Vitro and In Vivo Genetic

Fitness of *Pseudomonas aeruginosa* Using High-Throughput Sequencing of Transposon Libraries. *PLOS Pathog.* 9, e1003582.

Smith, J.M. (1976). A Comment on the Red Queen. *Am. Nat.* 110, 325–330.

Smith, E.E., Buckley, D.G., Wu, Z., Saenphimmachak, C., Hoffman, L.R., D'Argenio, D.A., Miller, S.I., Ramsey, B.W., Speert, D.P., Moskowitz, S.M., et al. (2006). Genetic adaptation by *Pseudomonas aeruginosa* to the airways of cystic fibrosis patients. *Proc. Natl. Acad. Sci.* 103, 8487–8492.

Sneppen, K., Semsey, S., Seshasayee, A.S.N., and Krishna, S. (2015). Restriction modification systems as engines of diversity. *Front. Microbiol.* 6.

Stern, A., and Sorek, R. (2011). The phage-host arms race: Shaping the evolution of microbes. *BioEssays* 33, 43–51.

Sweeney, M.T., Lubbers, B.V., Schwarz, S., and Watts, J.L. (2018). Applying definitions for multidrug resistance, extensive drug resistance and pandrug resistance to clinically significant livestock and companion animal bacterial pathogens. *J. Antimicrob. Chemother.* 73, 1460–1463.

Sybesma, W., Rohde, C., Bardy, P., Pirnay, J.P., Cooper, I., Caplin, J., Chanishvili, N., Coffey, A., De, D.V., Scholz, A.H., et al. (2018). Silk Route to the Acceptance and Re-Implementation of Bacteriophage Therapy-Part II. *Antibiot. Basel Switz.* 7.

Tanji, Y., Shimada, T., Yoichi, M., Miyanaga, K., Hori, K., and Unno, H. (2004). Toward rational control of *Escherichia coli* O157:H7 by a phage cocktail. *Appl. Microbiol. Biotechnol.* 64, 270–274.

Thébault, E., and Fontaine, C. (2010). Stability of Ecological Communities and the Architecture of Mutualistic and Trophic Networks. *Science* 329, 853–856.

Thingstad, T.F. (2000). Elements of a theory for the mechanisms controlling abundance, diversity, and biogeochemical role of lytic bacterial viruses in aquatic systems. *Limnol. Oceanogr.* 45, 1320–1328.

Tilman, D., Knops, J., Wedin, D., Reich, P., Ritchie, M., and Siemann, E. (1997). The Influence of Functional Diversity and Composition on Ecosystem Processes. *Science* 277, 1300–1302.

Toju, H., Yamamichi, M., Jr, P.R.G., Olesen, J.M., Mougi, A., Yoshida, T., and Thompson, J.N. (2017). Species-rich networks and eco-evolutionary synthesis at the metacommunity level. *Nat. Ecol. Evol.* 1, 0024.

Torres-Barceló, C. (2018). Phage Therapy Faces Evolutionary Challenges. *Viruses* 10, 323.

Torres-Barceló, C., and Hochberg, M.E. (2016). Evolutionary Rationale for Phages as Complements of Antibiotics. *Trends Microbiol.*

Torres-Barceló, C., Arias-Sánchez, F.I., Vasse, M., Ramsayer, J., Kaltz, O., and Hochberg, M.E. (2014). A Window of Opportunity to Control the Bacterial Pathogen *Pseudomonas aeruginosa* Combining Antibiotics and Phages. *PLoS ONE* 9.

Totten, P.A., Lara, J.C., and Lory, S. (1990). The *rpoN* gene product of *Pseudomonas aeruginosa* is required for expression of diverse genes, including the flagellin gene. *J. Bacteriol.* *172*, 389–396.

Trautmann, M., Lepper, P.M., and Haller, M. (2005). Ecology of *Pseudomonas aeruginosa* in the intensive care unit and the evolving role of water outlets as a reservoir of the organism. *Am. J. Infect. Control* *33*, S41–S49.

Van Valen, L. (1973). A new evolutionary law. *Evol. Theory* *1*, 1–30.

Vayssier-Taussat, M., Albina, E., Citti, C., Cosson, J.F., Jacques, M.-A., Lebrun, M.-H., Le Loir, Y., Ogliastro, M., Petit, M.-A., Roumagnac, P., et al. (2014). Shifting the paradigm from pathogens to pathobiome: new concepts in the light of meta-omics. *Front. Cell. Infect. Microbiol.* *4*.

Verbeken, G., De Vos, D., Vaneechoutte, M., Merabishvili, M., Zizi, M., and Pirnay, J.-P. (2007). European regulatory conundrum of phage therapy. *Future Microbiol.* *2*, 485–491.

Verbeken, G., Pirnay, J.-P., Vos, D.D., Jennes, S., Zizi, M., Lavigne, R., Casteels, M., and Huys, I. (2012). Optimizing the European Regulatory Framework for Sustainable Bacteriophage Therapy in Human Medicine. *Arch. Immunol. Ther. Exp. (Warsz.)* *60*, 161–172.

Vogwill, T., Fenton, A., Buckling, A., Hochberg, M.E., and Brockhurst, M.A. (2009). Source Populations Act as Coevolutionary Pacemakers in Experimental Selection Mosaics Containing Hotspots and Coldspots. *Am. Nat.* *173*, E171–E176.

Watanabe, R., Matsumoto, T., Sano, G., Ishii, Y., Tateda, K., Sumiyama, Y., Uchiyama, J., Sakurai, S., Matsuzaki, S., Imai, S., et al. (2007). Efficacy of Bacteriophage Therapy against Gut-Derived Sepsis Caused by *Pseudomonas aeruginosa* in Mice. *Antimicrob. Agents Chemother.* *51*, 446–452.

Waterbury, J.B., and Valois, F.W. (1993). Resistance to Co-Occurring Phages Enables Marine *Synechococcus* Communities To Coexist with Cyanophages Abundant in Seawater. *Appl. Environ. Microbiol.* *59*, 3393–3399.

Waters, E.M., Neill, D.R., Kaman, B., Sahota, J.S., Clokie, M.R.J., Winstanley, C., and Kadioglu, A. (2017). Phage therapy is highly effective against chronic lung infections with *Pseudomonas aeruginosa*. *Thorax*.

Weinbauer, M.G. (2004). Ecology of prokaryotic viruses. *FEMS Microbiol. Rev.* *28*, 127–181.

Weinbauer, M.G., and Rassoulzadegan, F. (2004). Are viruses driving microbial diversification and diversity? *Environ. Microbiol.* *6*, 1–11.

Weiner, L., Brissette, J.L., and Model, P. (1991). Stress-induced expression of the *Escherichia coli* phage shock protein operon is dependent on sigma 54 and modulated by positive and negative feedback mechanisms. *Genes Dev.* *5*, 1912–1923.

- Weitz, J.S., Poisot, T., Meyer, J.R., Flores, C.O., Valverde, S., Sullivan, M.B., and Hochberg, M.E. (2013). Phage–bacteria infection networks. *Trends Microbiol.* *21*, 82–91.
- Westra, E.R., van Houte, S., Oyesiku-Blakemore, S., Makin, B., Broniewski, J.M., Best, A., Bondy-Denomy, J., Davidson, A., Boots, M., and Buckling, A. (2015). Parasite Exposure Drives Selective Evolution of Constitutive versus Inducible Defense. *Curr. Biol.* *25*, 1043–1049.
- Wilhelm, S.W., and Suttle, C.A. (1999). Viruses and Nutrient Cycles in the Sea Viruses play critical roles in the structure and function of aquatic food webs. *BioScience* *49*, 781–788.
- Willner, D., Haynes, M.R., Furlan, M., Schmieder, R., Lim, Y.W., Rainey, P.B., Rohwer, F., and Conrad, D. (2012). Spatial distribution of microbial communities in the cystic fibrosis lung. *ISME J.* *6*, 471–474.
- Winstanley, C., O'Brien, S., and Brockhurst, M.A. (2016). *Pseudomonas aeruginosa* Evolutionary Adaptation and Diversification in Cystic Fibrosis Chronic Lung Infections. *Trends Microbiol.* *0*.
- World Health Organization (2014). Antimicrobial resistance: global report on surveillance.
- Wright, A., Hawkins, C.H., Änggård, E.E., and Harper, D.R. (2009). A controlled clinical trial of a therapeutic bacteriophage preparation in chronic otitis due to antibiotic-resistant *Pseudomonas aeruginosa*; a preliminary report of efficacy. *Clin. Otolaryngol.* *34*, 349–357.
- Yen, M., Cairns, L.S., and Camilli, A. (2017). A cocktail of three virulent bacteriophages prevents *Vibrio cholerae* infection in animal models. *Nat. Commun.* *8*, 14187.
- Yin, B., Crowley, D., Sparovek, G., Melo, W.J.D., and Borneman, J. (2000). Bacterial Functional Redundancy along a Soil Reclamation Gradient. *Appl Env. Microbiol* *66*, 4361–4365.
- Zhang, Q.-G., and Buckling, A. (2011). Antagonistic coevolution limits population persistence of a virus in a thermally deteriorating environment. *Ecol. Lett.* *14*, 282–288.
- Zhang, Q.-G., and Buckling, A. (2016). Resource-dependent antagonistic coevolution leads to a new paradox of enrichment. *Ecology* *97*, 1319–1328.
- Zhao, X.-F., Hao, Y.-Q., and Zhang, Q.-G. (2017). Stability of A Coevolving Host-parasite System Peaks at Intermediate Productivity. *PLOS ONE* *12*, e0168560.